The role of hormones in the development of the adrenal gland

by

Huifei Zheng

A dissertation submitted to the Graduate Faculty of
Auburn University
in partial fulfillment of the
requirements for the Degree of
Doctor of Philosophy

Auburn, Alabama
August 05, 2023

Keywords: Adrenal gland, Development, Thyroid hormone, Progenitor cell

Approved by

Chen-Che Jeff Huang, Chair, Associate Professor of Anatomy, Physiology and Pharmacology
Ya-Xiong Tao, Co-chair, Professor of Anatomy, Physiology and Pharmacology
Satyanarayana R. Pondugula, Professor of Anatomy, Physiology and Pharmacology
Ramesh B. Jeganathan, Bruno Endowed Professor of Nutrition

Abstract

The adrenal cortex, a crucial endocrine gland, is comprised of three distinct regions: the zona glomerulosa, zona fasciculata, and zona reticularis (referred to as the X-zone in mice). This organ plays a critical role in maintaining adult homeostasis by generating steroid hormones. In order to meet the hormonal needs for steroid production, it has the ability to naturally replace aging cells. The innermost zone's cells are considered the aged cell population, which ultimately undergoes apoptosis. The factors influencing the fate of this aged cell population remain incompletely understood. My dissertation aims to address three fundamental questions: 1) What factors affect the aged cell population's fate? 2) What are the potential functions of the aged cell population? 3) What is the origin of the aged cell population? To address these questions, conditional knockout mice and transgenic mice were used in this thesis. In Chapter 2, we utilized tissue-specific gene editing techniques to eliminate the *Ncor1* gene, which encodes the main corepressor in the thyroid hormone signaling pathway, in adrenocortical cells of the adrenal gland. The removal of *Ncor1* was shown to delay cell regression in the adrenal inner cortex. In Chapter 3, we also applied tissue-specific gene editing methods to remove *Dhcr24* in adrenocortical cells of the adrenal gland. In an earlier study, we had demonstrated that thyroid hormone upregulated cholesterol synthesis-related genes, with *Dhcr24* being one of them. In this study, we found that *Dhcr24* functioned as a key regulator of T3-mediated lipid accumulation. This inner cortex zone could potentially act as a reserve tissue for steroidogenesis. In Chapter 4, we studied the short- and long-term effects of glucocorticoids on adrenal gland function and development. RNA sequencing (RNA-seq) was conducted to identify early transcriptomic responses to the synthetic glucocorticoid dexamethasone (Dex) both *in vitro* and *in vivo*.

Adrenocortical Y-1 cells exhibited a transient early response to Dex treatment *in vitro*. Moreover, the differentially expressed genes (DEGs) had minimal overlap between the 1-hour Dex-treated groups *in vivo* and *in vitro*. In Chapter 5, we employed a lineage tracing approach to investigate the role of *Gli1* in the testis, another steroidogenesis organ. We successfully isolated cell-type-specific RNAs from heterogeneous tissue samples without the need for cell sorting. In Chapter 6, we performed a lineage tracing experiment to track Sonic hedgehog (*Shh*)-positive cells, which are progenitor cells, in post-weaning mice, revealing that the adrenal cortex undergoes replacement approximately every three months. *Shh*-positive cells reached the inner cortex, with a small portion becoming inner cortex marker-positive cells.

Acknowledgment

First and foremost, I would like to express my deepest gratitude to Dr. Jeff Huang, my mentor, who has not only guided and supported me throughout my research journey but has also instilled in me the valuable Chinese proverb, "To teach someone how to fish is better than to just give him a fish." The past four years, from 2019 to 2023, have been extraordinarily challenging due to the COVID-19 pandemic, but his relentless guidance, patience and support have made this journey much less daunting. His mentorship has truly shaped my academic and personal growth.

I am grateful to my committee members Drs. Ya-Xiong Tao, Vitaly J. Vodyanoy, Satyanarayana R. Pondugula, and Ramesh B. Jeganathan for their guidance, assistance, and expertise, which have been instrumental in the completion of my dissertation. Their invaluable suggestions and feedback have helped me to refine and improve my research.

I would like to extend my heartfelt appreciation to the Endocrine Society for granting me the Summer Fellowship Award, Early Career Award, and Eugenia Rosemberg Award. I am also grateful to the American Physiology Society for the Research Recognition Award and to Auburn University for the Outstanding Doctoral Student Award. These recognitions have not only validated my hard work and dedication but have also provided me with financial support and motivation to excel in my research endeavors.

My appreciation extends to the department faculty and staff, who have fostered a supportive and collegial environment that has enabled me to thrive academically. I am particularly grateful for their kindness and assistance throughout my time in the program.

I would like to express my sincere gratitude to our lab manager, Dr. Yuan Kang, for her help in breeding mice and ensuring smooth operations in the lab. Her knowledge and expertise have been crucial to the success of my research.

My heartfelt thanks go to my family—my parents, my sister, and my adorable nephew—for their unwavering love, encouragement, and support. Their belief in me and my abilities has been a constant source of strength and motivation throughout my academic journey.

Finally, I would like to extend my deepest appreciation to my fiancé, Michael, whose love, support, and understanding have been invaluable in helping me navigate the challenges and demands of pursuing a Ph.D. I am truly grateful for his unwavering commitment to our shared future.

To all who have contributed to my journey in their own unique ways, thank you. Your support has made this accomplishment possible, and I am eternally grateful.

Table of Contents

List of Tables

List of Figures

List of Abbreviations

11βHSD: 11β-hydroxysteroid dehydrogenase

3βHSD: 3 beta-hydroxysteroid dehydrogenase

ACTH: Adrenocorticotropic hormone

AD: Aldosterone synthase

AGP: Adrenogonadal primordium

Ang II: Angiotensin II

AP: Adrenal primordial

APC: Adenomatous polyposis coli

ATR1: Angiotensin II receptor type 1

CBG: Corticosteroid binding globulin

CK1: Casein kinase 1

cKO: Conditional knockout

CYB5A: Cofactor cytochrome b5

CYP11A1: Cytochrome P450 cholesterol side chain cleavage (P450scc) enzyme

CPY17A1: 17a-hydroxylase/17,20-lyase

CYP11B1: Cytochrome P450 family 11 subfamily b member 1

CYP11B2: Cytochrome P450 family 11 subfamily b member 2

CYP2F2: Cytochrome P450, family 2, subfamily f, polypeptide 2

DEGs: Differentially expressed genes

Dex: Dexamethasone

DHCR24: 24-dehydrocholesterol reductase

DHEA: Dehydroepiandrosterone

DHEAS: DHEA-sulfate

Dhh: Desert hedgehog

DZ: Definitive zone

EZH2: Histone- lysine N- methyltransferase

FZ: Fetal zone

GC: Glucocorticoid

Gli: Glioma-associated oncogene

GRE: Glucocorticoid response element

GSK3: Glycogen synthase kinase 3

Hh: Hedgehog

HPA: Hypothalamic-pituitary-adrenal

IGV: Integrative genomics viewer

Ihh: Indian hedgehog

KO: Knock out

LDL: Low-density lipoprotein

LH: Luteinizing hormone

MC2R: Melanocortin 2 receptor

NCOR1: Nuclear receptor corepressor 1

MCT: Monocarboxylate transporter

NuTRAP: Nuclear tagging and Translating Ribosome Affinity Purification

PBS: Phosphate-buffered saline

PKA: Protein kinase A

PFA: Paraformaldehyde

PRC2: Polycomb repressive complex 2

RRID: Research resource identifiers

SF1: Steroidogenic factor 1

Shh: Sonic hedgehog

SMO: Smoothened

StAR: Steroidogenic acute regulatory protein

T3: Triiodothyronine

TCF: T cell-specific factors

TH: Tyrosine hydroxylase

TR: Thyroid hormone receptor

ZF: Zona fasciculata

ZG: Zona glomerulosa

ZR: Zona reticularis

Chapter 1: Literature review

1.1 The development of the adrenal gland

The adrenal gland is an endocrine organ in the body. It is mainly composed of three parts: the capsule, which acts as a signaling center for adrenal zonation maintenance throughout life; the outer cortex, which synthesizes and secretes steroid hormones; and the medulla, which produces norepinephrine and epinephrine in response to stress. The outer cortex possesses three distinct concentric zones from outside inward: the outer layer, the zona glomerulosa (ZG) produces mineralocorticoids such as aldosterone that regulate water reabsorption thereby increasing blood volume and blood pressure. The second layer, the zona fasciculata (ZF) produces glucocorticoids whose major function is to control glucose metabolism and immune response. The innermost layer, the zona reticularis (ZR) in humans and X-zone in mice. ZR is the site of androgen biosynthesis, and the function of X-zone in mice is not well understood.

1.1.1 Embryonic development of the adrenal cortex

During embryonic development, the urogenital ridge of mesoderm gives rise to the adrenal cortex on both sides of the midline (1-3). During approximately the fourth week postconception in humans (embryonic day [E] 9.0 in mice), the adrenogonadal primordium (AGP) is a thickening of the coelomic epithelium that represents the initial stage of the adrenal cortex when it first appears (4). The bilateral AGP is marked by the presence of steroidogenic factor 1 (SF1/Ad4-binding protein; NR5A1) (4,5), which continues to be expressed in the adrenal cortex until adulthood. Afterward, AGP cells that are positive for SF1 delaminate from the epithelium and infiltrate the intermediate mesoderm's underlying mesenchyme (1). After delamination, a

particular group of AGP cells with higher expression of SF1 move in the dorsomedial direction to form the adrenal primordial at 33 days postconception (E10.5 in mice) (6). Cells of adrenal primordial (AP) continue to proliferate and form two morphologically distinct regions: the inner fetal zone (FZ) and the definitive zone (DZ) (7,8). FZ accounts for approximately 80-90% of the adrenal cortex, which consists of sizable eosinophilic cells that possess the ability to produce steroids (8). DZ is composed of a thin outer layer of small, tightly packed basophilic cells that are less capable of steroidogenesis (8). By 14 weeks of gestation in humans, the area between the two zones becomes evident and is known as the transitional zone (TZ) (9). It comprises cells that share histological characteristics similar to both the DZ and FZ. By late gestation, the DZ starts to resemble the ZG, and the TZ starts to resemble the ZF of the adult adrenal cortex (10).

1.1.2 Postnatal and adult adrenal cortex

The adrenal cortex undergoes significant changes during the neonatal and pubertal stages (10). This remodeling of the adrenal cortex after birth is a complex process that involves a series of differentiation phases, resulting in the rapid apoptosis of the fetal zone and the development of the glomerulosa and fasciculata zones (11). At around 6-8 years of age, human adrenal ZR starts to form in the region situated between ZF and the medulla. This process is also referred to as adrenarche, which is marked by elevated synthesis of adrenal androgens (12).

1.1.3 Murine X-zone development

In mice, the analogous structure to the human ZR is known as the X-zone, which is a cortex layer situated between ZF and the medulla (13). Cells of the X-zone appear for the first time on

postnatal day 8 (P8) and establish a layer at the boundary between the cortex and medulla between P10-P14 (14,15). In males, the X-zone starts to regress at P28 and disappears entirely by P35 (16,17). In female mice, X-zone cells experience a gradual degeneration that begins at P32 and disappears between 3 to 7 months of age (17). In pregnant female mice, the entire X-zone disappears within 5 to 15 days of the first pregnancy (17,18) (Figure 1.1).

1.1.4 Adrenal medulla development

The adrenal medulla originates from neural crest cells that are located near the dorsal aorta. Following their migration towards the midline and arrival at the dorsal aorta, a subset of neural crest cells undergoes lineage segregation and subsequently gives rise to sympathetic neurons and chromaffin cells located in the medulla (19). Recent research has identified Schwann cell precursors, which descend from the neural crest, as an additional source of chromaffin cells found in the adrenal medulla (20). The functions of chromaffin cells in the adrenal medulla include responding to stress, regulating respiration, monitoring the body's carbon dioxide and oxygen levels, as well as playing a role in blood pressure regulation (21).

1.1.5 Adrenal cortex zonation and self-renewal

In humans, the adrenal cortex is composed of three zones: ZG, ZF, and ZR (X-zone in mice). The adrenal cortex is a dynamic organ that is capable of adapting its size and functionality in response to changing physiological requirements. In terms of morphology, there are distinct variations in cellular structure and arrangement among the three cortical zones. Electron microscopic analysis showed that ZG cells are characterized by a high number of mitochondria that possess

lamelliform cristae and a few lipid droplets (22). Cord-like arrangements of ZF cells are accompanied by fenestrated blood vessels that aid in the swift exchange of hormones between steroidogenic cells and the bloodstream (23). While ZR cells share similarities with ZF cells, they typically contain fewer lipid droplets and a greater amount of lysosomes and lipofuscin pigment granules (24). Compared to ZF cells, the cells found in the mouse X-zone are smaller and exhibit varying degrees of cytoplasmic density (25). The absence of physical barriers between the different zones in the adrenal cortex, along with their distinct morphologies, suggests the presence of molecular signals that closely regulate the unique identity of each zone (26).

The adrenal cortex plays a crucial role in maintaining adult homeostasis by synthesizing steroid hormones through reciprocal hormonal regulation (13). It has the ability to spontaneously replace aging cells that undergo rapid changes in response to hormonal demands for steroid biosynthesis (27,28). The adrenal renewal is facilitated by the adrenocortical stem cell population, which ensures that the adrenal gland can sustain physiological and homeostatic conditions despite constant cellular turnover throughout an individual's lifespan (29). These specialized cells migrate towards the corticomedullary boundary (Figure 1.2). The centripetal migration hypothesis was proposed as an explanation to better understand the critical pathways involved in maintaining adrenocortical homeostasis and regeneration (30). In the centripetal migration model, undifferentiated stem/progenitor cells located in the capsular/outer cortex region are responsible for generating differentiated cells (31). These cells then move inward to the inner layers of the cortex, ultimately replacing aged or damaged cells at the corticomedullary boundary (32). This process is regulated by various signaling pathways and molecular factors. In the

following section, several essential regulatory factors involved in the regulation of zonation are presented.

1.1.5.1 Signaling pathways control adrenal cortex development

Wnt/β-catenin signaling pathway

The canonical Wnt/β-catenin signaling pathway plays a crucial role in the formation of the adrenal cortex during embryonic development, as well as its homeostatic maintenance in adulthood (33). The pathway depends on extracellular WNT ligands and the multifunctional protein β-catenin, which serves as an intracellular signaling mediator for transcriptional regulation and chromatin interactions (34). In the absence of WNT ligands, the cytoplasmic pool of β-catenin is maintained at low levels due to the action of the destruction complex (35). This complex consists of two serine/threonine kinases, casein kinase 1 (CK1) and glycogen synthase kinase 3 (GSK3), as well as two tumor suppressors, scaffolding proteins Axin and adenomatous polyposis coli (APC) (35). Within the complex, CK1α phosphorylates serine 45 on β-catenin, enabling further phosphorylation of serine residues 33 and 37 by GSK3β. The E3 ubiquitin ligase β-TrCP recognizes phosphorylated β-catenin and targets it for proteasomal degradation. Consequently, this prevents the accumulation and nuclear translocation of β-catenin (36). Upon binding of a Wnt ligand to the seven-pass transmembrane Frizzled (Fz) receptor and its coreceptor, low-density lipoprotein receptor-related protein 6 (LRP6) or LRP5, the Wnt/β-catenin pathway becomes activated (37,38). The Wnt-Fz-LRP6 complex forms, along with the involvement of the scaffolding protein Dishevelled (Dvl), leading to the phosphorylation and activation of LRP6 and the recruitment of the destruction complex to the receptors (39). These

processes inhibit β-catenin phosphorylation, resulting in the stabilization of β-catenin. Consequently, β-catenin accumulates and translocates to the nucleus, where it acts as a transcriptional co-regulator. For its nuclear function, β-catenin interacts with the N-terminus of DNA-binding proteins in the T cell-specific factors (TCF) and lymphoid enhancer-binding factor (Lef-1) family (40). The interaction between β-catenin and TCF/LEF-1 leads to the recruitment of histone acetylases, the Legless family docking protein (Bcl9), and CBP/p300, which in turn converts TCF/LEF-1 into a transcriptional activator for their target genes (34,41,42).

The zonal expression of several component elements implies a role for Wnt signaling in the development of the adrenal cortex. Out of nineteen Wnt ligands, only a few have been found in the mouse adrenal gland (43). Wnt4, one of these ligands, is expressed in the cortical region of the developing adrenal gland, particularly in the zona glomerulosa (44). In *Wnt4* mutant animals, the expression of *Cyp11b2* is reduced, resulting in a substantial decrease in aldosterone production in newborn mutants. CPY11B2 functions as the final enzyme in the aldosterone production process and is typically restricted to the zona glomerulosa. This indicates that Wnt4 might be crucial for the appropriate development of the zona glomerulosa (44). Cells exhibiting β-catenin accumulation are found along the outer edges of the adrenal cortex (33,45). The continuous activation of β-catenin in a particular group of steroidogenic cells in the adrenal cortex caused an atypical buildup of undifferentiated cells in both the subcapsular and capsular regions (46). Because mice with a global deficiency in β-catenin, known as knockout (KO) mice, experience embryonic lethality during gastrulation and do not develop mesoderm, it is impossible to use a global KO approach to analyze any potential abnormalities in adrenal

development (47). However, targeted inactivation of beta-catenin expression in the adrenal cortex resulted in adrenal aplasia in newborn mice (33). These findings highlight the essential roles of β-catenin, particularly as a component of the WNT canonical signaling pathway, in the development of adrenal cortical cells.

SHH signaling pathway

The Hedgehog (Hh) signaling pathway is a significant evolutionarily conserved pathway which involves essential functions such as embryonic development, adult stem cell maintenance, and cancer regulation (48-50). There are three Hh ligands: Sonic hedgehog (*Shh*), Desert hedgehog (*Dhh*), and Indian hedgehog *(Ihh*) (51). The initiation of Hh protein signaling depends on the binding of Hh ligands to a 12-transmembrane receptor known as Patched (PTCH) (52,53). The binding triggers a downstream signaling cascade that regulates target genes, which are responsible for proliferation, survival, metastasis, invasion, and self-regulation of the pathway (52). In the absence of Hh, PTCH1 localizes to the primary cilium's base and functions to prevent the seven-pass transmembrane protein Smoothened (SMO) from entering the primary cilium.

The SMO then controls the activation of Glioma-associated oncogene (Gli). The Gli family transcription factors consist of three members: GLI1, GLI2, and GLI3 (54). Gli1 is a transcriptional activator and a target of Hh signaling. GLI2 and GLI3 possess both transcriptional activator and repressor functions. When SMO is not activated, GLI2 undergoes proteolytic processing, and GLI3 is cleaved to produce a transcriptional repressor (55-57). This leads to the inhibition of a subset of Hh target genes. In contrast, when Hh binds to PTCH1, it leads to the deactivation of PTCH1, causing SMO to accumulate in the cilium. The activation of SMO results in the suppression of the

breakdown of these factors, which results in the disappearance of the repressor form of GLI and the buildup of the full-length activator form (mainly GLI1). This, in turn, leads to the stimulation of transcriptional activation (58).

Studies have demonstrated the expression of *Shh* in the adrenal gland of rodents, and its role in regulating the growth and differentiation of adrenal gland cells. As early as E12.5 (59), expression of *Shh* is detected in clusters of cells located at the edge of the adrenal cortex underneath the adrenal capsule (60). Mice lineage tracing studies revealed that descendants of *Shh*-positive cells also display markers for functional steroidogenic cells including *Sf1*-positive cells, but the vast majority do not exhibit either CYP11B2 or CYP11B1 (59). Several studies have investigated the effects of conditional ablation of *Shh* utilizing *Sf1-Cre* transgenic mice (59-61). All the reported results indicate that the adrenal glands in the mutant mice were significantly smaller compared to those in control mice and the cortex is disproportionately smaller in mutant mice. By utilizing inducible genetic lineage tracing similar to the method used for *Shh*, *Gli1*-positive cells were also marked in the adrenal gland (59,60). The offspring of *Gli1*-positive cells situated in the cortex also displayed expression of *Sf1*. Taken together, *Shh* and *Gli1* expression as markers for adrenal stem or progenitor cells both play a role in both adrenal renewal and homeostasis. Mechanistically, the sustained activation of the SHH signaling pathway is associated with the activation of the Wnt signaling pathway. Constitutive activation of β-catenin results in excessive accumulation of *Shh* mRNA level (46). This suggests β-catenin may be involved in the recruitment of adrenal stem/progenitor cells and that this process may involve the direct regulation of *Shh* expression by the WNT signaling pathway (62).

ACTH/PKA signaling pathway

The hypothalamic-pituitary-adrenal (HPA) axis regulates the production of cortisol and androgen (in humans) and corticosterone (in mice) by adrenocortical steroidogenic cells (63). Cortisol production in the adrenal ZF is stimulated by adrenocorticotropic hormone (ACTH) from the pituitary gland, which activates the cAMP-dependent protein kinase A (PKA) signaling pathway (64,65). When ACTH binds to its receptor, composed of melanocortin 2 receptor (MC2R) and its accessory protein (MRAP), it initiates the release of the alpha subunit of the stimulatory G protein that leads to elevated intracellular cAMP production and ultimately results in increased PKA activity, which further facilitates subsequent steroidogenesis (66-68). The predominant activity of the cAMP signaling pathway in the ZG is evidenced by the presence of molecular components of the cAMP cascade (69,70). In mice, persistent PKA activation in ZF is a key driver of WNT inhibition and lineage conversion, which subsequently prevents ZG differentiation (71). Histone-lysine N- methyltransferase (EZH2), a component of the polycomb repressive complex 2 (PRC2), is accountable for upholding elevated PKA signaling levels. Its removal results in ZF-specific hypoplasia, diminished steroidogenic identity, and primary glucocorticoid insufficiency in mice (69).

1.1.5.2 Molecular factors control adrenal cortex development

Steroidogenic Factor 1 (SF1)

SF1 is a crucial regulator required for adrenal development. It was first discovered as a transcription factor that controls the expression of several adrenal hydroxylase genes involved in

producing steroids (72). SF1 is also capable of transforming embryonic and mesenchymal stem cells into steroid-producing cells, which implies a role for SF1 in lineage conversion (73,74).

Aldosterone synthase (AS)

AS (encoded by cytochrome P450 family 11 subfamily b member 2 (*Cyp11b2*), a steroidogenic enzyme, is necessary for the final stages of aldosterone synthesis, and its gene expression is limited to fully differentiated cells within the ZG (75). In a *Cyp11b2-Cre* mouse model, ZG cells expressing *Cyp11b2* underwent lineage conversion into ZF cells (27). This implies that *Cyp11b2*-positive cells might possess the ability to self-renew as ZG cells.

Angiotensin II (Ang II)

.Ang II impacts blood pressure through its effects on the adrenal cortex, which includes stimulating the production of aldosterone and promoting the growth of ZG cells (76,77). This is accomplished through the transcriptional regulation of CYP11B2 and the stimulation of the Angiotensin II receptor type 1 (AT1R). The efficacy of AT1R blockers such as losartan and candesartan in reducing aldosterone synthesis, inhibiting ZG cell proliferation, and decreasing the width of the zone supports the critical role of AT1R in these processes (78,79). In addition to Ang II, a low sodium diet or high potassium intake can also lead to the proliferation of ZG cells and result in an expansion of the zone (76,80).

1.1.6 Adrenal steroidogenesis and function

The adrenal cortex is responsive for producing mineralocorticoids, glucocorticoids, and sex steroids (81). Cholesterol serves as the precursor for steroid hormones and is then transformed into intermediate substances for steroid hormone production (82). There are several potential sources for cellular cholesterol: (1) cholesteryl esters (CEs) from circulating lipoproteins acquired through low-density lipoprotein (LDL) receptor-mediated endocytic pathways (83), (2) Scavenger receptor class B type I (SR-BI) -mediated selective lipid uptake (84,85), (3) the conversion of cholesteryl esters into free cholesterol by cholesterol ester hydrolase (86), and (4) *de novo* cholesterol synthesis (87,88). Steroidogenesis begins with the transfer of free cholesterol from the outer mitochondrial membrane to the inner membrane, facilitated by the steroidogenic acute regulatory protein (StAR) (89). This is the rate limiting step in the steroidogenesis regulated by ACTH, which involves ACTH binding to cell membrane receptors associated with G-proteins. This binding promotes elevated cytoplasmic cAMP levels and enhances the accessibility of cholesterol to cytochrome P450 cholesterol side chain cleavage (P450scc) enzyme (CYP11A1) (90). In the inner mitochondrial membrane, CYP11A1 then catalyzes the conversion of cholesterol into pregnenolone (91). From this point on, the synthesis of all other steroid hormones is possible, depending on the specific type of cytochrome P450 isoform present.

Aldosterone biosynthesis and ZG function

Aldosterone, the primary mineralocorticoid, is generated predominantly in the ZG due to the exclusive presence of CYP11B2 in this region. 3 beta-hydroxysteroid dehydrogenase (3βHSD) coverts pregnenolone into progesterone (92), which then can be converted into 11-deoxycorticosterone by the action of 21-hydroxylase (CYP21A2). Following this, aldosterone

synthase (CYP11B2), which is exclusively located in the ZG, catalyzes 11b-hydroxylase, 18-hydroxylase, and 18-methyl oxidase and finally converts deoxycorticosterone to aldosterone.

Aldosterone plays a crucial role in regulating electrolyte and water balance to ensure optimal blood pressure is maintained. In the kidney, aldosterone acts on the epithelial cells of the distal colon and renal nephron, promoting the reabsorption of sodium ions and the secretion of potassium ions. Aldosterone is primarily regulated by angiotensin II and potassium, with ACTH and serotonin acting as additional acute regulators (93,94).

Cortisol biosynthesis and ZF function

Cortisol, a main glucocorticoid (GC) in humans, is produced in the ZF. 17a-hydroxylase/17,20-lyase (CYP17A1) catalyzes the 17α-hydroxylation and C17–20 cleavage of the pregnenolone and progesterone, then followed by the production of 17α-hydroxypregnenolone and 17α-hydroxyprogesterone, which then are converted to 11-deoxycortisol by the action of CYP21A2. Following this, 11b-hydroxylase (CYP11B1) catalyzes the 11β-hydroxylation of 11-deoxycortisol, resulting in the production of cortisol (91). In mice, due to the lack of CYP17A1, pregnenolone, and progesterone cannot undergo 17α-hydroxylation (95,96). As a result, mice are only capable of producing corticosterone rather than cortisol.

GCs are essential for maintaining both basal and stress-related homeostasis including cardiovascular, anti-inflammatory and metabolic responses (97). In humans, cortisol is the primary form of GCs, and almost 95% of it is tightly bound to corticosteroid binding globulin (CBG)

and albumin (98). Upon releasing from CBG, unbound cortisol represents the free form, which possesses biological activity (99). The interconversion of active form cortisol and inactive form cortisone is facilitated by 11β-hydroxysteroid dehydrogenase (11βHSD) types 1 and 2, which are responsible for regulating cortisol concentrations in peripheral tissues (99,100). In addition, cortisol levels follow a circadian and pulsatile secretion pattern, which is regulated by the HPA axis (101).

By binding to the ubiquitously expressed glucocorticoid receptor (GR), GCs exert a wide range of effects (102). GR belongs to the nuclear receptor family, which consists of ligand-dependent transcription factors (103). When a ligand binds, the GR undergoes conformational changes that lead to partial dissociation and subsequent nuclear translocation (104). Within the nucleus, the GR interacts with specific DNA binding sites, GC response elements (GREs) and coactivators, which further enhance gene expression (105). Conversely, inverted negative GREs (nGREs) are responsible for repressing gene transcription by recruiting corepressors and histone deacetylases (105). In addition, GR is capable of functioning via non-genomic actions. Non-genomic actions comprise GC-mediated alterations to membrane lipids, modifying their physicochemical properties (106). GR can also translocate to mitochondria and influence mitochondrial function (107,108).

Androgen biosynthesis and ZR function

As a C19 steroid, dehydroepiandrosterone (DHEA) is also the production of 17α-hydroxylation and C17–20 cleavage catalyzed by CYP17A1 (91). This process is facilitated by the cofactor

cytochrome b5 (CYB5A) (109). DHEA can be subsequently converted into DHEA-sulfate (DHEAS) through the activity of dehydroepiandrosterone sulfotransferase (110).

Adrenal androgens (AAs), which have weak androgenic activity, are typically secreted by the ZR. DHEA and DHEAS are the main precursors, which serve as a reservoir of circulating precursors that can be converted peripherally into more potent testosterone and estradiol. Other androgens including androstenediol (A5) and 11β-hydroxyandrostenedione (11βOHA4) can also contribute to the pool of circulating precursors (111). The binding of ACTH to its distinct G-protein coupled receptor melanocortin 2 receptor (MC2R) has been demonstrated to stimulate the production of not only aldosterone and cortisol but also DHEA. In response to ACTH, cAMP additionally promotes the phosphorylation of StAR, which then initiates steroidogenesis and promotes the production of androgen in the ZR (110).

1.2 Thyroid hormone actions

Thyroid hormone (TH) exerts crucial influences on regulating metabolic processes and cell development, differentiation, and survival (112-115). The two major forms of thyroid hormone are thyroxine (T4) and triiodothyronine (T3) in the circulatory system. T3 is the biologically relevant hormone molecule since it possesses a higher binding affinity to thyroid hormone receptors (TRs) (116,117). Upon reaching the target tissue, monocarboxylate transporters (MCT) at the cell membrane facilitate the cellular uptake of TH (118,119). Two other transporters also have been found, including the large neutral amino acid transporters (LAT1 and LAT2) and organic

anion transporting polypeptides (OATP) (120-122). Once in the cell, deiodinases convert T4 to its bioactive form T3, which further enters the nucleus and binds to TR (123) (Figure 1.3).

1.2.1 Thyroid hormone receptors

TRs belong to the nuclear receptor superfamily that contains steroids, retinoic acid receptors (RAR), and liver X receptors (LXR). In the early 1960s Tata and Widnell first showed that DNA-dependent RNA-polymerase activity in rat liver nuclei could respond to T3 stimulation by increasing transcriptional levels (124). Subsequently, two independent studies from Sap, *et al*., and Weinberger, *et al*., cloned TR cDNAs from chicken and humans (123,125). They demonstrated that TRs are highly related to viral oncogene product v-erbA and they presented a similar sequence with steroid hormone receptors. There are two major TR isoforms, designated as TRα and TRβ. They are encoded by separate genes on different chromosomes. In humans, the TRα gene located on chromosome 17 encodes TRα1, which binds T3 and mediates gene regulation (112). TRα encodes other additional splicing variants TRα2 and TRα3 (126). The major TRα variant TRα2 cannot bind to T3 and does not act as authentic TRs (127,128). Both TRβ1 and TRβ2 are encoded by the TRβ gene, which is located on chromosome 3 (129). These two TRβ isoforms can bind T3 and further regulate gene expression (112,130).

TR isoform expression varies depending on the tissue (131). TRβ1 exhibits predominant expression in the liver, brain, heart, thyroid, kidneys, and adrenal glands (132). The main expression sites of TRβ2 are the retina and pituitary gland (130,133). The brain shows the highest levels of expression for both TRα1 and TRα2, while the lung, heart, testis, and kidneys exhibit

lower levels of expression (134). Mice in which TRα and TRβ are deleted exhibit HPA axis dysfunction (135), whereas mice with the deletion of TRα have a disability in heart function (136). These findings indicate the possibility of TRs mediating subtype-specific functions.

1.2.2 Thyroid hormone receptor interaction with cofactors

The primary function of TRs is to regulate gene expression of target tissues by interacting with thyroid hormone elements (TREs) located in the regulatory regions of target genes (137,138). TR also heterodimerizes with the retinoid X receptor (RXR) and the heterodimer further binds to TRE to mediate the T3 induction of target genes (139). To activate or repress gene transcription, TR needs to recruit nuclear proteins called coregulators (coactivators and corepressors) (113,140). The coactivator complexes are composed of the steroid receptor coactivator (SRC) family and the CREB-binding protein/p300. Upon ligand (T3) binding, TR undergoes a conformational change, resulting in the recruitment of a set of activator proteins. This leads to chromatin decondensation and the subsequent transcription stimulation (132,141). The corepressor complex includes nuclear receptor corepressor (NCOR1, NCOR2) and a silencing mediator of retinoid and thyroid hormone receptors (SMRT) (142). In the absence of T3, the unliganded TR recruits corepressors, such as NCOR (nuclear receptor corepressor) and histone deacetylase (HDAC), leading to chromatin closing and transcription repression (142-145).

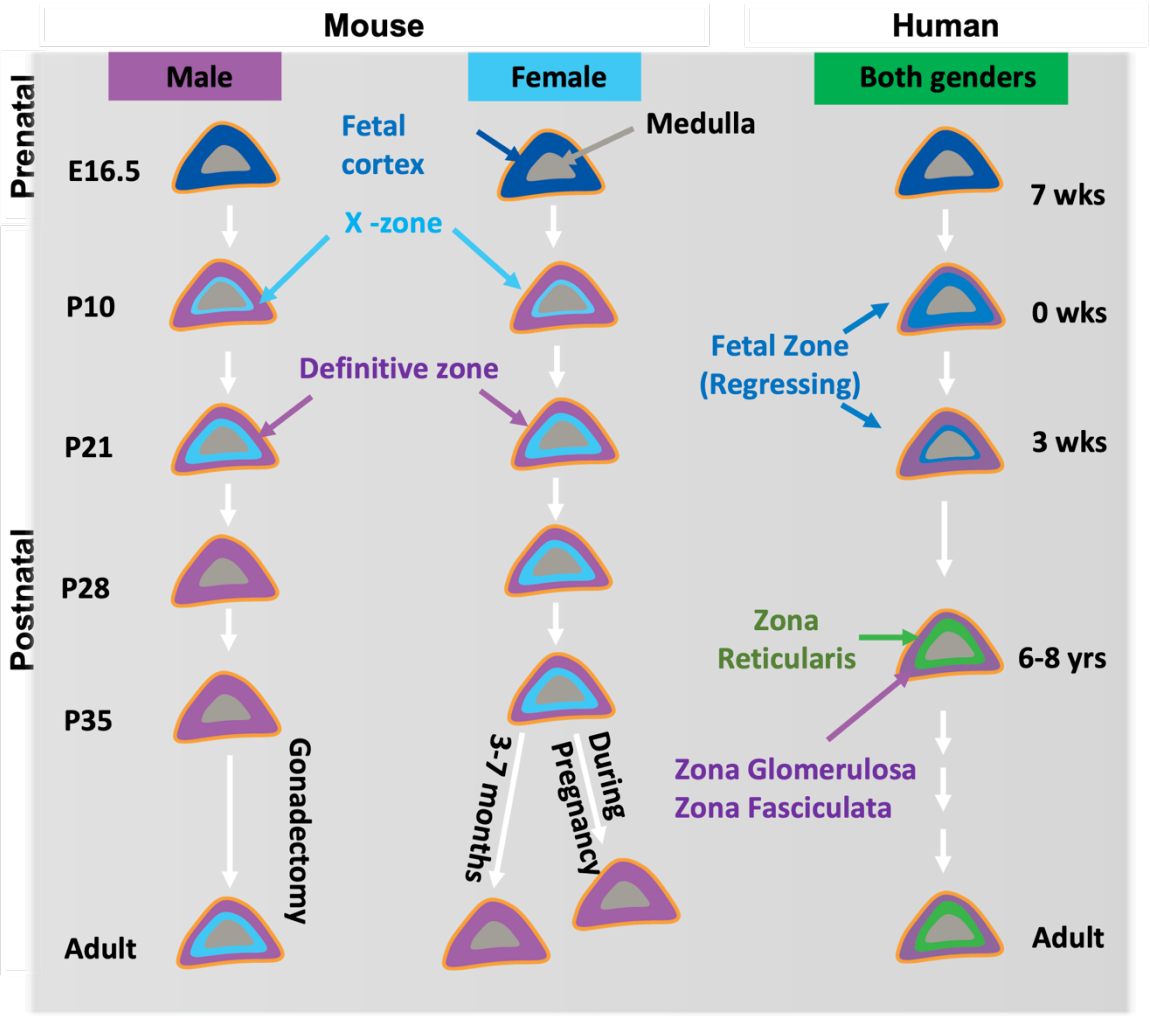

Figure 1.1 The formation and regression of human and murine adrenal inner cortex. In the embryonic stage, the enlarged fetal zone is progressively replaced by the outer definitive zone. After birth, the FZ undergoes regression through apoptosis, leading to the zonation of the DZ into the zona glomerulosa, zona fasciculata, and zona reticularis. In contrast to humans, mice have an additional transient cortical compartment called the X-zone, which is situated at the boundary between the adrenal cortex and the medulla. The regression of the X-zone exhibits sexual dimorphism. This figure was generated by Adobe Illustrator.

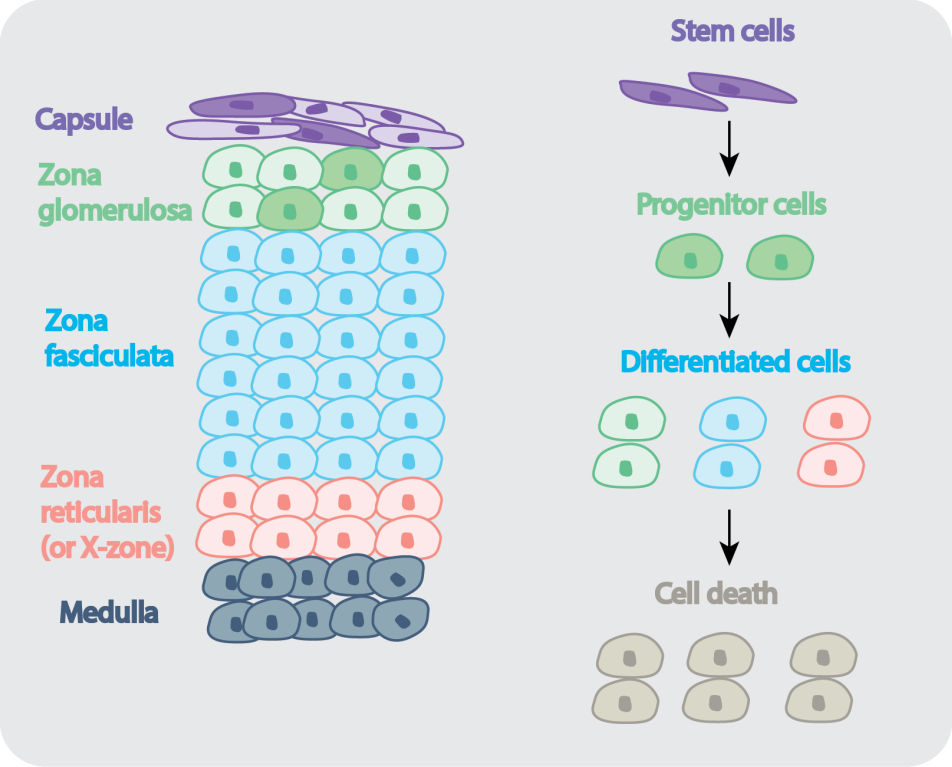

Figure 1.2 Homeostasis and renewal of the adult adrenal cortex. The adrenal gland consists of three parts: the capsule, the cortex, and the medulla. In humans the cortex has three subzones: zona glomerulosa, zona fasciculata and zona reticularis. In mice, X-zone is the third subzone instead of zona reticularis. Stem cells from capsule give rise to undifferentiated progenitor cells and differentiated cells of the adrenal cortex. Cells undergo apoptosis when they reach the cortical-medullary boundary. This figure was generated by Adobe Illustrator.

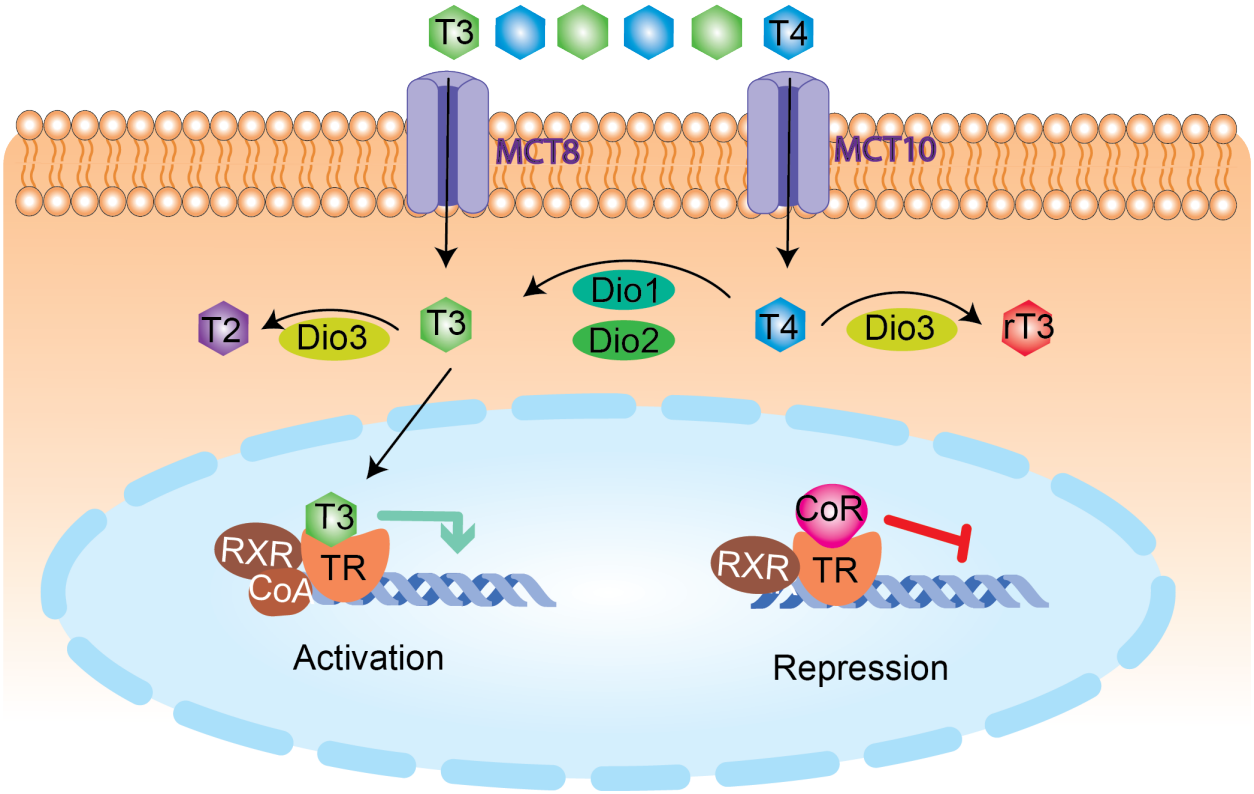

Figure 1.3 Schematic illustration of thyroid hormone (T3) action in the nucleus. T3 and T4 enter the cell via thyroid hormone transporters (MCT8 and MCT10). Thyroxine (T4) is converted into T3, the predominant form of TH, by deiodinases 1 and 2 (Dio1 and Dio2). Deiodinase 3 (Dio3) converts T4 to the inactive rT3. Deiodinase 3 (Dio3) also converts T3 to T2. In the nucleus, T3 binds to dimers containing thyroid hormone receptors (TRs). These dimers then bind to genomic thyroid hormone response elements (TREs) to activate gene transcription. In the absence of T3, a corepressor is bound to the RXR–TR heterodimer, then inhibiting gene expression. RXR, retinoic acid receptor; TR, thyroid hormone receptor; CoA, coactivator; CoR, corepressor. This figure was generated by Adobe Illustrator.

Chapter 2: Loss of *Ncor1* postpones cell regression of the adrenal inner cortex

2.1 Abstract

The nuclear receptor corepressor 1 (NCOR1) interacts with different nuclear proteins to modulate gene expression. It is ubiquitously expressed in many tissues and has been shown to control the transcriptional activity of several nuclear receptors. Many studies demonstrated that NCOR1 is an important player in regulating many pathways, including the thyroid hormone signaling pathway. In the adrenal gland, our previous studies demonstrated that thyroid hormone elicits its function through the thyroid hormone receptor in the inner cortex to regulate the cell fate of this cell population. Because NCOR1 is a key corepressor controlling the thyroid hormone signaling pathway and is the major nuclear corepressor expressed in the adrenal gland, we hypothesized that NCOR1 is involved in the cell fate regulation of the adrenal inner cortex. To further study this ubiquitously expressed corepressor and its function in the adrenal cortex, we conditionally deleted *Ncor1* in the adrenal cortex by crossing *Ncor1*-floxed (*Ncor1*$^{f/f}$) mice with steroidogenic factor 1 (SF1)-Cre mice. The *Ncor1*$^{f/f}$*;Sf1-Cre* mice (*Ncor1* cKO mice) were viable. Immunostaining showed a delayed regression of the inner cortex in male *Ncor1* cKO mice, whereas in female cKO mice, the inner cortex was thicker compared to their wild-type littermates. Interestingly, RNA sequencing analysis revealed that the top differentially expressed genes between WT and cKO mice were highly related to lipid metabolism. This result helps decipher the connection between the cell-protective effect and the lipid metabolic reprogramming, a hallmark of many developmental events and disease progression such as cancer aggressiveness.

2.2 **Introduction**

In mammals, the adrenal cortex is an endocrine organ that consists of three definitive zones: ZG, ZF, and ZR. In mice, a transient X-zone deriving from the fetal cortex takes place of the ZR zone in humans. During the early stages of development, adrenal cortex formation requires the expression of SF1. In the adult adrenal cortex, stem/progenitor cells from the capsule and the outer zone differentiate and migrate to replenish the adrenal cortex. As a consequence of the zonation, the aged cells in the ZR zone or X-zone undergoing cell death at the corticomedullary boundary are replaced by the younger cells that come from the outer layer. This aged cell population regresses at puberty in male mice and during the first pregnancy in female mice (146,147). Our previous reports showed that thyroid hormone treatment delayed the regression of the innermost cortex zone in prepubertal mice (148,149). However, the effect of the thyroid hormone signaling pathway on cell fate is not at present clear.

TRs act as nuclear hormone receptors (150) and are responsible for activation or repression of gene expression by recruiting coregulators (151,152), depending on the presence or absence of TH. Under normal conditions, T3, the active form of TH, binds to TR and recruits coactivators, leading to a conformational change of the multiprotein coactivator complex thereby activating gene transcription. In the absence of T3, TR could recruit nuclear corepressor 1 (NCOR1), which serves as a scaffold protein to form the corepressor complex and ultimately inhibit transcription. NCOR1 is broadly expressed in many tissues. Deletion of *Ncor1* in immune regulatory cells (Tregs) restrained Treg differentiation and maturation and further promoted inflammation (153). To test whether NCOR1 is a regulator in adrenocortical cells that alters the cell fate of the inner cortex,

we employed tissue-specific gene editing approaches. We crossed *Ncor1*$^{f/f}$ mice with *Sf1-Cre* mice to ablate NCOR1 in adrenocortical cells of the adrenal gland. This helps us to decipher whether T3- mediated delay of cell regression is a result of relief from NCOR1's repressive activity.

2.3 Materials and Methods

2.3.1 Animals *Ncor1*$^{flox/flox}$ mice, which possess *loxP* sites flanking exon 11 of the *Ncor1* gene, were purchased from the Jackson Laboratory. *Sf1-Cre* mice (gift from Dr. Keith L. Parker) express Cre recombinase in SF1-positive cells in the adrenal gland as well as pituitary gland, brain, and gonad. We generated mice with a conditional deletion of *Ncor1* in the adrenal gland by crossing *Ncor1*$^{flox/flox}$ mice with *Sf1-Cre* mice. There were three wild-type littermate controls: *Ncor1*$^{flox/flox}$, *Ncor1*$^{flox/+}$, *Ncor1*$^{flox/+}$*;Sf1Cre*. All mice were housed in a 12:12 h light-dark cycle (lights on at 6 am) with free access to regular rodent chow and water until sample collection. Mice were euthanized between 2 pm and 4 pm using carbon dioxide, followed by decapitation. Tissues were collected immediately and fixed in ice-cold 4% (v/v) paraformaldehyde (PFA) in 1X phosphate-buffered saline (PBS) or frozen by liquid nitrogen. All procedures followed the protocols approved by the Institutional Animal Care and Use Committee at Auburn University.

2.3.2 Immunostaining Tissues were fixed using 4% (vol/vol) buffered paraformaldehyde at 4°C overnight and rinsed three times in phosphate-buffered saline (PBS) at 4°C, 10 min each. Following graded ethanol (50%, 70%, 95%, 100%) dehydration, samples were embedded in paraffin. Embedded samples were sectioned at a thickness of 4 μm and were collected on uncharged slides. Then sections were deparafinized and rehydrated in graded ethanol (100%,

95%, 70%). Slides were heat-treated in the microwave in boiling 0.1 mM citric acid with pH 6.0 for 8 minutes. After preincubating with blocking buffer (2% normal donkey serum in PBS with 0.1% Tween 20), sections were incubated with primary antibodies (anti-3βHSD, Research resource identifiers (RRID): AB_2722746, 1:250; anti-Tyrosine Hydroxylase (TH), RRID: AB_628422, 1:1000; anti-CYP2F2, RRID: AB_10987684, 1:250; anti-20αHSD, RRID: AB_2832956, 1:500). For double staining, two primary antibodies were co-incubated at 4 °C overnight followed by incubation with secondary antibodies at room temperature for 1 hour. For CYP2F2 and 3βαHSD antibodies, sections were further incubated with avidin-biotin-peroxidase complex for 10 minutes and fluorescent tyramide was used to amplify the signal (TSA kit, PerkinElmer). Fluorescent images were obtained using an ECHO Revolve4 microscope. ImageJ was used to adjust the brightness, contrast, orientation, and channel merging. At least 3 sections that were 4 µm or farther apart were examined for each adrenal gland. For each group, at least 3 adrenal glands from 3 mice were analyzed.

2.3.3 RNA extraction and sequencing Total RNA was extracted from tissues using PicoPure RNA Isolation Kit (Thermo Fisher Scientific). The total RNA was sent to Novogene for further analysis.

2.3.4 Bioinformatic analysis of RNA-sequencing data The read count data was normalized using regularized logarithm (rlog) transformation in R/Bioconductor package DESeq2 (1.26.0). For differential expression analysis, the raw reads were adjusted for sequencing depth using size factors. The differential expression analysis was performed using a negative binomial generalized linear model implemented in DESeq2. To compare the effects of lack of *Ncor1* gene expression

in males and females, we performed 5 separate differential expression analyses using DESeq2. Gene expressions with a false discovery rate (FDR) of less than 0.05 were considered statistically significant. Gene Ontology (GO) analysis was performed by ShinyGO 0.77 online tools.

2.4 Results

2.4.1 Validation of *Ncor1* cKO in the adrenal gland.

The *loxP* sites of *Ncor1*$^{flox/flox}$ flank a region from exon 37 to exon 40. We used RNA-seq data to detect the expression levels from exons 37 to 40. The peaks of exons within the targeted region were dramatically reduced in the *Ncor1* cKO mice adrenal glands (Figure 2.1). This means we successfully removed the target exons of *Ncor1* from the mouse adrenal gland.

2.4.2 The inner cortex was the primary affected area in the *Ncor1* cKO mouse adrenal glands in both sexes.

Several proteins are specifically expressed in cells in the adrenal inner cortex, including 20αHSD (encoded by *Akr1c18*) and CYP2F2. The adrenal glands of male and female mice were harvested at various ages and stained with antibodies for 20αHSD and CYP2F2 to identify cells of the inner cortex. The expression pattern of 20αHSD in the adrenal glands showed differences between males and females. In wild-type male mice, the first occurrence of abundant 20αHSD-positive cells was observed at around P21. Starting from P35, cells that were positive for 20αHSD could not be detected (Figure 2.2A, 2.3A). In wild-type female mice, the expression of 20αHSD was consistently observed throughout different stages (from P14 to P56) (Figure 2.2B, 2.3B). Compared to wild-type mice, the thickness of 20αHSD-positive zone was 50% of the CYP2F2-

positive zone at P21. However, in *Ncor1* cKO female mice, the thickness of 20αHSD-positive zone was similar to the CYP2F2-positive zone (Figure 2.2B, 2.3B). CYP2F2 is a newly discovered marker in the inner cortex of the mouse adrenal gland. Cells that were positive for CYP2F2 were discovered in the inner cortex as early as P7 for both sexes. At P14, CYP2F2-positive cells formed a layer surrounding the medulla. In *Ncor1* cKO male mice, CYP2F2-positive cells remained in the adrenal inner cortex, while in wild-type mice, these cells had completely disappeared from this area at P35 (Figure 2.2A, 2.3A). In female mice, even at P56, a small number of cells that were positive for CYP2F2 were still detected in the inner cortex (Figure 2.2B, 2.3B). CYP2F2 in female *Ncor1* cKO mice also showed expression in a broader band of cells than in wild-type mice at P35 and P42. The adrenal cortical marker gene 3βHSD was also detected. The immunostaining result showed no difference in 3βHSD expression between WT and *Ncor1* cKO mice in both sexes (Figure 2.4). Comparison of mRNA expression levels of *Akr1c18* and *Cyp2f2* at P42 in WT and *Ncor1* cKO female mice by RNA-seq confirmed higher *Cyp2f2* expression in female *Ncor1* cKO mice (Figure 2.5). The comparison also suggested higher *Akr1c18* RNA expression in female *Ncor1* cKO mice than in WT, but the difference was not statistically significant.

2.4.3 Difference in gene expression profiles between WT and cKO mice.

To further characterize the *Ncor1* effects on the adrenal gland, we used RNA-Seq to detect differentially regulated transcriptome at P42. Within male groups, 24 differentially expressed genes (DEGs) were identified between WT and *Ncor1* KO mice, and 56 DEGs were identified within female groups (Figure 2.6). The relative expression levels of the 76 DEGs are shown in a clustered heatmap (Figure 2.7). Interestingly, gene ontology (GO) enrichment analysis indicated

DEGs were mainly enriched in cholesterol and lipid metabolism. The three terms of the DEGs with greatest fold enrichment were sterol biosynthetic process, secondary alcohol biosynthetic process, and cholesterol biosynthetic process (Figure 2.8). These synthesis pathways shared similar genes including *Dhcr24*, *Cyp51*, *Lpcat3*, *Tm7sf2*, *Scp2*, *Msmo1*, *Sc5d, and Idi1.*

2.5 Discussion

The adrenal cortex, which typically functions as a self-renewing endocrine organ, adjusts in response to hormonal signals for steroid biosynthesis (13). The inner cortex cells of the adrenal gland are typically considered aging cells that undergo apoptosis (154). The source of the X-zone cells and the physiological processes controlling their formation and expansion remains unknown. It is thought that the X-zone is analogous to the ZR in humans, which is the site of biosynthesis of androgen precursors such as dehydroepiandrosterone (DHEA) and androstenedione from cholesterol. Our data demonstrated that conditional knockout of *Ncor1* in the definitive cortex of mouse played a crucial role in maintaining the homeostasis of mouse adrenal inner cortex cells, an area partially overlapping with the X-zone. This likely contributes to the delayed regression of the mouse X-zone. This was evidenced by elevated expression levels of two adrenal inner cortex marker genes, 20αHSD and CYP2F2. The role of ovary 20αHSD, which transforms progesterone into a biologically inactive derivative, is crucial in achieving the brief estrous cycle in rats (155,156). The expression of adrenal 20αHSD is limited to the X-zone in mice (146). It has been shown that 20αHSD has the ability to reduce the enzymatic activity of 11-deoxycorticosterone (DOC), which is an intermediate in the biosynthesis of corticosterone and aldosterone, but the physiological function for adrenal steroidogenesis of 20αHSD remains unclear (146). CYP2F2 is highly abundant in the respiratory system and liver (157). In mice, CYP2F2-mediated metabolism

was accountable for both the short-term and long-term toxicity and development of tumors caused by styrene (158,159). Our recent study showed that CYP2F2 was also expressed in the inner cortex of adrenal gland (149). Although the absence of CYP2F2 had no impact on the formation and regression of the X-zone, it could still serve as a marker gene for the aging of adrenocortical cells (149). Notably, we observed a delayed regression of CYP2F2-positive cells in *Ncor1* cKO mice.

Eliminating *Ncor1* is predicted to have similar effects to T3 treatment, considering that *Ncor1* plays a repressive role in the thyroid hormone signaling pathway. Consistent with our previous findings that T3 treatment enlarged the area of the adrenal inner cortex zone including the CYP2F2-positive zone (149), *Ncor1* cKO mice also exhibited expansion of this area. This observation suggests functional changing of *Ncor1*-deficient adrenocortical cells and indicates that *Ncor1* controls the cell fate of CYP2F2-positive cells. However, the precise process through which *Ncor1* regulates the expression of CYP2F2 requires additional investigation. Our transcriptome data revealed that many DEGs with increased expression upon loss of *Ncor1* are linked to cholesterol synthesis of. Key enzymes such as *Dhcr24*, *Cyp51*, *Lpcat3*, *Tm7sf2*, *Scp2*, *Msmo1*, *Sc5d and Idi1* were upregulated in the absence of *Ncor1*. This observation aligns with our previous research that showed numerous key enzymes involved in cholesterol synthesis were upregulated as a result of T3 treatment (149). It remains to be determined whether the elevated expression of these key enzymes in *Ncor1* cKO mice contributes to the T3-induced cholesterol synthesis.

Taken together, our data demonstrate that disruption of *Ncor1* function in the adrenal gland postpones cell regression of the inner cortex and leads to altered cholesterol metabolism. In addition to our previous discoveries, our results suggest that *Ncor1* negatively regulates the expansion of the inner cortex and the alteration of cholesterol metabolism induced by T3.

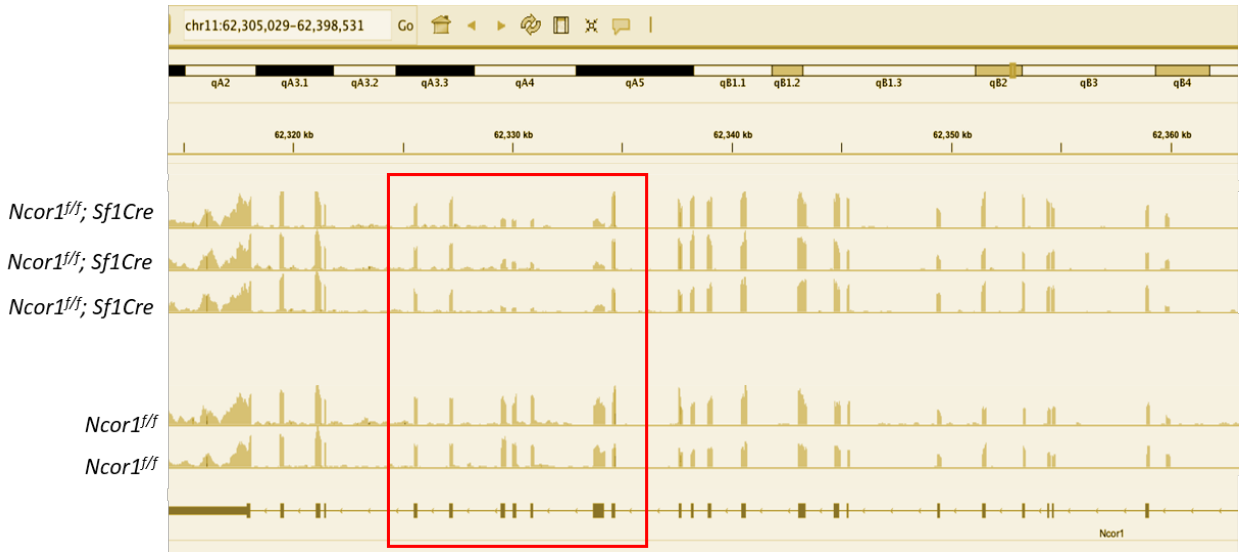

Figure 2.1 Integrative genomics viewer (IGV) visualization of RNA-seq reads from mapping results of RNA from adrenal glands of 3 cKO and 2 control mice at P42 for chromosome 11. In 3 cKO mice, the mapping results revealed deletion of exons 37, 38, 39, and 40 of the *Ncor1* gene. cKO, *Ncor1* conditional knockout mice.

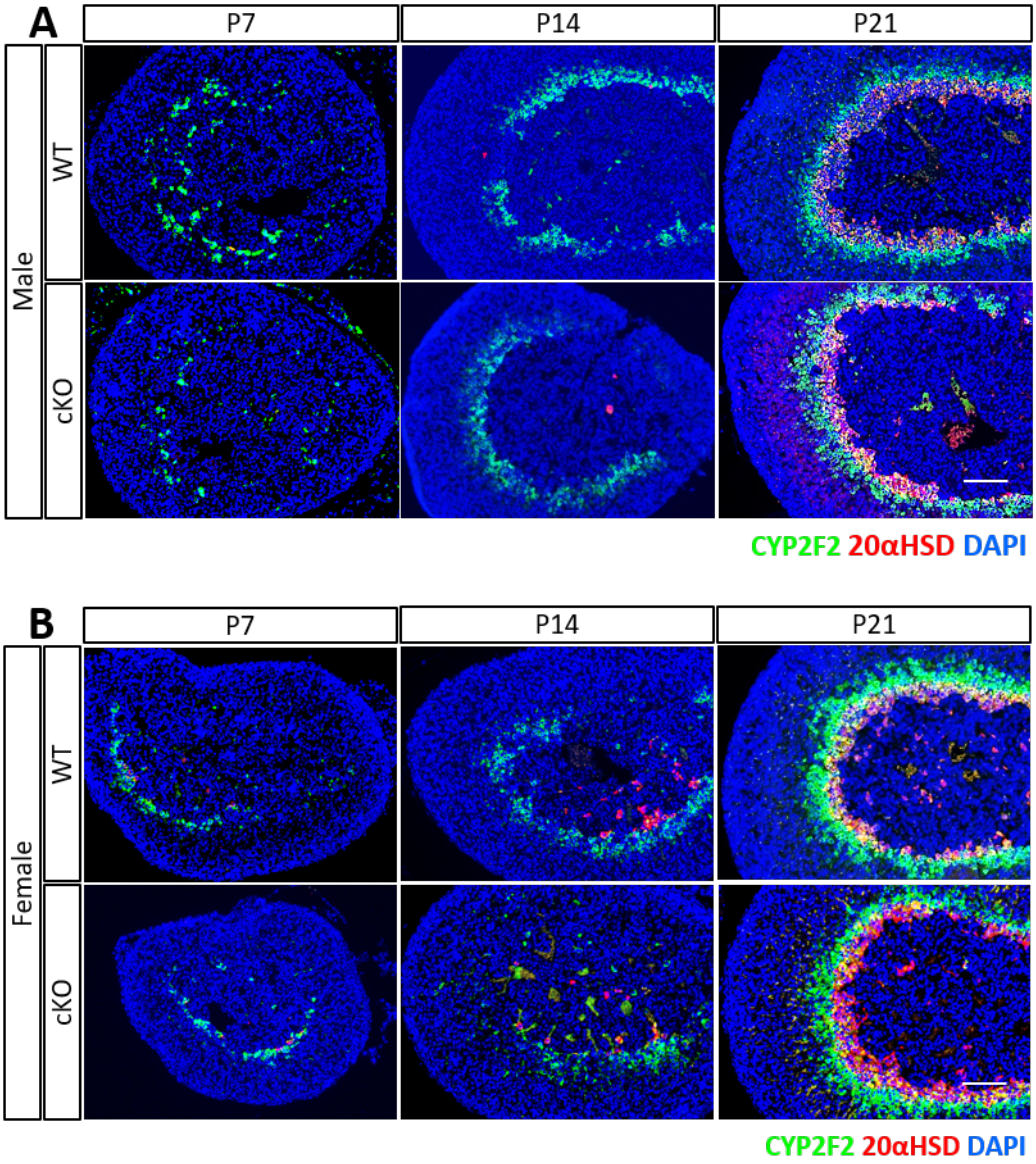

Figure 2.2 Immunostaining of CYP2F2 and AKR1C18 in the adrenal gland before weaning. Adrenal glands before weaning, from P7, P14, and P21 were immunostained with antibodies for CYP2F2 (green) and 20αHSD (red). DAPI (blue, cell nuclei). WT, wild-type mice. cKO*, Ncor1* conditional knockout mice. Scale bars, 100 µm.

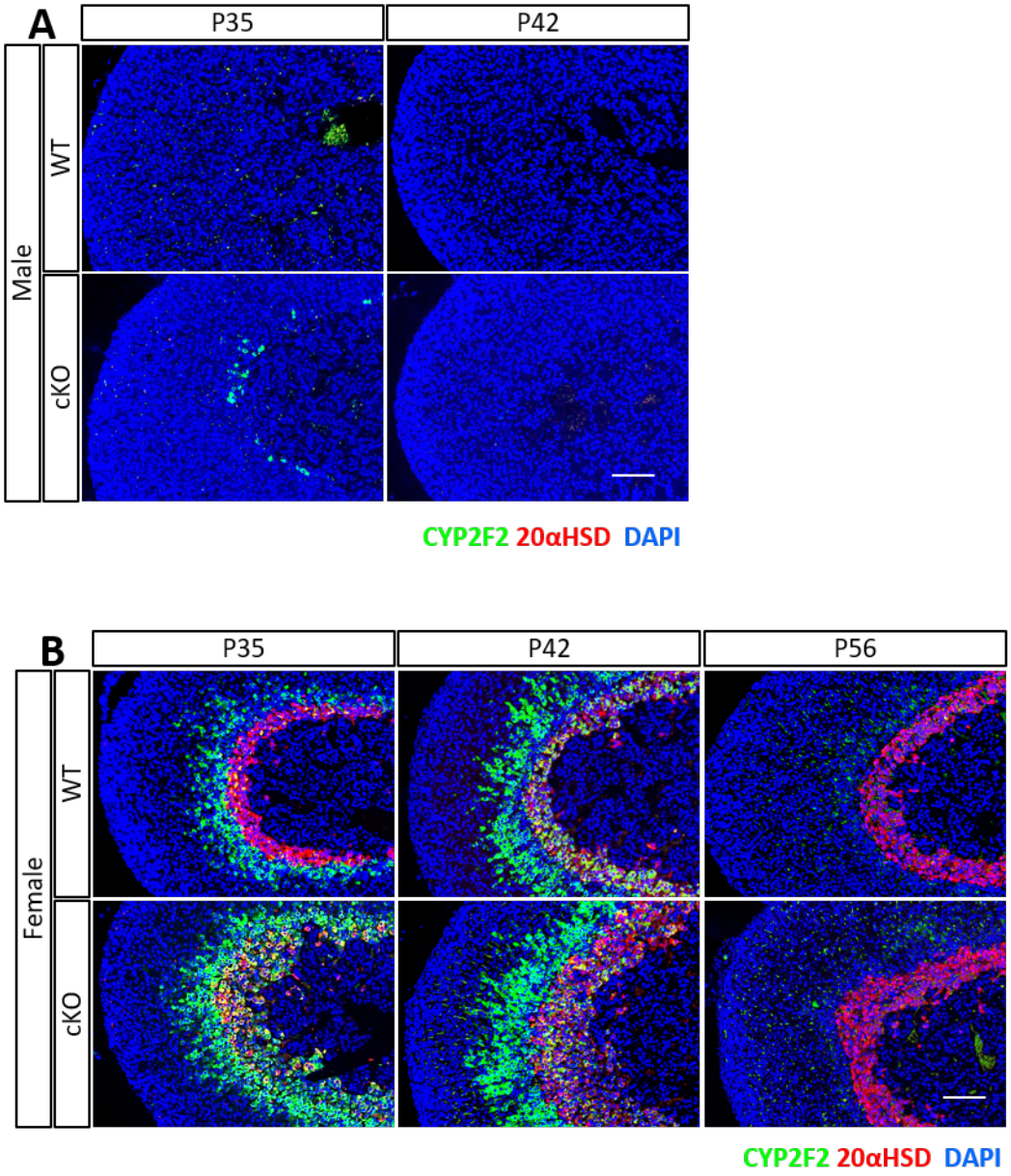

Figure 2.3 Immunostaining of CYP2F2 and AKR1C18 in the adrenal gland after weaning. Adrenal glands post-weaning, from P35, P42, and P56 were immunostained with antibodies for CYP2F2 (green) and 20αHSD (red). DAPI (blue, cell nuclei). WT, wild-type mice. cKO, *Ncor1* conditional knockout mice. Scale bars, 100 µm.

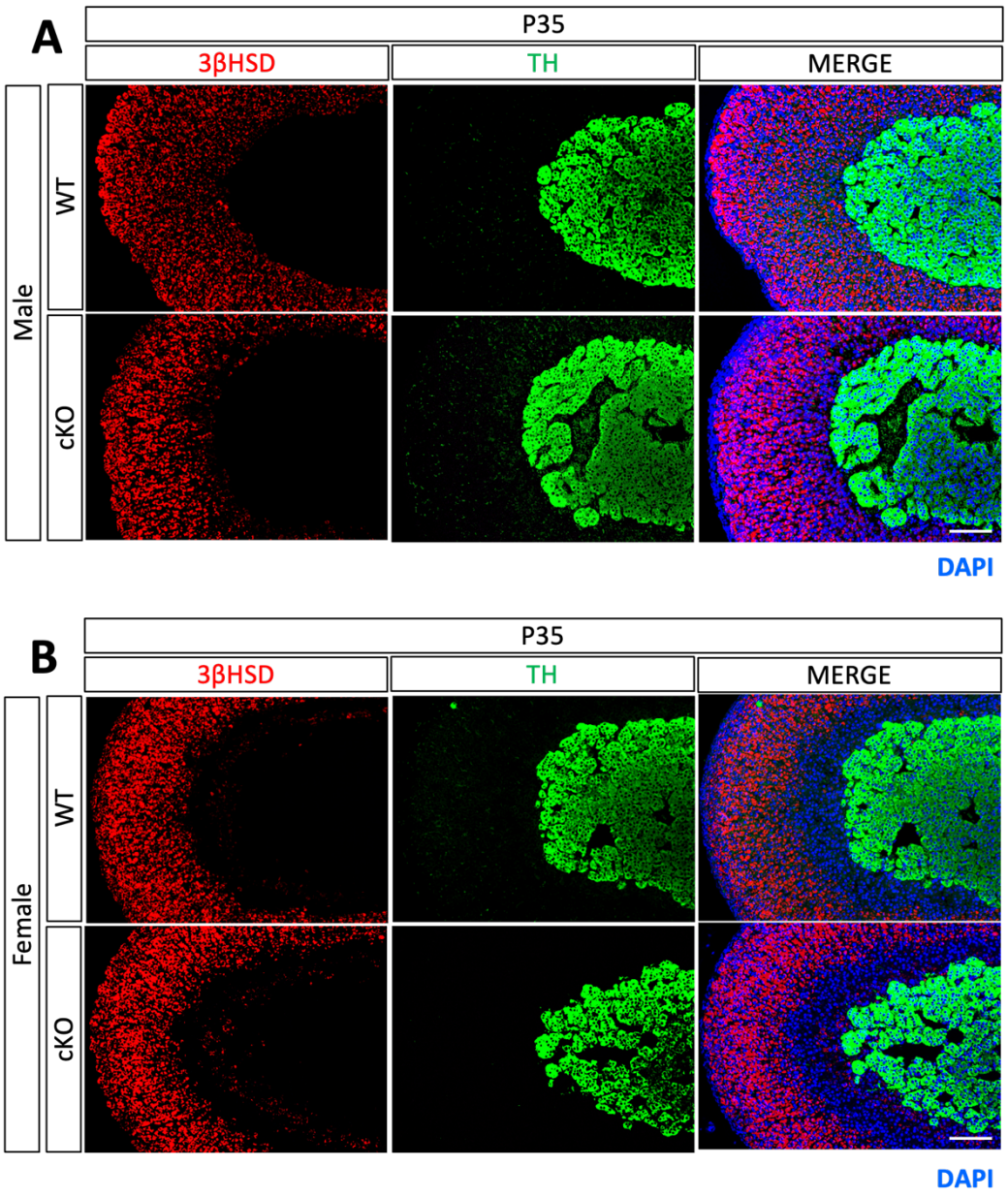

Figure 2.4 Immunostaining of 3βHSD and TH in euthyroid P35 mice. Double immunostaining using antibody against 3βHSD and TH in P35 mice. DAPI (blue, cell nuclei). WT, wild-type mice. cKO, *Ncor1* conditional knockout mice. Scale bars, 100 µm.

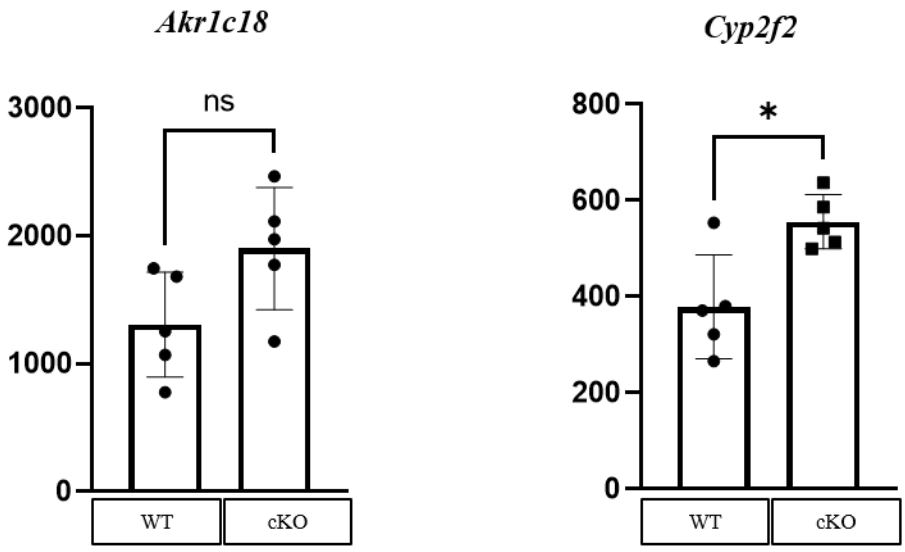

Figure 2.5 The FPKM levels of *Akr1c18* and *Cyp2f2* in cKO and WT at P42 female mice. Data are expressed as mean ± SEM (n=5). WT: wild-type mice. cKO: *Ncor1* conditional knockout mice. ns, no significant difference. * represents $P < 0.05$.

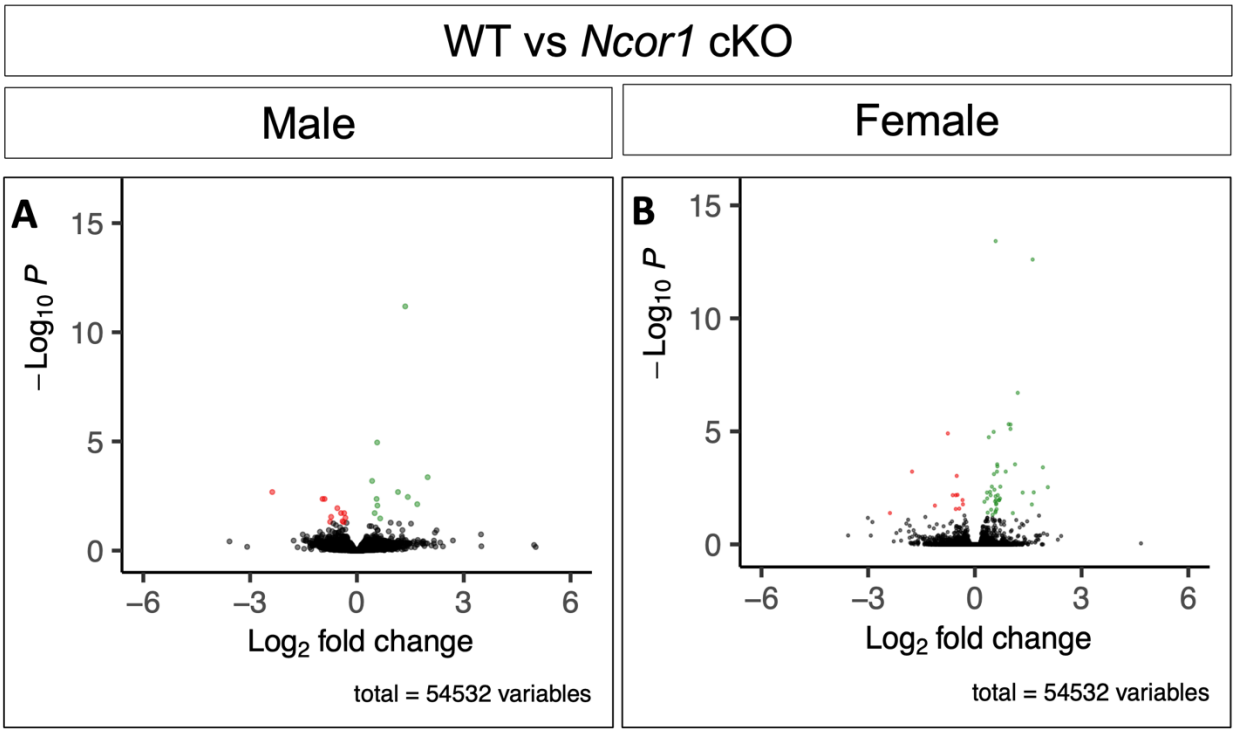

Figure 2.6 Volcano plot of differentially expressed genes (DEGs). A. Volcano plot showing 24 DEGs (11 are down-regulated genes, 13 are up-regulated genes) between WT and KO male mice. B. Volcano plot showing 56 DEGs (13 are down-regulated genes, 43 are up-regulated genes) between WT and KO female mice. Red dots represent down-regulated genes. Green dots represent up-regulated genes. $P < 0.05$. WT: wild-type mice. cKO: *Ncor1* conditional knockout mice.

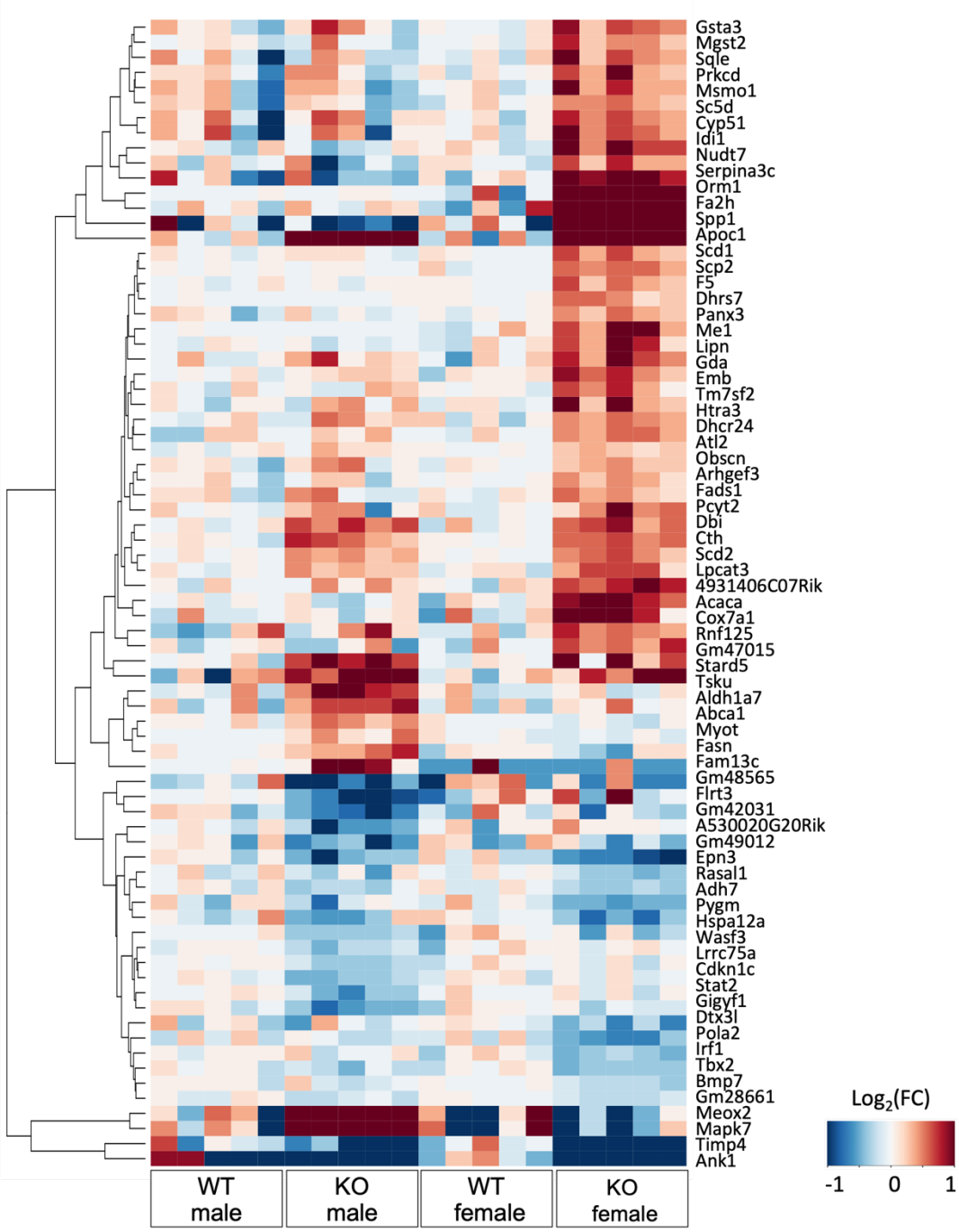

Figure 2.7 The clustered heatmap of the differentially expressed genes. The fold change used for heatmaps was calculated based on FPKM+0.001. WT: wild-type mice. cKO: *Ncor1* conditional knockout mice.

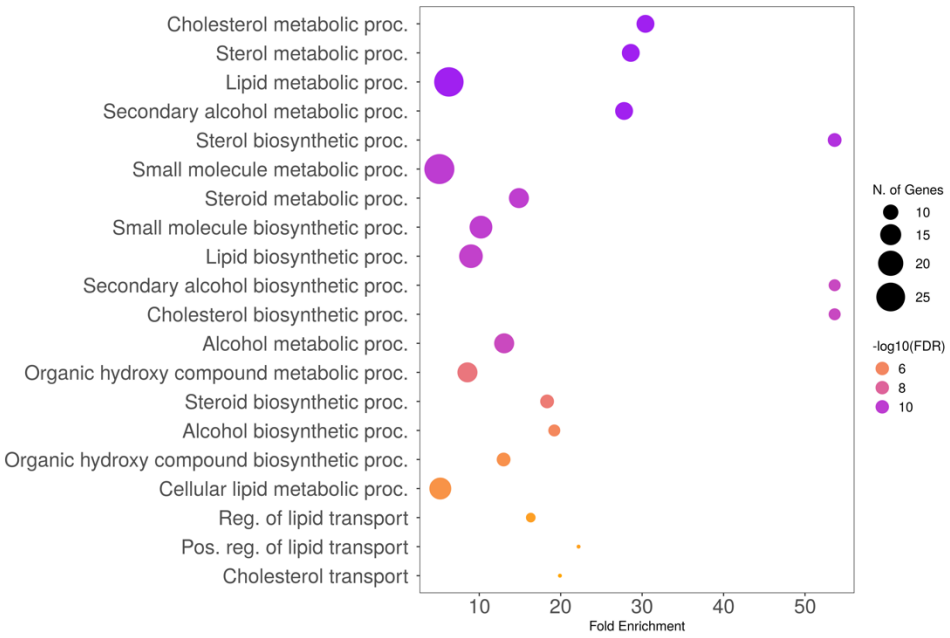

Figure 2.8 Gene Ontology (GO) analysis of the DEGs. The 13 most significant terms are provided on the left of the plot. FDR p-value cutoff = 0.05.

Chapter 3: *Dhcr24*, a key enzyme involved in *de novo* cholesterol synthesis in the adrenal inner cortex

3.1 Abstract

Steroid hormones are synthesized through enzymatic reactions using cholesterol as the substrate. In steroidogenic cells, the required cholesterol for steroidogenesis can be obtained from blood circulation or synthesized *de novo* from acetate. One of the key enzymes that controls cholesterol synthesis is 24-dehydrocholesterol reductase (encoded by DHCR24). In humans and rats, DHCR24 is highly expressed in the adrenal gland, especially in the zona fasciculata. We recently reported that DHCR24 is expressed in the mouse adrenal gland's inner cortex. We also recently found that thyroid hormone treatment significantly upregulates the expression of *Dhcr24* in the mouse adrenal gland. To study how DHCR24 is involved in this T3-induced lipid accumulation, we generated a conditional deletion of *Dhcr24* in the adrenal gland. We found that the T3-induced lipid accumulation in the inner cortex was partially decreased in *Dhcr24*;*Sf1-Cre* conditional knockout mice. This finding indicates *Dhcr24* is a key gene involved in T3-induced lipid accumulation.

*This chapter is a revised version of the manuscript published in International Journal of Molecular Sciences (Zheng HS, Kang Y, Lyu Q, Junghans K, Cleary C, Reid O, Cauthen G, Laprocina K, Huang CC. DHCR24, a Key Enzyme of Cholesterol Synthesis, Serves as a Marker Gene of the Mouse Adrenal Gland Inner Cortex. International Journal of Molecular Sciences. 2023 Jan;24(2):933).

3.2 Introduction

The mitochondrial cytochrome P450 cholesterol side-chain cleavage enzyme (P450scc, encoded by *CYP11A1*) controls the first step of the steroidogenesis pathway, which converts cholesterol into pregnanolone (160). Steroidogenic cells can obtain the required cholesterol for steroidogenesis by taking up circulating cholesterol via receptors on the cell membrane, using the cholesterol stored in lipid droplets in the cytoplasm, or synthesizing cholesterol *de novo* from acetate (161). Similar to many other steroid-producing cells, adrenocortical cells can synthesize cholesterol locally (162). In human adrenal glands, *de novo* synthesized cholesterol contributes to 20% of cortisol production (163). One of the key enzymes that controls cholesterol synthesis is DHCR24, which is highly expressed in the adrenal gland in both humans (164) and rats (165), especially in the ZF. DHCR24 is also named Selective Alzheimer disease indicator 1 (Seladin-1) because it was first identified using neuronal cells from Alzheimer's disease (AD) patients (166). In humans, the adrenal gland is the tissue with the highest expression of DHCR24 (166). The expression of DHCR24 has been reported to be altered in human adrenal adenomas and carcinomas (167,168). Patients carrying mutations in DHCR24 show the accumulation of cholesterol precursor, desmosterol, resulting in desmosterolosis, which is a disorder characterized by multiple congenital anomalies, neurological complications, and developmental delays (169). We recently reported that DHCR24 is expressed in the mouse adrenal gland inner cortex and is responsive to T3 treatment (149).

Thyroid hormones are essential regulators of growth, development, and metabolism across all tissues, and alterations in thyroid hormone levels can impact various organs and systems. There

is a significant amount of evidence demonstrating that thyroid hormones influence steroidogenesis during testicular development (79,170-172). The way T3 affects steroidogenesis is through its coordination of the levels of steroidogenic acute regulatory (StAR) protein and *Star* mRNA, leading to an increase in steroid production in mouse Leydig cells (172,173). The adrenal gland, much like the testis, is also involved in steroidogenesis, however, the influence of T3 on adrenal gland function, including steroidogenesis, is yet to be fully understood.

Moreover, as noted in our previous study, the expression level of DHCR24 was increased in the adrenal gland of mice under T3 treatment. A recent study utilized a mouse model with liver-specific deletion of *Dhcr24* to show an increase in the level of plasma desmosterol, which is the immediate precursor of cholesterol in the Bloch pathway of cholesterol synthesis (174). This finding suggests that DHCR24 is involved in cholesterol synthesis and metabolism in mice. To characterize the expression of the zonal-restricted marker gene, DHCR24, in the mouse adrenal gland inner cortex, immunostaining was used to determine the time-course of expression of DHCR24. A conditional knockout (cKO) mouse model was used to define the potential role of DHCR24 in the development and function of the adrenal gland under both normal conditions and after T3 treatment.

3.3 Materials and Methods

3.3.1 Animals and treatment C57BL/6J mice were purchased from the Jackson Lab. The Dhcr24tm1a(EUCOMM)Wtsi (C57BL/6 background) mutant mice (*Dhcr24*^{lacz}) were obtained from The European Conditional Mouse Mutagenesis Program (EUCOMM). To generate the conditional

knockout mice, the *Dhcr24*^{lacz} mice were first crossed with the Flp deleter strain (C57BL/6 background, #7089 from Taconic) to generate the 'conditional ready' strain (*Dhcr24*^{flox}). Then, the mice were crossed with C57BL/6J mice to remove the Flp. The *Dhcr24*$^{flox/flox}$ mice were then crossed with the *SF1-Cre* mice (gift from Dr. Keith Parker, has been back-crossed to C57BL/6 for more than 10 generations) to obtain the cKO mice (*Dhcr24*$^{flox/flox;}$ *Sf1-Cre*). All mice were housed in a 12:12 h light-dark cycle (lights on at 6 am) with free access to regular rodent chow and water until sample collection. Mice were euthanized between 2 pm and 4 pm using carbon dioxide, followed by decapitation. Tissues were collected immediately and fixed in ice-cold 4% (v/v%) paraformaldehyde (PFA) in 1X phosphate-buffered saline (PBS) or frozen by liquid nitrogen. All procedures followed the protocols approved by the Institutional Animal Care and Use Committee at Auburn University. For the T3 treatment, mice were provided with drinking water containing 1 µg/l of T3 (Sigma-Aldrich, MO, USA) for a continuous 10 days, from P25 to P35.

3.3.2 Immunohistochemistry Tissues were fixed at 4 °C overnight and processed according to standard immunostaining procedures (149). In short, deparaffinized sections were incubated with primary antibodies (anti-DHCR24, #sc-398938, RRID: AB_2832944, 1:100; anti-DHCR24, #ab137845, RRID: AB_2923496, 1:100; anti-Tyrosine Hydroxylase (TH), RRID: AB_628422, 1:500; anti-20αHSD, RRID: AB_2832956, 1:500; anti-CYP2F2, #sc-374540, RRID: AB_10987684, 1:250) followed by appropriate fluorescein-conjugated secondary antibodies. DHCR24 was detected by a biotinylated secondary antibody followed by a fluorescent tyramide (175). Fluorescent images were obtained using a Revolve 4 microscope (ECHO). ImageJ (http://rsb.info.nih.gov/ij/) was used for adjusting the brightness and contrast.

3.3.3 Oil Red O Staining For cryosection preparation, tissues were fixed using 4% (vol/vol) buffered paraformaldehyde at 4°C overnight and rinsed three times in phosphate-buffered saline (PBS) at 4°C, 10 min each. Samples were infiltrated with 30% sucrose overnight at 4°C on a shaker. After tissues sunk to the bottom of the vial (usually more than 24 hours), tissues were put into Tissue-Tek O.C.T compound and stored at -80°C. Sections (8 µm) were mounted onto positive charged slides and rinsed in PBS. Slides were incubated in Oil Red O solution (Electron Microscopy Sciences, PA, USA) for 5 min. After washing with ddH_2O, slides were covered with an aqueous mounting medium. For each group, at least 3 adrenal glands from 3 mice were analyzed.

3.3.4 Measurement of plasma hormone levels Mice were killed by decapitation. Plasma was collected in EDTA-coated tubes and stored at −80°C until use. Corticosterone was quantitated with Corticosterone Enzyme Immunoassay Kit (Arbor Assays Inc, MI, USA) according to the manufacturer's instructions. 5 µl of plasma were used for the corticosterone test of each mouse. ACTH was quantitated with the mouse ACTH ELISA kit (NBP3-14759, Novus Biologicals, Centennial, CO, USA) according to the manufacturer's instructions. 25 µl of plasma were used for the ACTH test of each mouse.

3.3.5 Statistical Analysis The two-tailed unpaired Student's t-test function in GraphPad Prism 9.0 software (GraphPad, San Diego, CA, USA) was used to calculate P values. P values less than 0.05 were considered statistically significant.

3.4 Results

3.4.1 Cellular expression of DHCR24 in mouse adrenal glands.

Under the euthyroid condition, the DHCR24-positive cells were mainly in the 3βHSD low-expressing inner cortex (Figure 3.1A), which is also the X-zone in mouse adrenal glands (146). To obtain the spatial and temporal expression profile of DHCR24 in mouse adrenal glands, adrenal glands of both male and female mice were analyzed by immunostaining (Figure 3.1B). The results showed that DHCR24 was expressed in postnatal adrenal glands with a sexually dimorphic pattern. The sexually dimorphic cellular expression and the expression timeline were similar to those of the X-zone marker gene 20αHSD (148,149). At P14, immunostaining results showed that a few DHCR24-positive cells were found at the cortical–medullary boundary in both sexes. A clear DHCR24-positive zone existed in the inner-cortical region at P21. At P28 and P35, the DHCR24-positive zone remained in the adrenal glands in female mice. However, in male mice, only a few DHCR24-positive cells were found at P28; immunostaining did not detect any DHCR24-positive cells in males at P35 (Figure 3.1B). Unlike the 20αHSD-positive zone that regresses soon during the first pregnancy (176), immunostaining showed that the DHCR24-positive zone remained present in parous females (Figure 3.1C), suggesting that pregnancy does not lead to loss of the DHCR24-positive zone in the adrenal glands of female mice.

3.4.2 Deletion of *Dhcr24* in steroidogenic cells did not affect the outer zone of the adrenal gland.

To understand the role of DHCR24 in the adrenal gland, we used *Sf1-Cre* to remove *Dhcr24* in steroidogenic cells. Immunostaining showed that even after thyroid hormone treatment, the adrenal glands in cKO mice remained negative for DHCR24 immunostaining signals (Figure 3.2A),

confirming the deletion of DHCR24 in adrenal glands of cKO mice. To determine if the structure of the concentric cortical layers was affected in cKO adrenal glands, we performed immunostaining to label the outer layers and medulla of the adrenal gland. The lack of DHCR24 did not lead to any significant change in adrenal cortex zonation at P35 (Figure 3.2B).

3.4.3 The role of *Dhcr24* in T3-mediated expansion of the inner cortex zone.

Our previous study showed that T3 treatment expanded the innermost zone of the adrenal gland; both the number of 20αHSD-positive cells and the number of newly-identified-inner-cortex-marker-CYP2F2-positive cells were expanded (149). Under the euthyroid condition, the number of CYP2F2-positive cells declined slightly in *Dhcr24* cKO mice compared with the wild-type group in females at P35 (Figure 3.3B). In males, the inner cortex had regressed under normal conditions (Figure 3.3B). When mice were given T3 treatment (Figure 3.3A) for 10 days, immunofluorescence showed the expansion of CYP2F2-positive and 20αHSD-positive zones in mice (Figure 3.3C), suggesting that T3 can postpone the regression of the inner cortex. The deletion of *Dhcr24* partially blocked the inner cortex expansion by reducing the number of CYP2F2-positive cells (Figure 3.3C).

3.4.4 The effect of T3 on the outer cortex zone.

To determine the impact of T3 treatment on the outer cortex, we conducted immunostaining to identify the outer layers of the adrenal gland. In WT mice, with T3 treatment, the DHCR24-positive area expanded and partially overlapped with the 3βHSD-positive region (Figure 3.4), which is a crucial component in the biosynthetic process for the production of potent adrenal

steroid hormones. This implies that the outer cortex is not the primary region that responds to T3 treatment.

3.4.5 The deletion of *Dhcr24* partially blocked T3-mediated lipid accumulation in the inner cortex.

Phenotypic analyses using Oil Red O were performed and showed that under the euthyroid condition, the oil accumulation was not affected in adrenal glands at the histological level in cKO mice (Figure 3.5A). We reported that genes differentially expressed in response to T3 treatment were enriched in the cholesterol synthesis pathway (149). Oil Red O staining showed that lipids mainly accumulated in the inner cortex-T3-responsive zone (Figure 3.5B). The inner cortex from *Dhcr24* cKO male and female mice displayed a reduction in lipid accumulation following T3 treatment, compared to the wild-type mice (Figure 3.5B). This indicates that the deletion of *Dhcr24* partially inhibits T3-mediated lipid accumulation.

3.4.6 The effect of *Dhcr24* on blood corticosterone and ACTH levels with T3 treatment.

Because DHCR24 is the key enzyme that controls cholesterol synthesis, it is possible that the *de novo* synthesis of cholesterol is affected in adrenocortical cells in *Dhcr24* cKO mice, thus altering steroidogenesis. Under the euthyroid condition, phenotypic analyses using hormone assays showed that the corticosterone and ACTH levels in blood circulation and the ACTH/corticosterone ratios were not significantly changed in either sex of the cKO mice (Figure 3.6A, B, C). It is important to note that these mice were euthanized by carbon dioxide inhalation, which is considered to be a stressor that leads to elevated corticosterone secretion (177). The

comparable stress-stimulated corticosterone and ACTH levels in cKO and WT mice suggest that the lack of *de-novo*-synthesized cholesterol does not significantly affect steroidogenesis under certain stress levels, such as the stress caused by CO_2 euthanasia. X-zone is not considered a primary contributor to the steroidogenic function. Thus, the level of corticosterone was not changed in our experiment. In *Dhcr24* cKO male mice, the corticosterone level in T3 treatment group was found to be higher compared to the level in euthyroid group (Figure 3.6D). Additionally, in WT female mice, the corticosterone level during T3 treatment was higher compared to the level during saline treatment (Figure 3.6E). This finding is similar to the Oil Red O result. Altogether, These results indicate that T3-induced *de novo* synthesized cholesterol in the inner cortex may also contribute to steroidogenesis.

3.5 Discussion

The adrenal gland maintains body homeostasis and responding to stress by producing hormones and neurotransmitters. The outer cortex of the gland specializes in producing steroid hormones which are crucial for physiological processes including metabolism, blood pressure, and immunity. Although there is information regarding the origin (27,178,179) and developmental timeline of the inner cortex (X-zone) (146,148,149,176,178,180), more research is needed to uncover the physiological role of cells in the inner zone of the adrenal gland. Here, we demonstrate that DHCR24 is a key factor in the response to T3-induced reprogramming and functional changes in the inner cortex. It accomplishes this process by controlling the production of *de novo* cholesterol synthesis and preventing the regression to a state of cellular aging. This may provide new insight into the function of the inner cortex, which has the capability to produce steroids.

The mice X-zone cells are characterized as a distinct cluster of eosinophilic cells in the inner cortex that is located adjacent to the medulla. Previous observations provided strong evidence for 20αHSD being a dependable marker of the X-zone in mice. Despite the absence of 20αHSD in mice, the growth rate of the X-zone remained unchanged (146). Our data demonstrated that DHCR24 was specifically expressed in the inner cortex (Figure 3.1), with temporal and spatial expression patterns that were very similar to those of the X-zone marker gene 20αHSD, which has a sexually dimorphic expression pattern. The major difference between DHCR24 and 20αHSD is that there are DHCR24-positive cells in the adrenal glands of parous female mice (Figure 3.1), but there is no X-zone in these mice because it regresses during pregnancy (176).

Thyroid hormones significantly influence various metabolic processes related to energy balance under different nutritional circumstances (181). It is well-established that thyroid hormones directly impact cholesterol and fatty acid synthesis and metabolism (182,183). It has been reported that T3 has a direct impact on the numbers of luteinizing hormone (LH) receptors in Leydig cells and the mRNA levels of steroidogenic enzymes, resulting in an increased secretion of progesterone, testosterone, and estradiol both in mouse Leydig cell lines and in primary Leydig cells (170,184).

Different sources or supply routes of cholesterol ensure the high demand for cholesterol for steroidogenesis is met in steroid hormone-producing cells. Other than taking up high- and low-density lipoproteins from the blood circulation and deriving cholesterol from cholesterol esters stored as lipid droplets, synthesizing cholesterol *de novo* in the endoplasmic reticulum is another

way steroidogenic cells obtain cholesterol (161,185). Even though the removal of DHCR24 in steroidogenic cells did not cause significant histological and functional changes in the adrenal gland under euthyroid conditions, the mouse adrenal gland displayed different responses between the *Dhcr24* cKO and wild-type groups when subjected to thyroid hormone treatment. The restricted spatial expression of DHCR24 in the inner cortex of the mouse adrenal gland, combined with the observation of elevated corticosterone levels in WT female mice, implies that *de novo* cholesterol synthesis might serve as a source of cholesterol for steroid hormone production in the mouse adrenal gland when treated with T3. An initial hypothesis also suggested that the X-zone in mice could potentially serve as a backup tissue to meet the heightened need for glucocorticoids (186).

In addition to its involvement in the mevalonate pathway that controls cholesterol synthesis, DHCR24 has also been linked to many cellular functions and diseases. DHCR24 is also named 'selective Alzheimer's disease indicator-1' or Seladin-1 because of its connection with AD (166). Patients with AD suffer from massive neuronal death due to apoptosis in both neurons and glial cells [28]. In the brain, DHCR24 is less abundant in the areas affected by AD (166,187). Over-expression of DHCR24 in neurons prevents β-amyloid accumulation and oxidative stress. This neuroprotective function that prevents neuronal loss has been seen both in vitro and *in vivo* (188-192). Additionally, it has been demonstrated that DHCR24 has a protective effect against apoptosis by inhibiting caspase-3 activity (193,194). Indeed, in our study *Dhcr24* ablation is associated with a strong reduction of T3-induced inner cortex expansion, characterized by decreased expression of 20αHSD-positive and CYP2F2-positive cells (Figure 3.3) in the context of

unchanged 3βHSD expression level. This is consistent with our previous study that T3 did not noticeably alter the differentiation state of outer cortical cells, but it did affect inner cortex cells (148,149). We thus reasoned that *Dhcr24* acts as a cell protective effect in response to T3 treatment in the inner cortex of the adrenal gland. However, the molecular mechanism for the DHCR24-mediated cell protective effect is not fully understood. Our previous study showed that TRβ1 is specifically expressed in the adrenal gland's inner cortex, especially in the X-zone (148). Because T3 treatment has been shown to increase the size of inner-cortical cells and delay their regression (148,186,195), the T3-mediated delayed regression of the X-zone is possibly a direct effect of the T3-induced high expression of DHCR24 in the inner cortex.

Altogether, our data show a novel role of the *Dhcr24* as a master regulator of T3-mediated lipid accumulation and delayed cell regression in the adrenal inner cortex.

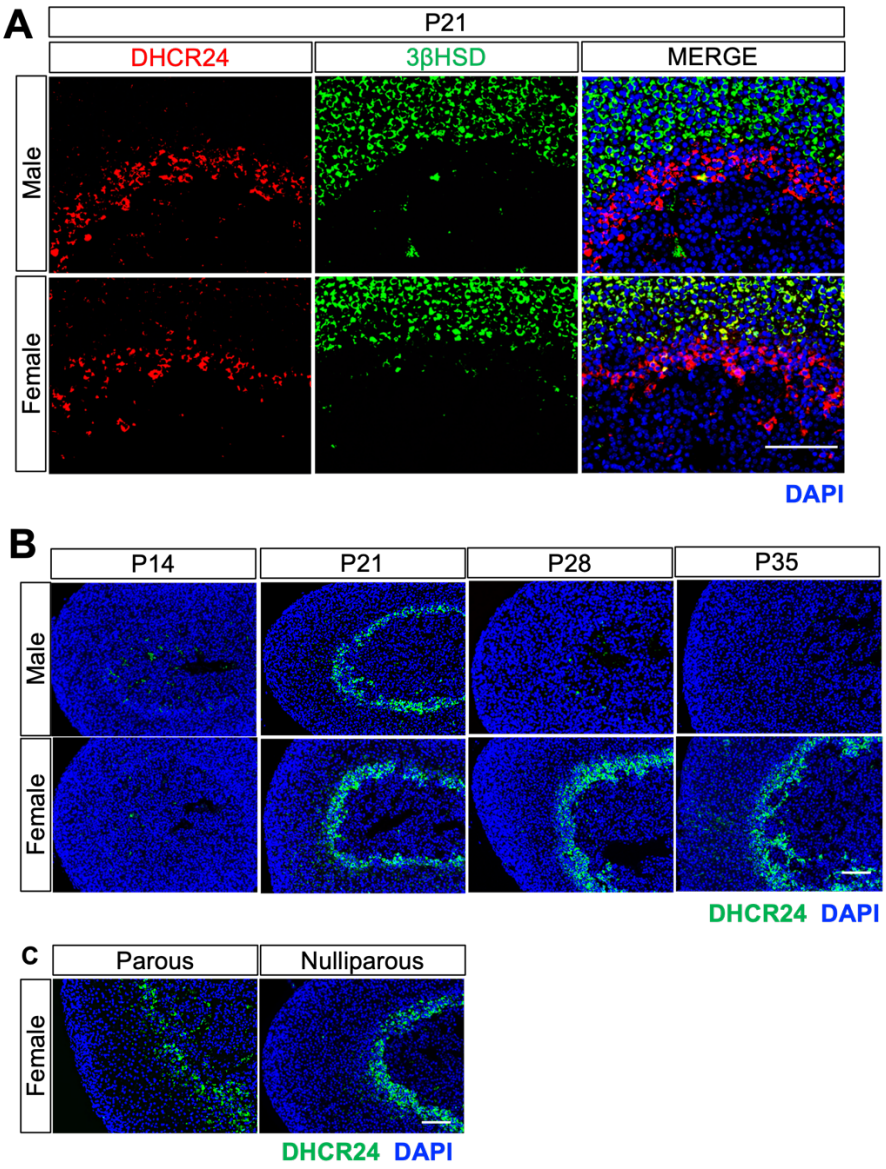

Figure 3.1 DHCR24 expression in the adrenal gland. (A) Double immunostaining using anti-DHCR24 and anti-3βHSD on euthyroid wild-type B6 mice of both sexes. (B) The time course of DHCR24-positive cells (green) during development in both sexes was determined by immunofluorescence. (C) Immunostaining using DHCR24 antibody of tissue from parous and nulliparous euthyroid wild-type B6 mice. Scale Bar 100 μm.

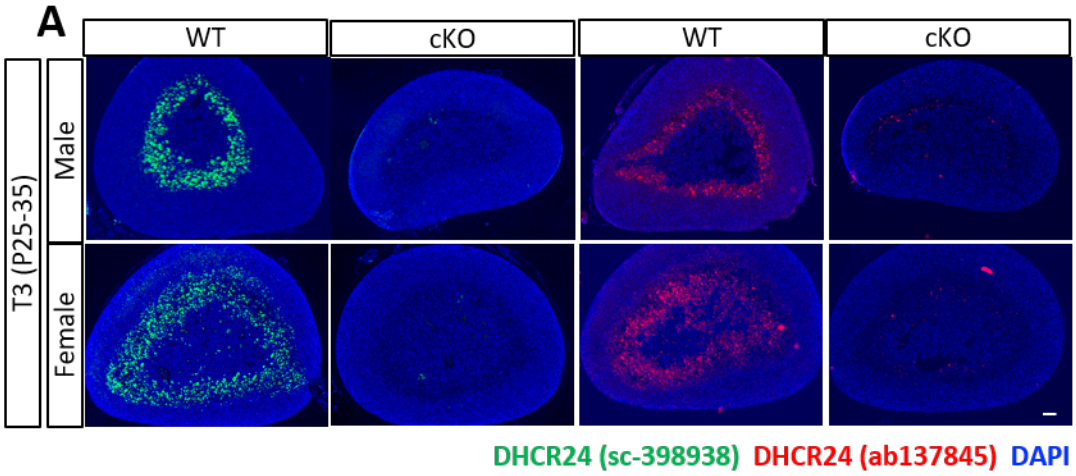

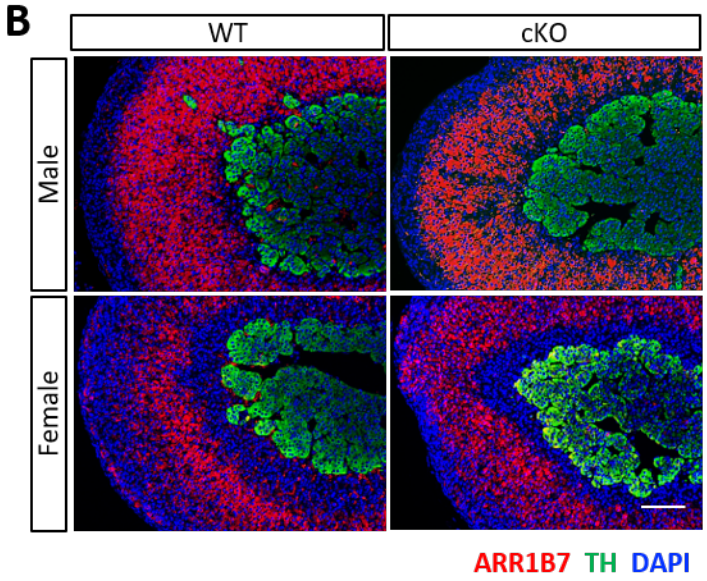

Figure 3.2 Phenotypic analyses of *Dhcr24* cKO mice. (A) Immunostaining using DHCR24 antibodies #sc-398938 (green) and #ab137845 (red). The mice were treated with T3 drinking water for 10 days to increase the expression level of DHCR24. (B) Immunostaining showed areas of zona fasciculata (AKR1B7-positive) and medulla (tyrosine hydroxylase (TH)-positive in euthyroid P35 mice. The cell nuclei were counterstained with DAPI (blue). WT: wild-type mice, cKO: *Dhcr24* conditional knockout mice. Scale Bar 100 μm.

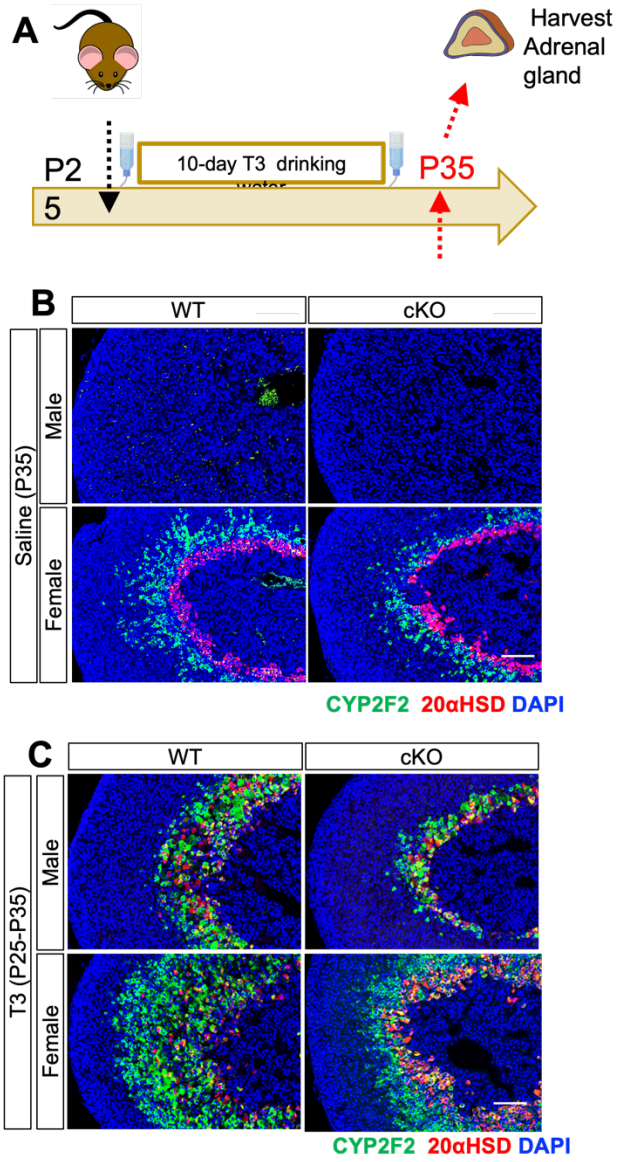

Figure 3.3 Effect of T3 treatment on adrenal glands of *Dhcr24* cKO mice. (A) Schematic of T3 administration to mice. (B, C) Immunostaining showed areas of the inner cortex (CYP2F2- or 20αHSD-positive) in euthyroid and T3-treated P35 mice. The cell nuclei were counterstained with DAPI (blue). WT: wild-type mice, cKO: *Dhcr24* conditional knockout mice. Scale Bar 100 μm.

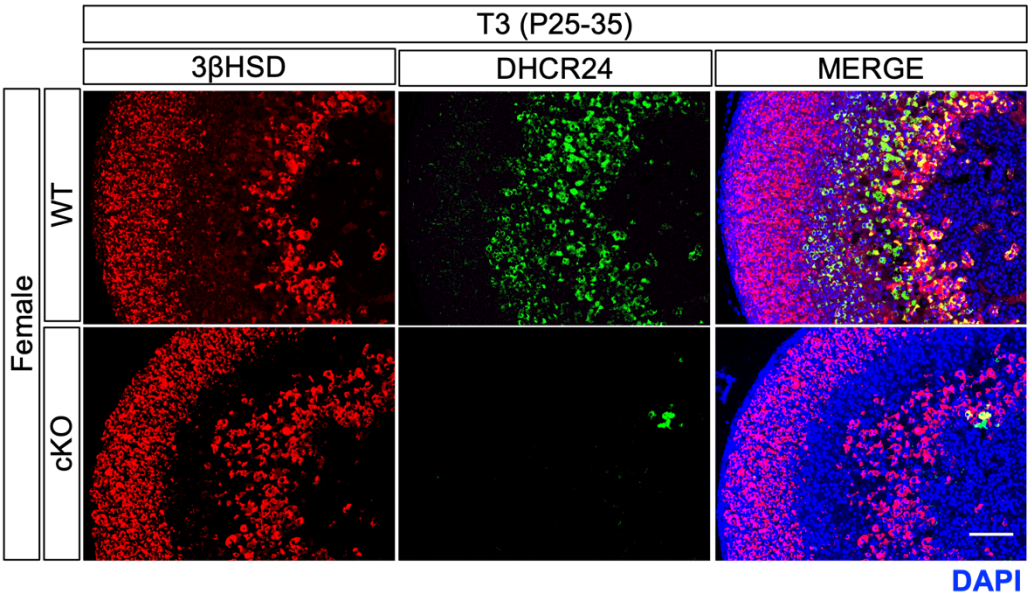

Figure 3.4 T3 treatment effect on *Dhcr24* cKO mice adrenal outer cortex. Immunostaining showed areas of the outer cortex (3βHSD-positive) in T3 treated P35 mice. The cell nuclei were counterstained with DAPI (blue). WT: wild-type mice, cKO: *Dhcr24* conditional knockout mice. Scale Bar 100 μm.

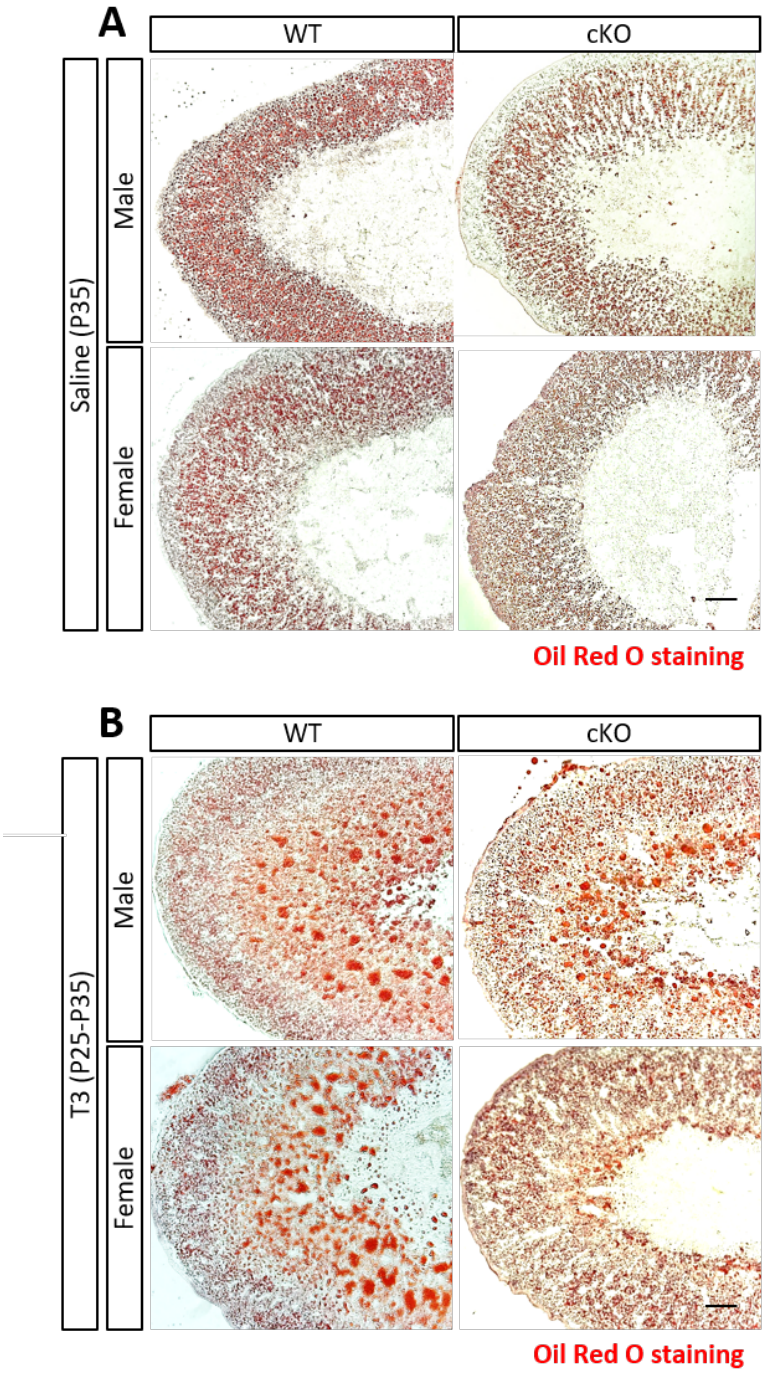

Figure 3.5 Phenotypic analyses of *Dhcr24* cKO mice. (A) Oil Red O staining showing lipid droplets in the adrenal glands of euthyroid P35 mice. (B) Oil Red O staining showing lipid droplets in the adrenal glands with T3 treatment at P35. WT: wild-type mice. cKO: *Dhcr24* conditional knock-out mice. Scale bars, 100 µm.

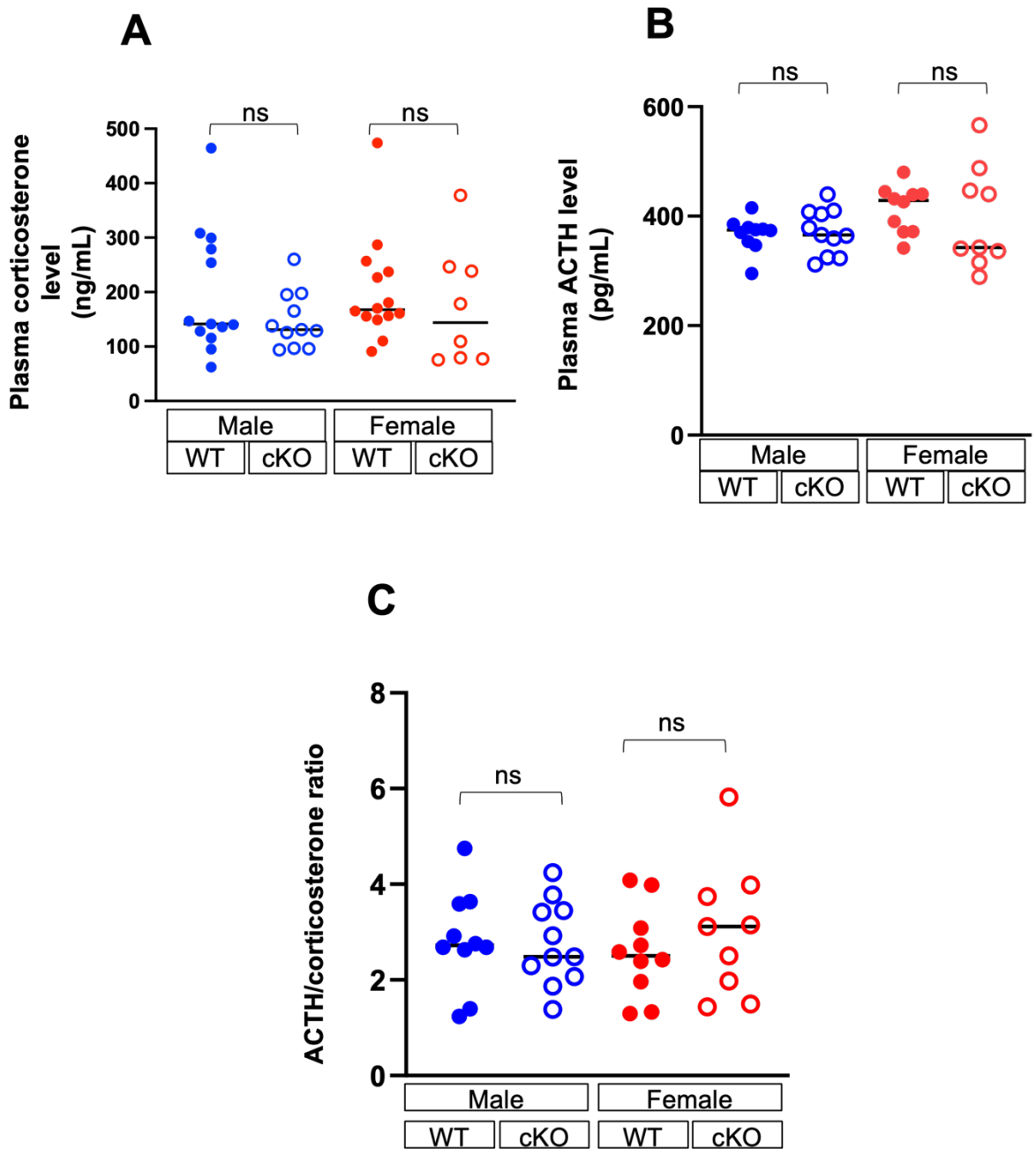
A
Plasma corticosterone level (ng/mL)
500
400
300
200
100
0
ns
ns
Male
Female
WT
cKO
WT
cKO
B
Plasma ACTH level (pg/mL)
600
400
200
0
ns
ns
Male
Female
WT
cKO
WT
cKO
C
ACTH/corticosterone ratio
8
6
4
2
0
ns
ns
Male
Female
WT
cKO
WT
cKO

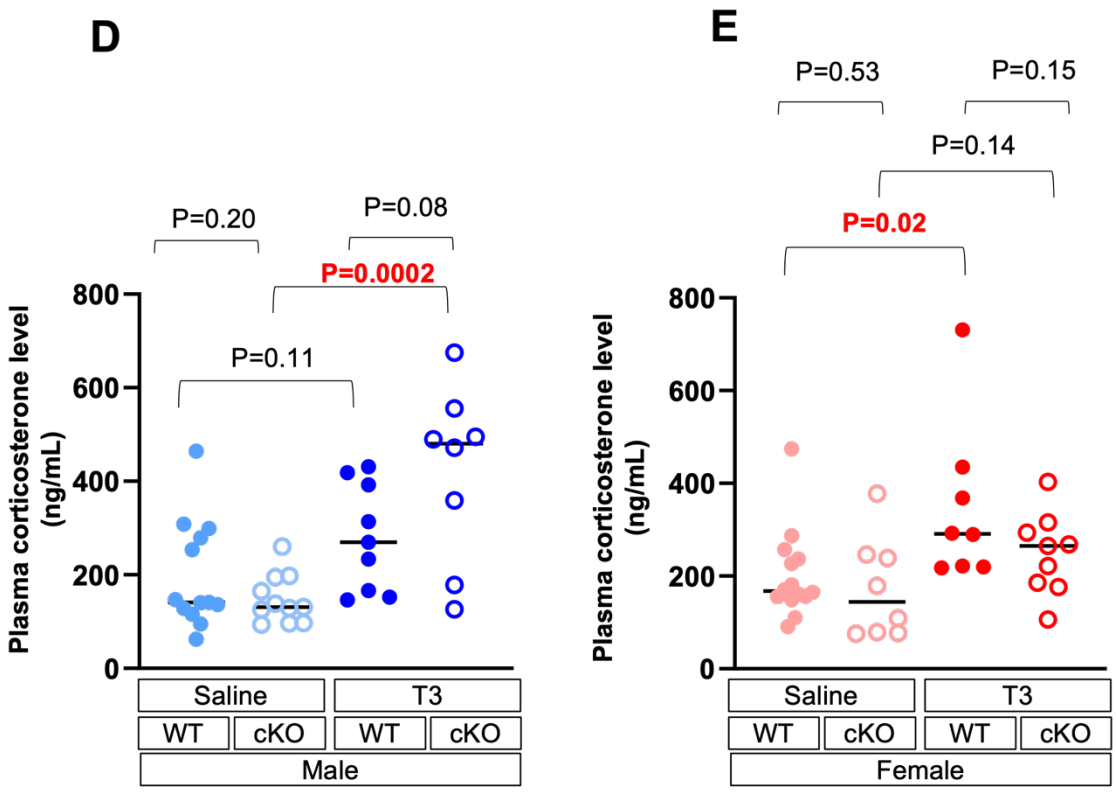

Figure 3.6 Plasma corticosterone and ACTH levels. (A) Plasma level of corticosterone in euthyroid P35 mice. (B) A) Plasma level of ACTH in euthyroid P35 mice. (C) Plasma ACTH/ corticosterone ratio in euthyroid P35 mice. (D) Plasma level of corticosterone in euthyroid and T3-treated P35 male mice. (E) Plasma level of corticosterone in euthyroid and T3-treated P35 female mice. WT, wild-type mice. cKO, *Dhcr24* conditional knockout mice. ns, no significant difference.

Chapter 4: Early transcriptomic response of mouse adrenal gland and Y-1 cells to dexamethasone

4.1 Abstract

Glucocorticoids have short- and long-term effects on adrenal gland function and development. RNA sequencing (RNA-seq) was performed to identify early transcriptomic responses to the synthetic glucocorticoid, dexamethasone (Dex), *in vitro* and *in vivo*. In total, 1711 genes were differentially expressed in the adrenal glands of the 1-h Dex-treated mice. Among them, only 113 were also considered differentially expressed genes (DEGs) in murine adrenocortical Y-1 cells treated with Dex for 1 h. Gene ontology analysis showed that the upregulated DEGs in the adrenal gland of the 1-h Dex-treated mice were highly associated with the development of neuronal cells, suggesting the adrenal medulla had a rapid response to Dex. Interestingly, only 4.3% of Dex-responsive genes in the Y-1 cell line after 1-h-Dex treatment were differentially expressed after 24-h-Dex treatment. Heatmaps revealed that most early responsive DEGs in Y-1 cells during 1-h treatment exhibited a transient response. The expression of these genes under treatment for 24 h returned to basal levels similar to those during control treatment. In summary, this research compared the rapid transcriptomic effects of Dex stimulation *in vivo* and *in vitro*. Notably, adrenocortical Y-1 cells had a transient early response to Dex treatment. Furthermore, the DEGs had a minimal overlap in the 1-h Dex-treated group *in vivo* and *in vitro*.

*This chapter is a revised version of the manuscript published in Endocrine Connections (Zheng HS, Daniel JG, Salamat JM, Mackay L, Foradori CD, Kemppainen RJ, Pondugula SR, Tao YX, Huang CC. Early transcriptomic response of mouse adrenal gland and Y-1 cells to dexamethasone. Endocrine Connections. 2022 Aug 8;11(8)).

4.2 Introduction

Glucocorticoids (GCs) are primary stress hormones and critical regulators of several physiological mechanisms. GCs commonly elicit their function through glucocorticoid receptor (GR)-mediated genomic effects. However, other than nuclear GR, these hormones can also stimulate several non-genomic mechanisms via the membrane-bound GR (196). Non-transcriptional effects have short-term outcomes that control several critical physiological processes, including inflammation, behavioral changes, and even negative feedback from the hypothalamic-pituitary-adrenal (HPA) axis (197). Although GCs have non-transcriptional actions, they may still rapidly affect gene expression via different mechanisms such as mRNA destabilization and coactivator competition (198,199). Transcriptional responses can occur within 1 hour after the initial stimulus (200,201). Therefore, the rapid response of gene expression is observed immediately after GC administration via both genomic and non-genomic actions.

Synthetic GC dexamethasone (Dex) is widely used for therapeutic and diagnostic purposes in clinical settings due to its potent GR activity and predominant effects. Treatment with Dex suppresses HPA axis activity leading to decreased steroidogenesis in the adrenal cortex, eventually reducing endogenous GC secretion. The mechanisms of the abovementioned Dex-mediated negative feedback have been widely assessed (202). However, the immediate transcriptomic response (i.e., within approximately 1 h) of the adrenal gland to Dex administration is not completely elucidated at the genome-wide level. In this study, RNA sequencing (RNA-seq) and downstream bioinformatics analysis were performed to explore the early transcriptional response to Dex exposure *in vivo* and *in vitro*. This study provides data about

the transcriptomic response of Y-1 cells, a widely used murine adrenocortical cell line, to Dex treatment for 1 and 24 h. The rapid responses (within 1 h) *in vitro* vs. *in vivo* were also compared to highlight the differences between Y-1 adrenocortical cells and the adrenal glands in C57BL/6 mice.

4.3 Materials and Methods

4.3.1 Animals and dexamethasone treatment Male C57BL/6 mice aged 35-60 days were housed in a 14:10-h light/dark cycle, were given free access to water and rodent chow and were treated with Dex as previously described (203). In short, mice were familiarized with general handling, weighing procedures, and intraperitoneal injections for 4 days (once a day with 0.25 ml of sterile 1X phosphate-buffered saline (PBS)). On the fifth day in the morning, animals were weighed, injected with 0.25 ml of either vehicle (sterile 1X PBS) or 10 μg dexamethasone (1DEX027, Covetrus, Portland, ME), and returned to their cages. Mice were euthanized by CO_2 inhalation 1 hour after injection, and all samples were collected immediately after euthanasia. Adrenal glands were quickly removed from mice, and the surrounding adipose tissue was trimmed away. The right adrenal gland from each mouse was snap-frozen in liquid nitrogen and stored at -80°C until use. All procedures followed the protocols approved by the Institutional Animal Care and Use Committee at Auburn University.

4.3.2 Cell culture Y-1 mouse adrenocortical cells (ATCC #CCL-79) were purchased from American Type Culture Collection (ATCC). Y-1 cells were cultured in DMEM/F12 medium supplemented with 10% fetal bovine serum and 1% streptomycin/penicillin (E490-20ml, VWR, Radnor, PA). Cells

were subcultured separately into three groups (control, 1-h Dex-treated, and 24-h Dex-treated) using six-well plates with 400,000 cells per well. After reaching 70% confluency, the growth medium was aspirated and replaced by either vehicle-containing (0.05% ethanol) or Dex-containing (0.05% ethanol and 100 nM Dex) medium. The 100 nM Dex is commonly used in the cell culture system for studying the Dex effect and is considered a high-dose treatment (204-207). At the end of the treatment, the culture medium was aspirated, and RNA immediately extracted. Vehicle-treated control groups were harvested along with the 1-h Dex-treated group and the 24-h Dex-treated group. For the RNA-seq study, the 24-h vehicle-treated samples were used as the control group. Three experimental replicates were performed independently on different days starting from different cell passages.

4.3.3 RNA isolation and sequencing Total RNA from cell cultures was extracted using 400 µL TRIzol (Invitrogen, Waltham, MA). Total RNA from tissues was extracted from frozen adrenal glands using Monarch Total RNA Miniprep Kit (New England Biolabs, Ipswich, MA) according to the manufacturer's instructions. Adrenal glands from 2-3 animals were pooled as one biological replicate, with two biological replicates per condition (a total of 5 mice were included in each condition). Total RNA was sent to Novogene Life Sciences Co., Ltd. for the PE150 RNA-seq service. All samples that passed the quality control (concentration > 25 ng/µl, RIN ≥ 7.5) were used for library preparation and subsequent RNA-seq.

4.3.4 Bioinformatics data analysis Unstranded paired-end read files were first analyzed using the FASTQ error check feature of Chipster (208). Quality control was then run on the raw read files

using FastQC. The trimmed reads were then aligned to the mouse genome (mm10, GRCm38.95) using STAR (v. 2.5) (209). Reads were mapped to each gene and counted using HTSeq (v.0.6.1) (210). The Maximal Mappable Prefix (MMP) method ensures precise mapping results for exon-exon junction reads. Differential expression analysis between control and Dex-treated groups was performed using the DESeq2 (211) in R version 3.6.2 with FDR cutoff α=0.05. Differential expression analysis between the 1-h and 24-h Dex treatment groups was also performed using the same parameter. Three replicates per group were included in the *in vitro* study and two replicates per group were used for the *in vivo* study. Statistical significance of differential expression was assigned to genes with adjusted p-values < 0.05, irrespective of fold change. Genes must have at least one fragment per kilobase per million mapped reads (FPKM) in at least one sample to be considered differentially expressed genes (DEGs). Heatmaps for DEGs were generated using heatmap.2 in R, with Ward's minimum variance method for clustering (ward.D2) and Euclidean distance measurement method. The Panther Gene Ontology website (geneontology.org) was used for GO analysis. GO-Figure! was used to generate Fig. 4.2d. GO enrichment analysis in Fig. 4.3 was analyzed using g:Profiler and the enrichGO function in the clusterProfiler package (3.16.0) in R with P < 0.05 as the cutoff value (212,213).

4.3.5 Statistical analysis Differential expression analysis between control and Dex-treated groups was performed using the DESeq2 (211) in R version 3.6.2 with FDR cutoff α=0.05. Differential expression analysis between the 1-h and 24-h Dex treatment groups was also performed using the same parameter. Three replicates per group were included in the *in vitro* study and two

replicates per group were used for the *in vivo* study. Statistical significance of differential expression was assigned to genes with adjusted p-values < 0.05, irrespective of fold change.

4.4 Results

4.4.1 Differentially expressed genes had a minimal overlap in the 1- and 24-h Dex-treated Y-1 cells.

RNA-seq analysis identified 313 and 319 DEGs in Y-1 cells in the 1- and 24-h Dex-treated groups, respectively (Figure 4.1). There were 203 upregulated genes and 110 downregulated genes in the 1-h Dex-treated group. Meanwhile, 200 and 119 genes were upregulated and downregulated, respectively, in the 24-h Dex-treated group. The clustered heatmap showed that these DEGs belong to four major groups, which were as follows: (1) upregulated mainly in the 1-h Dex-treated group, (2) upregulated mainly in the 24-h Dex-treated group, (3) downregulated mainly in the 24-h Dex-treated group, and (4) downregulated mainly in the 1-h Dex-treated group (Figure 4.1A). Interestingly, most DEGs in the 1-h Dex-treated group were not identified as DEGs in the 24-h Dex-treated group. After 24-h Dex treatment, the expression of these genes had returned to basal levels similar to those of the non-treated control group. Among 606 Dex-responsive genes found in Y-1 cells, only 26 (4.3%) were differentially expressed in both the 1- and 24-h Dex-treated groups, which is equivalent to 8.3% and 8.2% of DEGs in each group, respectively (Figure 4.1B). Interestingly, the heatmap showed that almost all of those 26 genes had a similar response to Dex treatment for 1 and 24 h.

4.4.2 Genes responsive to Dex treatment *in vivo* and *in vitro*.

To compare the early response to Dex treatment *in vitro* versus *in vivo*, adult C57BL/6 mice were also treated with high-dose Dex, which can have a sufficient effect on the HPA axis to stimulate the expression of *Rsd1* in the pituitary level within 1 h (203). Twenty six point two percent of 54,533 genes in the mouse genome had at least one FPKM in one sample. These genes were classified as adrenal-expressed genes (14,300 genes). The number of adrenal-expressed genes in the saline-treated group was similar to that in another genome-wide study of adult C57BL/6 mice (149). The *in vivo* 1-h Dex-treated group had 862 upregulated genes and 849 downregulated genes in the adrenal glands (Figure 4.2A). These 1,711 Dex early-responsive genes comprise 12.0% of all adrenal-expressed genes (Figure 4.2B). Thirteen point three percent of adrenal-expressed transcription factors (TFs) were differentially expressed in the 1-h Dex-treated group. The percentage of Dex early-responsive adrenal-expressed genes and Dex-responsive adrenal-expressed TFs was similar. Hence, the response rate to Dex treatment was similar between the TF and non-TF genes (Figure 4.2B). Interestingly, only a small percentage of DEGs identified *in vitro* was also identified *in vivo* (Figure 4.2C). 58 DEGs in the 1-h Dex-treated Y-1 cells were differentially expressed in the *in vivo* study, while 63 genes in the 24-h *in vitro* Dex-treated group were also identified in the *in vivo* treatment group. The Venn diagram shows that only a small portion of DEGs overlapped among three groups (58 + 63 - 113 = 8 genes). Gene ontology (GO) analysis showed that the 58 overlapped DEGs between the 1-h *in vitro* and *in vivo* groups were highly associated with the "Regulation of Response to Stress" (GO: 0080135, fold enrichment of > 5.00, FDR P = 0.0003) (Figure 4.2D).

4.4.3 Dynamic expression of differentially expressed genes *in vivo* and *in vitro*.

A clustered heatmap was used to better visualize the response of the 113 genes that responded to Dex both *in vivo* and *in vitro* (Figure 4.2E). Interestingly, genes that exhibited an opposite direction of response during *in vivo* and *in vitro* treatments were clustered together (highlighted in the green box in Figure 4.2E, containing 43 genes). For example, the expression of nuclear receptor genes *Nr4a1* and *Nr4a3* and the zona fasciculata marker gene *Akr1b7* was upregulated either in the 1- or 24-h Dex-treated Y-1 cells. However, their expression was downregulated *in vivo*. "Cellular Response to Corticotropin-Releasing Hormone Stimulus" (GO: 0071376, fold enrichment of > 100, FDR P = 0.047) was the leading GO term obtained from the 44 clustered genes. The other GO terms included "cell migration involved in sprouting angiogenesis" (GO:0002042, fold enrichment of 84.7, FDR P = 0.020), "blood vessel endothelial cell migration" (GO:0043534, fold enrichment of 53.6, FDR P = 0.035), and "tissue development" (GO:0009888, fold enrichment of 4.47, FDR P = 0.009).

4.4.4 Opposite response of genes associated with steroidogenesis and catecholamine synthesis.

We then compared the 1,711 Dex-early-responsive genes identified in the *in vivo* treatment, chromaffin-like genes, (214) and adrenocortical-related genes (215). In the Dex-treated adrenal glands of mice, 24.65% of the adrenocortical-related Dex-responsive genes and 68.09% of the chromaffin-like Dex-responsive genes were upregulated (Figure. 4.3A). This difference was in accordance with the current understanding that the effect of GCs in the adrenal cortex could be opposite to that in the adrenal medulla. GCs can both suppress adrenocortical steroidogenesis directly or indirectly (216) and can induce medullary function by upregulating the expression of phenylethanolamine N-methyltransferase (PNMT) (217,218), an epinephrine synthesis enzyme.

To further understand the functional meaning of this dynamic response at the transcriptome level, GO analysis was performed to evaluate the potential function of upregulated and downregulated genes. GO analysis revealed that several GO terms associated with the 862 Dex-upregulated genes were associated with the development or function of neuronal cells (Figure 4.3B). To provide a better visualization of the response of adrenal glands to Dex, the genes were classified based on their function, and clustered heatmaps were used to show the relative expression of genes both in the *in vivo* and *in vitro* treatment groups. Interestingly, results revealed that genes associated with catecholamine synthesis may be upregulated in general in the *in vivo* group (Figure 4.4), which was in accordance with the result of GO analysis in which many GO terms are linked to neuronal development (Figure 4.3). Although none of these catecholamine synthesis-associated genes were considered DEG, several genes associated with the regulation of neurotransmitter secretion (GO:0046928, fold enrichment of 4.0, FDR P = 0.000407) were included in the Dex-upregulated genes. Regarding steroid hormone production, several genes associated with steroidogenesis were downregulated primarily in the *in vivo* study (Figure 4.4). No specific trend was observed in expression of genes associated with nuclear receptors or cholesterol metabolism. Expression of most genes in these two categories did not change or was minimally affected in the *in vitro* treatment groups.

4.4.5 Dynamic response of nuclear receptors to Dex treatment *in vivo* and *in vitro*.

In Figure 4.4, it is interesting that downregulation of genes associated with steroidogenesis was observed particularly in the *in vivo* treatment groups. This result was in accordance with the long-term understanding that Dex can suppress the endogenous secretion of GCs via a negative

feedback loop. In the *in vivo* treatment group, *Nr5a1*, which is a nuclear receptor known as the master regulator of steroidogenesis, is downregulated (Figure 4.5A). The expression of several genes known as *Nr5a1*-induced genes (e.g., *Fdx1*, *Alas1*, and *Akr1b7*) was also downregulated (Table 1) (219-221). Moreover, the downregulation of *Nr5a1* may explain the overall suppression of steroidogenesis-related genes (Figure 4.4). *Nr0b2*, *Nr1d2*, *Nr4a1*, *Nr4a3*, *Nr1h4*, and *Pparg*, in addition to *Nr5a1*, were the nuclear receptors considered DEGs (Figure 4.5B-G).

4.5 Discussion

Rapid transcriptional effects of GCs

A typical action of GCs is that they bind cytosolic steroid receptors, which in turn migrate to the nucleus and regulate the expression of target genes. For example, GCs can activate or suppress gene expression via GR, mineralocorticoid receptors or other TFs that bind the glucocorticoid-responsive elements (222). Although the genetic effect of steroid hormones is not commonly short-term, several data have shown that steroid hormone exposure causes transcriptional changes more rapidly than previously believed. Our *in vitro* experiments revealed that Y-1 cells had a dynamic early response to Dex treatment. The DEGs identified in the 1-h Dex-treated group are extremely different from those identified in the 24-h Dex-treated group.

The rapid cytoplasmic movement of steroid receptors toward the cell nucleus occurs within minutes after steroid hormone administration (223). *In vitro* studies have shown that Dex-induced transcriptional changes can be a direct effect independent from other confounding external stimuli present in organismal model systems. For example, a 40-min exposure to

estrogen in human umbilical vein endothelial cell culture leads to an acute PI3K-mediated upregulation of 250 genes (224). GR ChIP-seq studies have shown a significant enrichment in GR binding sites after 1 h of Dex treatment in cells originating from different types of tissues (225,226). RNA-seq analysis using rat primary cardiomyocytes revealed 98 differentially regulated genes after 1 h of Dex stimulation. This indicated the upregulation of several genes involved in the development of hypertrophic cardiomyopathy, which is a common adverse effect of Dex (227). The same study revealed that the treatment with Dex in 10-week-old mice could mimic findings found in primary cardiomyocytes. These *in vivo* and *in vitro* studies provided important evidence showing that Dex treatment causes short-term expression changes at a genome-wide level.

Rapid and transient responses of the Nr4a subfamily

In Y-1 cells, Dex treatment leads to a rapid and transient upregulation of *Nr4a1* and *Nr4a3*, which are orphan nuclear receptors belonging to the *Nr4a* subfamily (containing *Nr4a1*, *Nr4a2*, and Nr4a3). Although the expression of *Nr4a1* and *Nr4a3* in Dex-treated Y-1 cells increased in the 1-h Dex-treated group, the expression was low in the 24-h Dex-treated group. This rapid and transient upregulation of genes of the *Nr4a* subfamily has been observed in several different types of cells when stimulated with Dex. The expression of *Nr4a1* and *Nr4a3* in 3T3-L1 preadipocytes increases only within the first 4 h during the cell differentiation process from preadipocyte to adipocyte (228). The upregulation of *Nr4a1* and *Nr4a2* in T cells reaches the peak level within the first hour after antigen stimulation (229). In addition, the expression of *Nr4a1* and *Nr4a3* increases within the first hour and then decreases in macrophages coincubated with

apoptotic thymocytes (230). Interestingly, *Nr4a1* and *Nr4a3* are included in the GO term 'cellular response to corticotropin-releasing hormone stimulus' (GO: 0071376), which is the leading biological process GO term identified using 44 genes that were classified as having opposite responses *in vitro* and *in vivo* (Figure 4.2E). Most of the 44 genes had a transient response in the *in vitro* treatment groups. Because our work does not specifically focus on the GR-dependent and/or GR-independent pathways, the data cannot confirm the possible crosstalk between GR and the *Nr4a* subfamily members (231). However, a previous GR ChIP-seq study did not detect GR binding to sites around the promotor region of *Nr4a1* in a Dex-treated human cell line (232).

Effects of Dex on steroidogenesis

GC suppresses the HPA axis activity partly by reducing the secretion of steroid hormones from the adrenal cortex. This GC-mediated suppression is commonly associated with an hour-to-day timescale. Although the short-term non-transcriptional and long-term transcriptional effects of GCs on steroid hormone secretion are known, most studies have focused on time points several hours after establishing baseline transcription levels at time zero. For example, efforts to classify GC-associated mechanisms in Leydig MA10 cells showed suppressed cAMP-mediated Star transcription via NR4A1 after 4 h of Dex incubation (205). In bovine adrenocortical primary cells, 48 h of Dex treatment resulted in a 50% suppression of the adrenocorticotropic hormone (ACTH) or forskolin-induced *CYP11A* and *CYP17* expression (204). Another study revealed that 24-h incubation with a physiological range of Dex concentrations inhibits steroidogenic gene expression including *STAR*, *CYP11A1*, and *HSD3B* in the human glial cell line via GR (206). All these *in vitro* studies have shown that the GC-mediated suppression of steroidogenesis could be direct

and independent of the HPA axis. At least immunostaining results showed that GR is expressed in all cortical zones and the adrenal medulla as well (233,234). Although GC was found to have an inhibitory effect on steroidogenesis, seemingly contradictory results have also been reported. For example, in the human adrenocortical (H295A) cell line, 24-h Dex treatment did not affect the transcription of *CYP11A1*, *CYP17*, *and HSD3B* (235).

In the 1-h *in vivo* treatment groups, the expression of several genes involved in steroidogenesis was downregulated, thereby indicating the suppression of steroidogenesis in mouse adrenocortical cells at the transcriptional level 1 h after Dex treatment. Because the expression of most downregulated genes identified in our *in vivo* treatment groups did not change in the *in vitro* treatment groups (except *Akr1b7*, which was upregulated after 24 h of treatment), a systemic effect from the HPA axis may influence the adrenal gland at the transcriptional level. Our previous data did show that 1 h of Dex treatment significantly increased the expression of pituitary *Rasd1*, a gene associated with mechanisms mediating the early response of GCs to negative feedback (203). Although a systemic effect from the HPA axis cannot be ruled out, a direct effect is more probable in our 1-h *in vivo* treatment study. Notably, carbon dioxide inhalation was used for euthanasia in our study. Euthanasia via CO_2 inhalation is a significant stress and can lead to high plasma ACTH and corticosterone levels in rodents (236). A possible influence from acute stress may still exist even though high-dose Dex treatment should significantly suppress the HPA axis activity via the negative feedback.

Effects of Dex on neuronal cells

GCs are critical regulators of neuronal cell development and function (237). They upregulate the expression of PNMT in the adrenal medulla, which converts norepinephrine to epinephrine. GC-induced PNMT expression has been evaluated using several models including hypophysectomized rats. The low levels of PNMT expression in hypophysectimized rats can be restored by ACTH or supraphysiological doses of external GC (217,238,239). The rich vasculature within the adrenal gland allows the rapid delivery of GCs to cortical layers and the medulla (240). Endogenous GCs are supplied to the adrenal medulla via the corticomedullary portal system. This phenomenon leads to extremely high GC concentrations in the adrenal medulla and an induction of PNMT expression. The lack of PNMT in *Cyp11a1* knockout embryos further confirms that a high concentration of intra-adrenal GC is required to stimulate adrenal PNMT expression (241). In the current study, although the heatmaps showed that the expression of several genes associated with catecholamine synthesis might be elevated in the Dex-treated groups, none of them were identified as DEGs. One possible explanation is that the Dex treatment suppresses endogenous GC secretion. Thus, the effect of Dex on the medulla, at least at the acute regulation of catecholamine synthesis, is attenuated due to the reduced quantity of endogenous GC entering the adrenal medulla. This would also explain why the adrenal *Pnmt* expression increases as early as 20 min after Dex treatment in hypophysectomized rats. However, there is no change of *Pnmt* expression in non-hypophysectomized rats (242). Although *Pnmt* expression did not significantly increase based on our data, GO analysis did show that the upregulated genes were associated with the function and development of neuronal cells. An RNA-seq study showed that the proliferation of cells is the leading functional network in hypothalamic neural-

progenitor/stem cells treated with Dex (243), thereby indicating the direct effect of Dex on neuronal cell development.

Difference between adrenal cortex and adrenocortical Y-1 cells

Notably, the Y-1 cells are adrenocortical tumor cells; therefore, the characteristics (i.e., pathways and mechanisms) of these cells significantly differ from those of normal adrenocortical cells. For example, Y-1 cells do not express 21-hydroxylase (*Cyp21a1*) and, thus, do not secrete corticosterone (244). Moreover, compared to the intact adrenal gland, Y-1 cells had a significantly lower expression of the lipid transport protein apolipoprotein E (encoded by *Apoe*), a key modulator of cholesterol homeostasis and corticosterone secretion in the adrenal gland (FPKM of approximately 5 in Y-1 cells vs. FPKM of > 500 in the whole adrenal gland RNA-seq) (245). In the current study, only 58 genes were differentially expressed during 1 h of Dex treatment both *in vivo* and *in vitro*. Notably, most Dex-responsive genes identified in the *in vitro* treatment were not observed in the *in vivo* treatment, and vice versa. It is understandable that data on the Y-1 cell line, which is an adrenocortical tumor cell line of a LAF1 (C57L × A/HeJ) male mouse, differs in an *in vivo* study using the whole adrenal glands of C57BL/6 mice. The difference could also be attributed to complex physiological responses, including the HPA axis negative feedback, in living animals. Although we did not use a cell-type-specific approach for our *in vivo* study, the whole adrenal gland RNA-seq still provides valuable resource data emphasizing the difference in the Dex-mediated effect between Y-1 cells and the *in vivo* mouse model at the transcriptome level.

Sexually dimorphic adrenal gland and effects of Dex

The histology and transcriptome of the adrenal gland are sexually dimorphic in mice (149,176,215,246). Moreover, Dex elicits its effect in a sex-specific manner in several aspects via complex mechanisms that are still not completely understood (247-250). Several immortalized adrenocortical cell lines from transgenic mice, which include a cell line generated using female mice (251), have been developed. However, the Y-1 cell line is most widely used. Because the Y-1 cell line was collected from a male mouse, only male mice were included in our study. With consideration of GR-mediated sexual dimorphism in several tissues (252-254), the Dex-mediated short-term effect in the adrenal gland and adrenocortical cells in female mice could differ from that in male mice. Further studies need to be conducted to assess the short-term effects mediated by Dex in the female adrenal gland and female-derived adrenocortical cells.

In conclusion, we assessed the early/rapid murine adrenal transcriptome response to Dex treatment *in vivo* and *in vitro*. Results showed that 1 h of Dex treatment had acute transcriptional effects in the adrenal gland and Y-1 cells. However, less than 10% of Dex-responsive genes were differentially expressed both *in vivo* and *in vitro*. Interestingly, a group of Dex-responsive genes had opposite directions of response *in vivo* and *in vitro*, indicating a diverse early response of the mouse adrenal gland and adrenocortical Y-1 cells to Dex at the transcriptomic level.

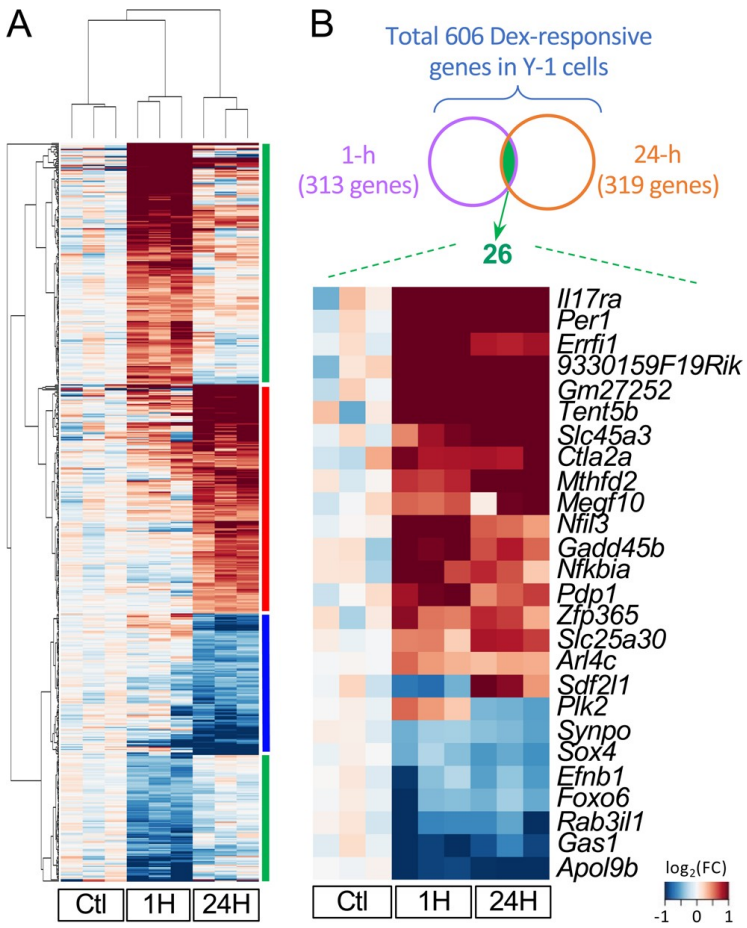

Figure 4.1 Y-1 cells responded differently to the 1-h and the 24-h dexamethasone treatment. (A) The clustered heatmap shows the fold change of all DEGs identified either in the 1-h- or the 24-h-Dex-treated Y-1 cells. Genes were clustered into four major groups. Genes in two clusters (marked by the red bar and the blue bar on the right) were either upregulated or downregulated mainly in the 24-h group with no or minor changes in the 1-h group. Genes in another two clusters (marked by green bars) had a transient response to Dex. In these two clusters, expression levels of genes after 24-h Dex treatment moved back toward levels in the non-treated control group. (B) There were 313 and 319 genes differentially expressed in the 1-h treatment group and the 24-h treatment group, respectively. A total of 26 genes were differentially expressed in both groups. Sdf2l1 and Plk2 are the only two genes that showed an opposite change between the 1-

h and 24-h treatment groups. Ctl, vehicle control. Genes must have at least one fragment per kilobase per million mapped reads (FPKM) in at least one sample to be DEGs. The fold change used for heatmaps was calculated based on FPKM +0.001.

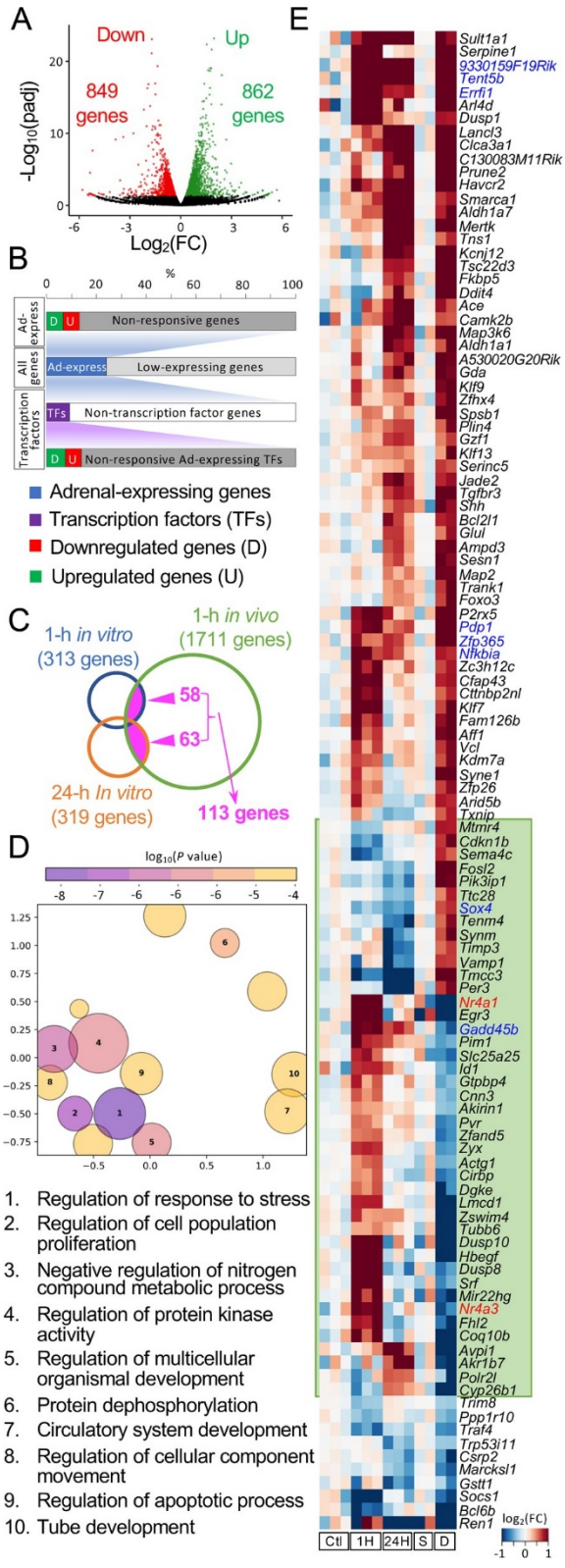
A
Down
Up
849 genes
862 genes
-Log10(padj)
Log2(FC)
B
%
Ad-express
All genes
Transcription factors
Non-responsive genes
Low-expressing genes
Non-transcription factor genes
Non-responsive Ad-expressing TFs
Adrenal-expressing genes
Transcription factors (TFs)
Downregulated genes (D)
Upregulated genes (U)
C
1-h in vitro (313 genes)
1-h in vivo (1711 genes)
24-h In vitro (319 genes)
58
63
113 genes
D
log10(P value)
1. Regulation of response to stress
2. Regulation of cell population proliferation
3. Negative regulation of nitrogen compound metabolic process
4. Regulation of protein kinase activity
5. Regulation of multicellular organismal development
6. Protein dephosphorylation
7. Circulatory system development
8. Regulation of cellular component movement
9. Regulation of apoptotic process
10. Tube development
E
Sult1a1
Serpine1
9330159F19Rik
Tent5b
Errfi1
Arl4d
Dusp1
Lancl3
Clca3a1
C130083M11Rik
Prune2
Havcr2
Smarca1
Aldh1a7
Mertk
Tns1
Kcnj12
Tsc22d3
Fkbp5
Ddit4
Ace
Camk2b
Map3k6
Aldh1a1
A530020G20Rik
Gda
Klf9
Zfhx4
Spsb1
Plin4
Gzf1
Klf13
Serinc5
Jade2
Tgfbr3
Shh
Bcl2l1
Glul
Ampd3
Sesn1
Map2
Trank1
Foxo3
P2rx5
Pdp1
Zfp365
Nfkbia
Zc3h12c
Cfap43
Cttnbp2nl
Klf7
Fam126b
Aff1
Vcl
Kdm7a
Syne1
Zfp26
Arid5b
Txnip
Mtmr4
Cdkn1b
Sema4c
Fosl2
Pik3ip1
Ttc28
Sox4
Tenm4
Synm
Timp3
Vamp1
Tmcc3
Per3
Nr4a1
Egr3
Gadd45b
Pim1
Slc25a25
Id1
Gtpbp4
Cnn3
Akirin1
Pyr
Zfand5
Zyx
Actg1
Cirbp
Dgke
Lmcd1
Zswim4
Tubb6
Dusp10
Hbegf
Dusp8
Srf
Mir22hg
Nr4a3
Fhl2
Coq10b
Avpi1
Akr1b7
Polr2l
Cyp26b1
Trim8
Ppp1r10
Traf4
Trp53i11
Csrp2
Marcksl1
Gstt1
Socs1
Bcl6b
Ren1
log2(FC)
Ctl
1H
24H
S
D

Figure 4.2 Transcriptomic response of adult mouse adrenal gland to 1-h dexamethasone treatment. (A) The volcano plot shows the DEGs in the whole adrenal gland transcriptome in male mice after a 1-h Dex treatment. (B) Twenty-six point two percent of genes were identified as adrenal- expressed genes. 12.0% of adrenal-expressed genes were differentially expressed after a 1-h Dex treatment. Transcription factors (TFs) had a similar response rate compared to non-TF genes. (C) Minimal overlap of DEGs among three groups. (D) GO analysis of the 58 overlapping DEGs in the 1-h treated *in vivo* and *in vitro* studies. GO terms that are most similar in semantic spaces (indicated on the X and Y axis) are placed nearest to each other. The ten most significant terms are labeled with numbers and their descriptions are provided below the plot. (E) Clustered heatmap of the 113 genes that were differentially expressed both *in vivo* and *in vitro*. Genes in the green box had opposing responses to Dex treatment *in vivo* vs *in vitro*. DEGs identified in all three conditions are in blue. DEGs identified as nuclear receptors are in red. The fold change used for heatmaps was calculated based on FPKM +0.001. Ctl, untreated control (*in vitro*); 1H, 1-h Dex-treated group (*in vitro*); 24H, 24-h Dex-treated group (*in vitro*); S, saline-treated group (*in vivo*); D, Dex-treated group (*in vivo*).

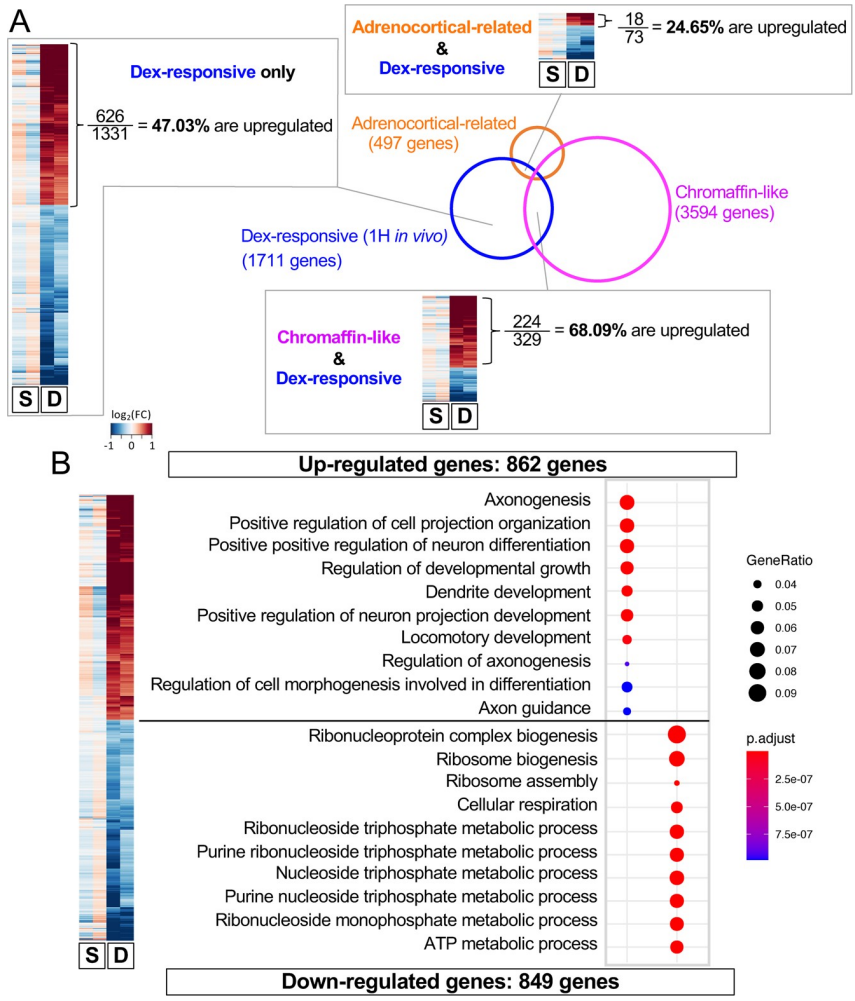

Figure 4.3 Following the *in vivo* 1-h dexamethasone treatment, the upregulated genes and the downregulated genes were linked to different functions and different groups of cells. (A) Venn diagram comparing Dex-responsive genes with 'adrenocortical-related genes' and 'chromaffin-like' genes. Clustered heatmaps show how genes were differentially expressed in each overlapping gene set. In the Dex-responsive genes that overlap with 'chromaffin-like' genes set,

68.09% were upregulated (significantly higher than the 'Dex-response only' gene set, $z = 6.84$, $P < 0.0001$). In the set of genes that were both 'Dex-responsive' and 'adrenocortical-related,' only 24.65% were upregulated (significantly lower than the 'Dex-response only' group, $z = -3.74$, $P < 0.0002$). (B) GO analysis showed that 864 upregulated genes in the *in vivo* 1-h Dex treatment group were highly associated with neural cell development and function. The fold change used for heatmaps was calculated based on FPKM +0.001. S, saline-treated group; D, Dex-treated group.

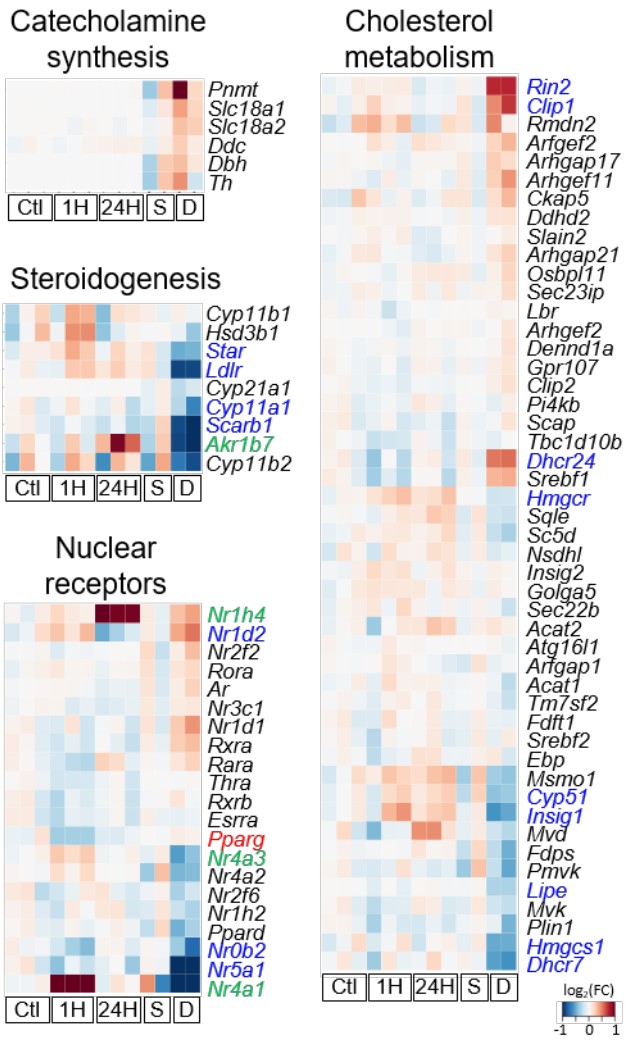

Figure 4.4 Heatmaps of the genes related to adrenal gland functions (catecholamine synthesis and steroidogenesis), cholesterol metabolism, and nuclear receptors in the adrenal gland. Heatmaps show the fold change of Dex-treated groups vs control groups. The fold change was calculated based on FPKM +10 to reduce the influence of low expressing genes. Genes must have an original FPKM > 10 in at least one sample to be included in these heatmaps. Gene names in blue, red, or green were identified as DEGs *in vivo*, *in vitro*, or both groups, respectively. Ctl, vehicle control (*in vitro*); 1H, 1-h Dex-treated group (*in vitro*); 24H, 24-h Dex-treated group (*in vitro*); S, saline-treated group (*in vivo*); D, Dex-treated group (*in vivo*).

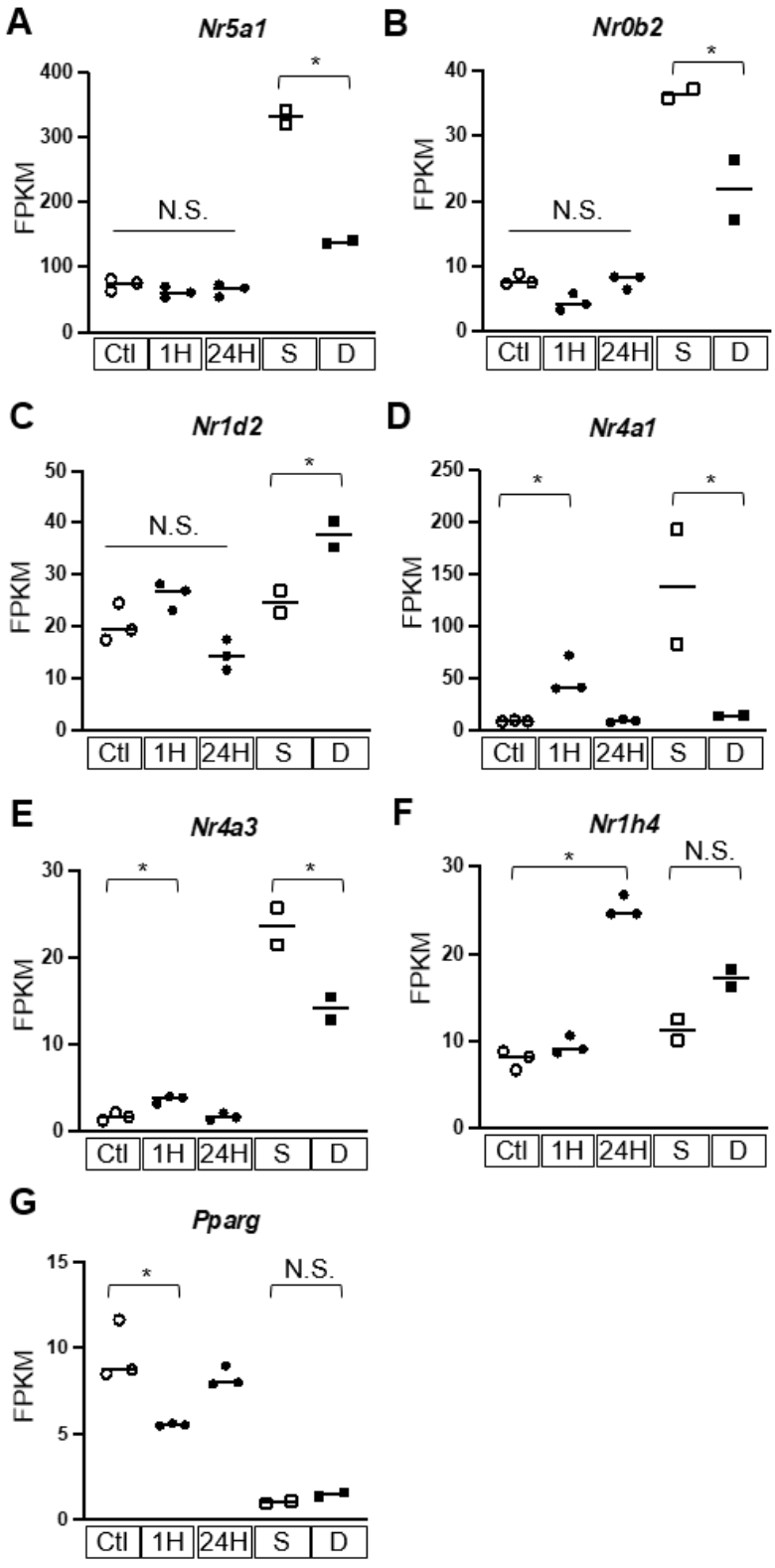
A
Nr5a1
FPKM
400
300
200
100
0
N.S.
*
Ctl
1H
24H
S
D
B
Nr0b2
FPKM
40
30
20
10
0
N.S.
*
Ctl
1H
24H
S
D
C
Nr1d2
FPKM
50
40
30
20
10
0
N.S.
*
Ctl
1H
24H
S
D
D
Nr4a1
FPKM
250
200
150
100
50
0
*
*
Ctl
1H
24H
S
D
E
Nr4a3
FPKM
30
20
10
0
*
*
Ctl
1H
24H
S
D
F
Nr1h4
FPKM
30
20
10
0
*
N.S.
Ctl
1H
24H
S
D
G
Pparg
FPKM
15
10
5
0
*
N.S.
Ctl
1H
24H
S
D

Figure 4.5 Expression of differentially expressed nuclear receptors. Dot plots show FPKM levels with means. *Identified as DEGs using DESeq2 in the RNA-seq; N.S., no significant difference (t-test); Ctl, vehicle control (*in vitro*); 1H, 1-h Dex-treated group (*in vitro*); 24H, 24-h Dex-treated group (*in vitro*); S, saline-treated group (*in vivo*); D, Dex-treated group (*in vivo*).

Table 1 Top differentially expressed genes in adrenal glands in Dex-treated male mice.

Top up-regulated genes

Gene Name	FPKM		Fold
	Saline	Dex.	Change
Abca1	10.2	42.8	4.20
Pdk4	3.0	11.7	3.83
Zbtb16	6.6	25.4	3.83
Chrna7	3.8	14.2	3.79
Ddit4	28.6	107.9	3.77
Fam107a	5.3	19.0	3.60
Nt5e	4.1	13.8	3.40
Fzd4	3.6	11.6	3.25
Greb1	20.3	63.4	3.12
Lrg1	9.2	28.3	3.07
Lnpep	8.2	24.2	2.94
Maf	4.6	13.3	2.87
Tsc22d3	28.3	80.4	2.84
Tbx20	4.8	13.6	2.83
Rin2	6.6	18.2	2.74
Vcam1	9.3	25.4	2.72
AW551984	3.9	10.4	2.70
Dock10	4.1	11.0	2.68
Klf15	9.5	25.5	2.67
Rab3c	8.7	23.1	2.65
Pde10a	6.0	15.8	2.65
Arl4d	5.6	14.5	2.60
Errfi1	14.2	36.6	2.58
Hmgcs2	4.8	12.3	2.54
Atp7a	5.4	13.7	2.54
Fkbp5	47.6	121.0	2.54
Bmp4	5.4	13.7	2.53
Ston1	8.1	20.5	2.52
Ptprn2	5.4	13.6	2.52
Irs2	4.3	10.8	2.49
Bdkrb2	4.5	11.2	2.47
Klhl24	6.0	14.9	2.47
Pdp1	11.9	29.3	2.47
Tgfbr3	38.4	93.2	2.43
Slc9a7	5.0	12.0	2.41
Rims3	5.1	12.3	2.40
Osbpl3	19.7	47.1	2.39
Cebpd	16.7	39.6	2.36
Arrdc2	4.4	10.1	2.32
Adcyap1r1	12.2	28.3	2.31
Klhl11	5.5	12.7	2.31
Ncoa7	5.8	13.4	2.30
Mcf2l	4.8	10.9	2.30
Map3k6	8.7	19.9	2.29

Only genes that have FPKM> 10 in the Dex-treated group are listed.

Top down-regulated genes

Gene Name	FPKM		Fold
	Saline	Dex.	Change
Nr4a1	138.0	14.0	0.10
2010003K11Rik	16.3	3.2	0.20
Gm13889	18.9	4.2	0.22
2010109I03Rik	14.7	4.1	0.28
Tnfrsf12a	225.4	70.5	0.31
Mob4	78.9	25.9	0.33
Apoc4	11.6	3.9	0.34
Coq10b	63.5	21.6	0.34
Cryba4	24.9	9.0	0.36
Yam1	6933.1	2565.2	0.37
Mapkapk3	13.9	5.3	0.38
Fdx1	2978.8	1129.6	0.38
Avpi1	60.7	23.1	0.38
Junb	44.5	17.0	0.38
Ldlr	31.9	12.3	0.38
Hba-a2	17.0	6.7	0.40
Tubb6	121.8	49.0	0.40
Ptp4a1	42.6	17.6	0.41
Smim3	31.0	12.8	0.41
Atf4	146.0	60.9	0.42
Nr5a1	330.6	138.7	0.42
Scx	32.3	13.6	0.42
Dusp10	10.0	4.2	0.42
Hes6	174.1	75.7	0.43
Srrd	11.4	5.0	0.44
Etnk2	22.9	10.1	0.44
Gm10275	16.6	7.5	0.45
Alas1	423.9	191.0	0.45
Tmem120a	29.4	13.6	0.46
Adamts1	12.6	5.9	0.46
Creb3l1	19.1	9.1	0.47
Zswim4	16.5	7.9	0.48
Dusp14	12.4	5.9	0.48
Fam222a	34.9	16.7	0.48
Akr1b7	1279.3	611.1	0.48
Cldn5	11.8	5.7	0.48
Naa38	20.3	9.8	0.48
2310009B15Rik	16.1	7.8	0.48
Agtr1b	13.5	6.6	0.49
RP24-139E15.1	16.4	8.1	0.49
Lsm5	14.5	7.2	0.49
Esm1	18.9	9.3	0.50
Mir22hg	15.2	7.5	0.50
Hbb-bt	19.5	9.7	0.50
Lars2	270.7	134.8	0.50

Only genes that have FPKM> 10 in the Dex-treated group are listed.

Chapter 5: Isolation of cell-type-specific RNAs from snap-frozen heterogeneous tissue samples without cell sorting.

5.1 Abstract

Cellular heterogeneity poses challenges to understanding the function of complex tissues at a transcriptome level. Using cell-type-specific RNAs avoids potential pitfalls caused by the heterogeneity of tissues and unleashes powerful transcriptome analysis. This protocol demonstrates how to use the Translating Ribosome Affinity Purification (TRAP) method to isolate ribosome-bound RNAs from a small number of EGFP-expressing cells in a complex tissue in a mouse animal model. This protocol is suitable for isolating cell-type-specific RNAs using the recently available *NuTRAP* mouse model and could also be used to isolate RNAs from any EGFP-expressing cells.

*This chapter is a revised version of the manuscript published in Journal of Visualized Experiments (Zheng HS, Huang CC. Isolate Cell-Type-Specific RNAs from Snap-Frozen Heterogeneous Tissue Samples without Cell Sorting. JoVE (Journal of Visualized Experiments). 2021 Dec 8(178):e63143).

5.2 Introduction

High-throughput approaches, including RNA sequencing (RNA-seq) and microarray, have made it possible to interrogate gene expression profiles at the genome-wide level. For complex tissues such as the heart, brain, and testis, cell-type-specific data will provide more details compared to the use of RNAs from the whole tissue (255-257). To overcome the impact of cellular heterogeneity, the Translating Ribosome Affinity Purification (TRAP) method has been developed since the early 2010s (258). TRAP is able to isolate ribosome-bound RNAs from specific cell types without cell sorting. This method has been used for translatome (mRNAs that are being recruited to the ribosome for translation) analysis in different organisms, including targeting an extremely rare population of muscle cells in Drosophila embryos (259), studying different root cells in the model plant Arabidopsis thaliana (260), and performing transcriptome analysis of endothelial cells in mammals (261).

TRAP requires a genetic modification to tag the ribosomes of a model organism. Evan Rosen and colleagues recently developed a mouse model called Nuclear tagging and Translating Ribosome Affinity Purification (*NuTRAP*) mouse (262) which has been available through the Jackson Laboratory since 2017. By crossing with a Cre mouse line, researchers can use this *NuTRAP* mouse model to isolate ribosome-bound RNAs and cell nuclei from Cre-expressing cells without cell sorting. In Cre-expressing cells that also carry the *NuTRAP* allele, the EGFP/L10a tagged ribosome allows the isolation of translating mRNAs using affinity pulldown assays. In the same cell, the biotin ligase recognition peptide (BLRP)-tagged nuclear membrane, which is mCherry positive, allows nuclear isolation by using affinity- or fluorescence-based purification. The same research

team also generated a similar mouse line in which the nuclear membrane is labeled only with mCherry without biotin (262). These two genetically modified mouse lines give access to characterization of paired epigenomic and transcriptomic profiles of specific types of cells of interest.

The hedgehog (Hh) signaling pathway plays a critical role in tissue development (263). GLI1, a member of the GLI family, acts as a transcriptional activator and mediates Hh signaling. *Gli1+* cells can be found in many hormone-secreting organs, including the adrenal gland and the testis. To isolate cell-type-specific DNAs and RNAs from *Gli1+* cells using the *NuTRAP* mouse model, *Gli1-CreER^{T2}* mice were crossed with the *NuTRAP* mice. *Shh-CreER^{T2}* mice were also crossed with the NuTRAP mice aim to isolate sonic hedgehog (Shh)-expressing cells. The following protocol shows how to use *Gli1-CreER^{T2};NuTRAP* mice to isolate ribosome-bound RNAs from *Gli1+* cells in adult mouse testes.

5.3 Protocol

The following protocol uses one testis (about 100 mg) at P28 from *Gli1-CreER^{T2};NuTRAP* mice (*Mus musculus*). Volumes of reagents may need to be adjusted based on the types of samples and the number of tissues. All animal experiments followed the protocols approved by the Institutional Animal Care and Use Committee (IACUC) at Auburn University.

1) Tissue Collection

a) Euthanize mice using a CO_2 chamber, and sanitize the abdomen surface with 70% ethanol. Open the lower abdomen with scissors and remove the testes. Snap-freeze freshly dissected testes using liquid nitrogen (LN_2) immediately upon collection.

b) Samples are stored in the vapor phase of LN2 until use.

2) Reagent and Bead Preparation

a) Prepare the homogenization stock solution: 50 mM Tris (pH7.4), 12 mM $MgCl_2$, 100 mM KCl, 1% NP-40, and 1 mg/ml heparin. Store at 4 °C until use (up to 1 month).

b) Prepare the homogenization working buffer from the homogenization stock solution freshly before use: Add DTT (1 mM), cycloheximide (100 μg/ml), recombinant ribonuclease (final concentration: 200 units/ml), and protease inhibitor cocktail (final concentration: 1X) to the homogenization stock solution to make the required amount of the homogenization working buffer. Store the freshly prepared working buffer on ice until use.

c) Prepare the low-salt and the high-salt wash buffers: The low-salt wash buffer contains 50mM Tris (pH7.4), 12 mM $MgCl_2$, 100 mM KCl, 1% NP-40. Add 1 mM DTT and 100 μg/ml cycloheximide before use. The high-salt wash buffer contains 50mM Tris (pH7.4), 12 mM $MgCl_2$, 300 mM KCl, 1% NP-40. Add 2 mM DTT and 100 μg/ml cycloheximide before use.

d) Prepare protein G beads: Each sample will need 50 μl of protein G beads. Place the required volume of beads in a 1.5 ml centrifuge tube and separate the beads from the solution on a magnetic rack. Remove the supernatant after 30-60 s. Wash beads three times with 1 ml of ice-cold low-salt wash buffer.

3) Tissue Lysis and Homogenization

a) Add 2 ml ice-cold homogenization working buffer (freshly prepared from 2b) to a glass tissue grinder set. Quickly place the frozen sample into the grinder and homogenize the tissue with 30 strokes on ice using a loose pestle.

b) Transfer homogenate to a 2 ml round-bottom tube and centrifuge at 12,000 x g for 10 min at 4°C.

c) Transfer the supernatant to a new 2 ml tube. Save 100 µl as the "input."

d) Incubate the supernatant with the anti-GFP antibody (5 µg/ml; 1:400) at 4°C on an end-over-end rotator (24 rpm) overnight.

4) Immunoprecipitation

a) Transfer the homogenate/antibody mixture to a new 2 ml round-bottom tube containing the washed protein G beads from 2d. Incubate at 4°C on an end-over-end rotator (24 rpm) for 2 h.

b) Separate magnetic beads from the supernatant using a magnet rack. Save the supernatant as the "negative fraction". The negative fraction contains (1) RNAs from EGFP-negative cells, and (2) RNAs from EGFP-positive cells that are not bound to ribosomes.

c) Add 1 ml of high-salt wash buffer to the beads and briefly vortex the tube to wash the beads. Place the tube in a magnet rack. Remove the wash buffer. Repeat the washing step two more times. The beads now contain the beads-ribosome-RNA complex from EGFP-positive cells.

5) RNA extraction

The following steps are adapted from the RNA isolation kit (PicoPure, CA, USA). Treat each fraction (*i.e.*, input, positive, and negative) as an independent sample and isolate RNAs independently.

a) Incubate beads from 4c with 50 µl Extraction Buffer (from the RNA isolation kit) in a thermomixer (42°C, 500 rpm) for 30 min to release RNAs from beads.

b) Separate the beads with a magnet rack, transfer the supernatant which contains the mRNA was captured ribosomes to a 1.5 ml tube. Centrifuge the tube at 3000 x g for 2 min, then pipette the supernatant to a new 1.5 ml tube. This tube contains the "positive fraction" of the TRAP step.

Note: For the input and the negative fractions, extract RNA from 25 µl of samples using 1 ml Extraction Buffer. Incubate in a thermomixer (42°C, 500 rpm) for 30 min.

c) Pre-condition the RNA purification column: Pipette 250 µl Conditioning Buffer onto the purification column. Incubate for 5 min at room temperature (RT). Centrifuge the column at 16,000 x g for 1 min.

d) Pipette equal volume (around 50 µl for the positive fraction and 1 ml for the input and the negative fractions) of 70% EtOH into the cell extract from Step 5b. Mix well by pipetting up and down.

e) Pipette the mixture into the column from step 5c.

f) Centrifuge at 100 x g for 2 min, then centrifuge at 16,000 x g for 30 s immediately. Discard the flow-through.

Note: For the input and the negative fractions, add 250 µl of the mixture to the column each time. Repeat Steps 5e and 5f until all mixtures are used.

g) Pipette 100 µl Wash Buffer 1 (W1) into the column and centrifuge at 8,000 x g for 1 min. Discard the flow-through.

h) Pipette 75 µl DNase solution mix directly onto the purification column membrane. Incubate at RT for 15 min.

i) Pipette 40 µl W1 into the column and centrifuge at 8,000 x g for 30 s. Discard the flow-through.

j) Pipette 100 µl Wash Buffer 2 (W2) into the column and centrifuge at 8,000 x g for 1 min. Discard the flow-through.

k) Pipette 100 µl W2 into the column and centrifuge at 16,000 x g for 2 min. Discard the flow-through. Re-centrifuge the column at 16,000 x g for 1 min to remove all traces of wash buffer prior to the elution step.

l) Transfer the column to a new microcentrifuge tube.

m) Pipette 12 µl RNase-free water directly onto the membrane of the purification column. Incubate at RT for 1 min. Centrifuge at 1000 x g for 1 min, then centrifuge at 16,000 x g for 1 min to elute RNA.

6) RNA Concentration and Quality

Use a bioanalyzer to assess the quality and quantity of the extracted RNA (264).

7) Storage and Further Analysis

Store RNA at -80 °C (up to one year) until further analysis (e.g., microarray, quantitative PCR (qPCR), and RNA-seq, etc.). Details of qPCR analysis, including cDNA synthesis, were described in our previous publication (149). Primers for qPCR are listed in Table 2 (Table of Materials).

5.4 Results

Gli1-CreER^{T2} mice (Jackson Lab Stock Number: 007913) were first crossed with the *NuTRAP* reporter mice (Jackson Lab Stock Number: 029899) to generate double-mutant mice. Mice carrying both genetically engineered gene alleles (i.e., *Gli1-CreER^{T2}* and *NuTRAP*) were injected with tamoxifen (1 mg/10 g body weight each) once a day, every other day, for three injections. Tissue samples were collected on the 7th day after the first day of the injection. Immunofluorescence analysis showed that the EGFP was expressed in interstitial cells in testes (Fig. 1). The adrenal gland capsule has been shown to be another cell population positive for Gli1 (59,60). EGFP was also found in adrenal capsular cells in *Gli1-CreER^{T2};NuTRAP* mice (Fig. 1). Our lab also carries *Shh-CreER^{T2};NuTRAP* mice. Note that in *Shh-CreER^{T2};NuTRAP* mice, the *EGFP+* cell population resides in the outer cortex of the adrenal gland underneath the capsule (Figure 5.1), the same expression site of *Shh+* cells (60), confirming the expression of EGFP in Cre-expressing cells.

After the extraction of the cell-type-specific RNAs, the quantity and quality of isolated RNAs from one testis were assessed using a bioanalyzer (Figure 5.2). The bioanalyzer result indicates that this protocol is able to obtain high-quality RNAs from all three fractions. All fractions have a similar RNA Integrity Number (RIN).

We sent the extracted RNA for microarray analysis using a commercial microarray service (mouse Clariom S Assay, ThermoFisher Scientific, CA, USA). The microarray result showed that about

3,000 genes were enriched in the positive fraction comparing to genes in the negative fraction, whereas about 4,000 genes were enriched in the negative fraction (Figure 5.3). Among these differentially expressed genes, Leydig-cell-associated genes *Hsd11b1* and *Hsd3b6* (265,266) were enriched in the positive fraction, whereas the Sertoli-cell-associated genes *Dhh* and *Gstm6* (267,268) were enriched in the negative fraction. Only a few differentially expressed genes were identified when comparing the negative fraction with the input.

Real-time quantitative RT-PCR (qPCR) was also used to confirm the expression of key genes in the positive fraction and the negative fraction. Similar to what was found in the microarray assay, RNAs encoding steroidogenic enzymes 3β-hydroxysteroid dehydrogenase (encoded by *Hsd3b*) and cholesterol side-chain cleavage enzyme (encoded by *Cyp11a1*) were enriched in the positive fraction, while RNAS encoding the Sertoli cell marker *Sox9* (Syr-box transcription factor 9) and the germ cell marker Synaptonemal complex protein 3 (encoded by*Sycp3*) were enriched in the negative fraction (Figure 5.4). Together these data demonstrate that the transcriptomes in *Gli1+* cells were successfully enriched by the above protocol.

5.5 Discussion

The usefulness of whole-tissue transcriptome analysis could be dampened, especially when studying complex heterogeneous tissues. The ability to obtain cell-type-specific RNAs becomes an urgent need to unleash the powerful RNA-seq technique. The isolation of cell-type-specific RNAs usually relies on the collection of a specific type of cells using micromanipulation, fluorescent-activated cell sorting (FACS), or laser capture microdissection (LCM) (269). Other

modern high-throughput single-cell collection methods and instruments have also been developed (270). These methods usually employ the microfluidics techniques to barcode single cells followed by single-cell RNA-seq. Cell dissociation is the required step to obtain the suspended cell solution which then will go through either a cell sorter or a microfluidic device to barcode each cell. The cell dissociation step introduces challenges to these methods for cell-type-specific studies because the enzymatic treatment not only breaks down tissues but also affects cell viability and transcriptional profiles (271). Moreover, the expense for single-cell RNA-seq is usually high and requires specialized equipment on site.

Recently, two studies successfully isolated specific cell types from whole tissues using the *NuTRAP* mice (262,272). Without using specific equipment and tools, the *NuTRAP* mouse model allows obtaining RNAs and DNAs from specific types of cells. The *NuTRAP* allele could target Cre-expressing cells without requiring dissociation of tissues into single cells, thus avoiding effects on cell viability and transcriptional profiles. Rol *et al*. used the *NuTRAP* mouse model to isolate nuclei and translating mRNA simultaneously from adipose tissue. The other study also demonstrated that the *NuTRAP* mouse model could work for glial cells in the central nervous system.

In our lab, we are interested in studying the stem cell populations in steroidogenic tissues such as *Gli1+* interstitial cells in the testis (273) and *Gli1+* capsular cells in the adrenal gland (60). The challenge of studying *Gli1+* cells in these two organs is that their numbers are small. Because the TRAP technique aims to specifically pull down translating ribosome-bound RNAs in a complex tissue, the *NuTRAP* mouse model could be a powerful tool suitable for studying a rare cell

population in a complex tissue (274). The previously published protocols using *NuTRAP* mice target adipocytes and glial cells that are more abundant in the brain and the adipose tissue comparing to *Gli1+* cells in the testis and the adrenal gland. To ensure obtaining required RNAs from a small number of cells in a complex tissue, we revised the existing protocols by (1) increasing the incubation time with the GFP antibody from one hour to overnight; (2) using another type of RNA extraction kit which aims to isolate a small amount of RNA at a picogram level.

We demonstrated that our protocol is able to obtain high-quality cell-type-specific RNAs from a small number of cells in a complex tissue. The quality and quantity of extracted RNAs are suitable for qPCR and a commercial microarray service. Results from microarray and qPCR confirmed that Leydig-cell-associated RNAs are enriched in the positive fraction coming from one testis in an adult mouse in which the targeted cell population only occupies 3.8% of the testis volume. We here provided a detailed protocol to isolate cell-type-specific translating ribosome mRNAs using the *NuTRAP* mouse model. This protocol may also be used to isolate RNAs from any cells in which the ribosomes are tagged with EGFP.

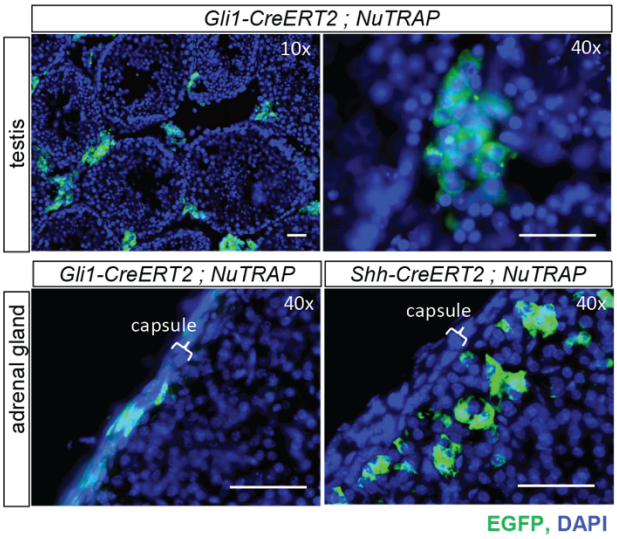

Figure 5.1 Immunofluorescence images of the EGFP expression in 6-month-old *NuTRAP* reporter mice. The *Gli1-CreER^{T2};NuTRAP* or the *Shh-CreER^{T2};NuTRAP* mice were treated with tamoxifen to activate the EGFP expression. In the testis, *Gli1+* cells were in the interstitium, whereas in the adrenal gland, *Gli1+* cells were in the adrenal capsule. In the adrenal gland, cells underneath the capsule were positive for SHH which is the ligand of the SHH signaling pathway eliciting its function in *Gli1+* capsular cells (60). Scale bars: 50 µm.

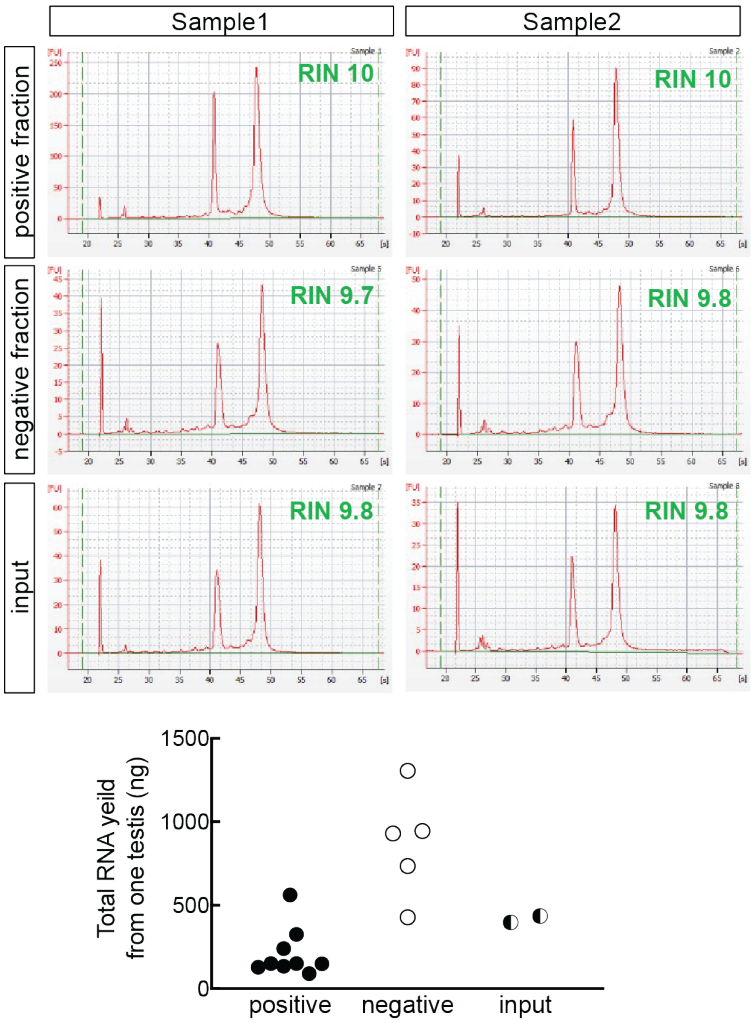

Figure 5.2 RNA quality and quantity from the TRAP extraction. RNAs of the positive fraction, the negative fraction, and the input were evaluated using an Agilent bioanalyzer. The positive fraction contains RNAs extracted from protein G beads after the incubation with the GFP antibody (Step 4c). The negative fraction contains RNAs that remain in the supernatant at Step 4b. The input contains RNAs from the homogenate (Step 3c. In the electropherogram, because the concentrations of the lower marker (displayed as the first peak at 20-25 seconds of the migration time of samples shown on the X-axis) and the ladder (not shown in these electropherograms) are known, the concentration of each sample can be calculated. The two

major peaks at 40-50 seconds represent the 18S and 28S rRNA. The ribosomal ratio (based on the fluorescence intensity shown on the Y-axis) is used to determine the integrity of the RNA sample. The RNA Integrity Number (RIN) of each sample is shown on the top right corner of each plot. The dot plot shows the amount of RNA that was extracted from one single testis. The amount of RNA of each sample in the negative fraction and the input was extracted from 25 µL of samples.

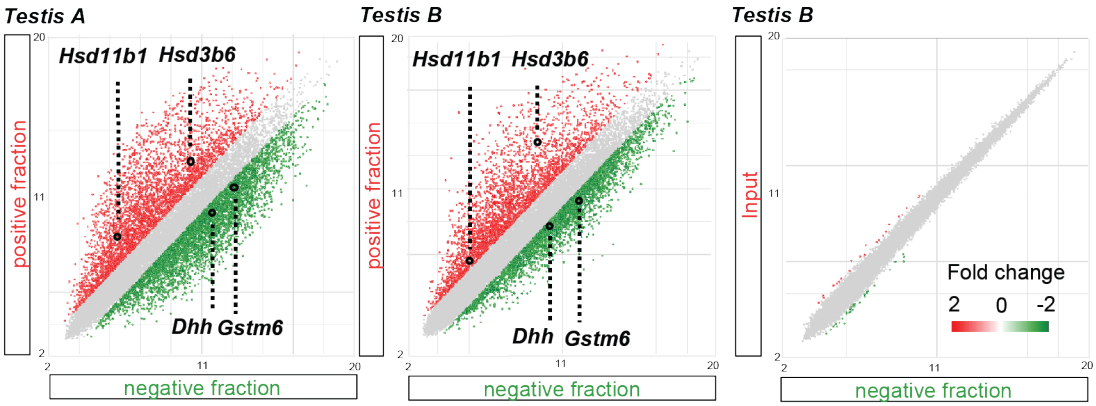

Figure 5.3 Microarray analysis for TRAP samples from P28 mice. Results of two extractions (one testis each) were shown. The microarray analysis identified a similar number of differentially expressed genes from each extraction. Around 4,000 genes were enriched (red dots) in the positive fraction, whereas ~3,000 genes were enriched (green dots) in the negative fraction. *Hsd11b1* and *Hsd3b6* were enriched in positive fractions. *Dhh* and *Gstm6* were enriched in negative fractions. Only a few genes were identified as differentially expressed genes between the negative fraction and the input, suggesting the testis only contains a very small number of *Gli1+* cells.

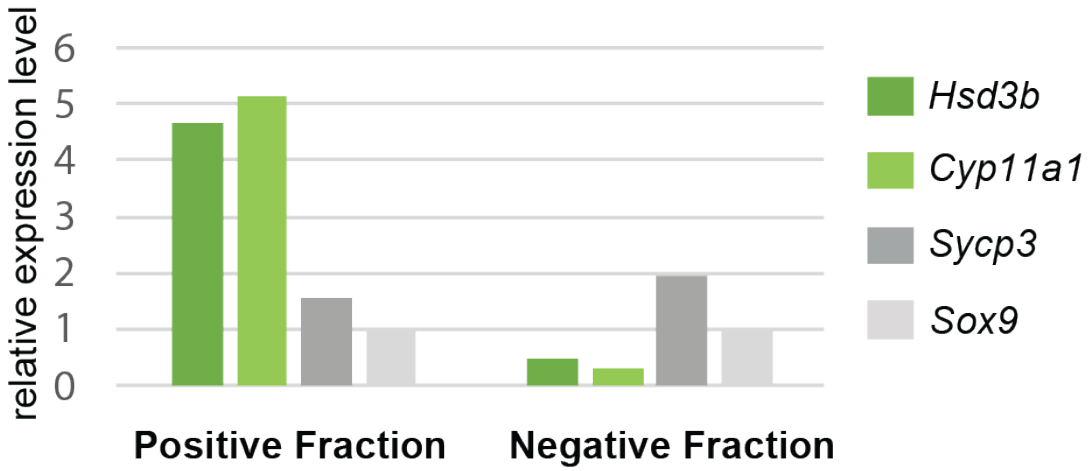

Figure 5.4 qPCR analysis for TRAP samples. qPCR analysis showed the relative expression of cell-type-specific genes in the positive fraction and the negative fraction. The expression of each gene was normalized with *Actb*. The relative expression in each fraction was then calculated based on the expression of *Sox9* (set as 1). Note that the relative expression of target genes can only be compared within each fraction. *Hsd3b* and *Cyp11a1*, which encode steroidogenic enzymes, were enriched in the positive fraction. *Sycp3* and *Sox9*, marker genes for germ cells and Sertoli cells, were enriched in the negative fraction. Two biological replicates were examined, and a similar trend was observed. Data from only one testis is shown here.

Table 2. Table of Materials

Name	Company	Catalog Number	Comments
Actb	eurofins	qPCR primers	ATGGAGGGGAATACAGCCC / TTCTTTGCAGCTCCTTCGTT (forward primer/reverse primer)
Bioanalyzer	Agilent	2100 Bioanalyzer Instrument	
cOmplete Mini EDTA-free Protease Inhibitor Cocktail	Millipore	11836170001	
cycloheximide	Millipore	239764-100MG	
Cyp11a1	eurofins	qPCR primers	CTGCCTCCAGACTTCTTTCG / TTCTTGAAGGGCAGCTTGTT (forward primer/reverse primer)
dNTP	Thermo Fisher Scientific	R0191	
DTT, Dithiothreitol	Thermo Fisher Scientific	P2325	
DynaMag-2 magnet	Thermo Fisher Scientific	12321D	
Falcon tubes 15 mL	VWR	89039-666	
GFP antibody	Abcam	ab290	
Glass grinder set	DWK Life Sciences	357542	
heparin	BEANTOWN CHEMICAL	139975-250MG	
Hsd3b	eurofins	qPCR primers	GACAGGAGCAGGAGGGTTTGTG / CACTGGGCATCCAGAATGTCTC (forward primer/reverse primer)
KCl	Biosciences	R005	
$MgCl_2$	Biosciences	R004	
Microcentrifuge tubes 2 mL	Thermo Fisher Scientific	02-707-354	
Mouse Clariom S Assay microarrays	Thermo Fisher Scientific		Microarray service
NP-40	Millipore	492018-50 Ml	
oligo (dT)20	Invitrogen	18418020	
PicoPure RNA Isolation Kit	Thermo Fisher Scientific	KIT0204	
Protein G Dynabead	Thermo Fisher Scientific	10003D	
RNase-free water	growcells	NUPW-0500	
RNaseOUT Recombinant Ribonuclease Inhibitor	Thermo Fisher Scientific	10777019	
Sox9	eurofins	qPCR primers	TGAAGAACGGACAAGCGGAG / CTGAGATTGCCCAGAGTGCT (forward primer/reverse primer
Superscript IV reverse transcriptase	Invitrogen	18090050	
SYBR Green PCR Master Mix	Thermo Fisher Scientific	4309155	
Sycp3	eurofins	qPCR primers	GAATGTGTTGCAGCAGTGGGA / GAACTGCTCGTGTATCTGTTTGA (forward primer/reverse primer)
Tris	Alfa Aesar	J62848	

Chapter 6: Lineage tracing sonic hedgehog-expressing cells in adrenal glands in post-weaning mice

6.1 Abstract

The Sonic Hedgehog (Shh) gene expressed in the subcapsular cortical region of the adrenal gland has been found to play a role in adrenal gland development. The *Shh*-positive cell population at the fetal stages contributes to different cortical layers in the adrenal gland. However, the (1) capability of these cells after weaning and (2) how soon they can renew the adrenal cortex in the postnatal stages is not fully understood. Here, we conducted a lineage tracing experiment to track *Shh*-positive cells and cells descended from them in post-weaning mice to ultimately better understand the processes of adrenal cortex renewal and remodeling over time in young adult mice. This experiment used *Shh-CreER^{T2};NuTRAP* mice as a Shh-reporter mouse model. This lineage tracing experiment found that *Shh*-positive cells and their descendant cells reached the margin of the CYP2F2-positive cortical zone in 2 months and the cortical-medullary boundary in 4 months. This finding indicates that the *Shh*-positive cell population in post-weaning mice can proliferate, differentiate, and eventually renew the entire adrenal cortex over a four-month period of time.

6.2 Introduction

As a critical endocrine organ, the adrenal cortex is responsible for generating various steroid hormones based on various physiological needs. ZG produces aldosterone which regulates sodium balance and blood volume and thus has an impact on blood pressure. ZF generates glucocorticoids, hormones that play a crucial role in the immune system response and glucose metabolism. In humans, ZR is responsible for the production and secretion of androgens. In mice, the ZR, located in the inner cortex zone, has a similar structure, but its function is still unknown. Given that the steroid hormones are essential for survival, the adrenal cortex must be constantly sustained throughout life. To keep up with this ongoing renewal, the adrenal cortex relies on populations of stem/progenitor cells.

The Hh signaling pathway plays a vital role in the growth and formation of various tissues during embryonic development (275). SHH, one of the three Hh proteins, is a secreted glycoprotein that initiates signaling in target cells. When the Shh ligand is present, PTCH loses the ability to inhibit SMO at the primary cilium. This leads to the transportation of Gli family transcription factors to the nucleus (276). In the adrenal cortex, *Shh* is expressed in the subcapsular cortical region (59,60). During mouse embryogenesis, cells that express *Shh* start to appear as early as E12.5 (59,60). These cells also contribute to the formation of different cortical layers in the adrenal gland. However, the capability of these cells after weaning and how soon they can renew the adrenal cortex in the postnatal stages is not fully understood. To better understand the processes of adrenal cortex renewal and remodeling over time in young adult mice, a lineage tracing experiment was conducted to track *Shh*-positive cells and cells descended from them in post-weaning mice.

6.3 Materials and Methods

6.3.1 Animals To generate *Shh-CreER^{T2};NuTRAP* mice, *Shh-CreER^{T2}* mice were crossed with *NuTRAP* reporter mice. All mice were housed in a 12:12 h light-dark cycle (lights on at 6 am) with free access to Envigo Teklad Global 18% protein rodent chow and water until sample collection. Tissue was harvested at the age of 1 month, 2 months, or 4 months. Before tissue collection, mice were euthanized between 2 pm and 4 pm using carbon dioxide, followed by decapitation. Tissues were collected immediately and fixed in ice-cold 4% (v/v%) paraformaldehyde (PFA) in 1X phosphate-buffered saline (PBS) or frozen in liquid nitrogen. All procedures followed the protocols approved by the Institutional Animal Care and Use Committee at Auburn University.

6.3.2 Tamoxifen (Tam) treatment On three days, at postnatal days (P)22, P24, and P26, mice were administered tamoxifen (1 mg/10 g body weight each, #T5648; Millipore Sigma, St. Louis, MO) through oral gavage. Tamoxifen was dissolved in 100% corn oil.

6.3.3 Immunohistochemistry Tissues were fixed at 4°C overnight and processed according to standard immunostaining procedures (149). For cryosection preparation, tissues were fixed using 4% (vol/vol) buffered paraformaldehyde at 4°C overnight and rinsed three times in phosphate-buffered saline (PBS) at 4°C, 10 min each. Samples were infiltrated with 30% sucrose overnight at 4°C on a shaker. After tissues sink to the bottom of the vial (usually over 24 hours), they were put into OCT and stored at -80°C. Sections (8 μm) were mounted onto positive charged slides and rinsed in PBS. In short, paraffin-embedded sections or cryosections were incubated with primary antibodies (anti-DHCR24, #sc-398938, RRID: AB_2832944, 1:100, anti-CYP2F2, #sc-374540, RRID: AB_10987684, 1:250; anti-EGFP, RRID: AB290, 1:500; anti-AKR1B7, 1:500) followed by

appropriate fluorescein-conjugated secondary antibodies. DHCR24 was detected by a biotinylated secondary antibody followed by a fluorescent tyramide (175). Fluorescent images were obtained using a Revolve 4 microscope (ECHO). ImageJ (http://rsb.info.nih.gov/ij/) was used for adjusting the brightness and contrast.

6.4 Results

6.4.1 *Shh*-expressing cells migrate from the outer cortex to the inner cortex of adrenal gland.

To shed light on the cellular dynamics involved in maintaining the stability of the adrenal cortex after weaning of mice, we used *Shh-CreER^{T2};NuTRAP* mice as the Shh-reporter mouse model. Tamoxifen was given at P22, P24, and P26 to enable the Cre recombinase activity driven by the Shh promoter (Figure 6.1A). Adrenal glands were then analyzed at the age of 1, 2, and 4 months. In male mice, shortly after tamoxifen induction, cells expressing *Shh* at the time of induction (GFP-labeled) are located mainly in the outer cortex zone of the adrenal gland. Over time, the number of GFP-positive cells increased and the entire cortex and was replaced with GFP-positive cells by 4 months of age both in males and females (Figure 6.1B, C).

6.4.2 Female-specific recruitment of outer cortex progenitor cells.

To address how the *Shh*-positive cells at the time of tamoxifen induction contribute to the adrenal cortex, we detected 3βHSD, an adrenal steroidogenesis marker and AKR1B7, a ZF marker, in the lineage tracing reporter mice. At 2 months of age, GFP-positive cells reached the middle of the adrenal cortex. Most of them were 3βHSD-positive and AKR1B7-positive (Figure 6.2A). We found that more GFP-positive cells became 3βHSD- and AKR1B7-positive cells at 4 months of age (Figure

6.3A). Some 3βHSD- and AKR1B7-positive cells were not GFP-positive. We also detected CYP2F2-positive and DHCR24-positive cells in the lineage tracing mice. Within 1 month after induction, GFP-positive cells had not reached the inner cortex zone, and CYP2F2-positive and DHCR24-positive cells were negative for GFP (Figure 6.2B). However, by after 3 months after induction, the GFP-positive cells reached the inner cortex, and a small proportion of them became CYP2F2 and DHCR24-positive (Figure 6.3B).

6.5 Discussion

Examining tissue homeostasis is a crucial goal when exploring aging, the response to tissue damage, and even its connection to cancer. The proliferation ability in the outer cortex and the migration of cells towards the cortico-medullary boundary indicate a mechanism to fulfill the need for rapid replacement within the adrenal cortex. Previous studies showed that *Shh*-expressing progenitor cells contribute to ZG and ZF zone using lineage tracing analysis at embryonic stages (59,60). In this study, we demonstrated that the *Shh*-positive cell population, even in post-weaning mice, has the ability to proliferate, differentiate, and renew the entire adrenal cortex over a three-month period.

Even in the context of the rapid turnover of the adrenal cortex, differences are observed in stem cell dynamics between males and females. Dumontet, *et al*., published a paper highlighting sex differences in the migration of adrenal steroidogenic cells during the postnatal period, as female mice exhibit quicker adult cortical cell regeneration compared to male mice with adrenal definite zone knockout from birth (215). An *Axin2-CreER*^{T2} lineage tracing study identified a stem and/or progenitor compartment located within the adrenal capsule and demonstrated that female mice

exhibit a 3-fold higher turnover rate compared to males (277). Our research presented here indicates no apparent sex difference regarding the renewal rate of progenitor cells in the adrenal cortex. Our results are consistent with previous studies that showed that the adrenal cortex undergoes replacement approximately every three months at least in female (215). Despite the observation that *Shh*-expressing progenitor cells can migrate centripetally and become part of the adrenal cortex, ablation of these cell populations does not affect steroidogenesis (60). The function of *Shh*-expressing progenitor cells in the adrenal cortex requires further investigation. The nuclear tagging and translating ribosome affinity purification (*NuTRAP*) system was first introduced by Roh *et al*. (262), and subsequently, other researchers successfully used it for labeling and isolating ribosomes and nuclei in the central nervous system (CNS) (272). The *Shh-CreER^{T2};NuTRAP* mouse model used in this experiment also allows for the isolation of cell-type-specific DNA/RNA, enabling further deciphering of the underlying genes/pathways that control the progenitor cell population of the adrenal gland cortex.

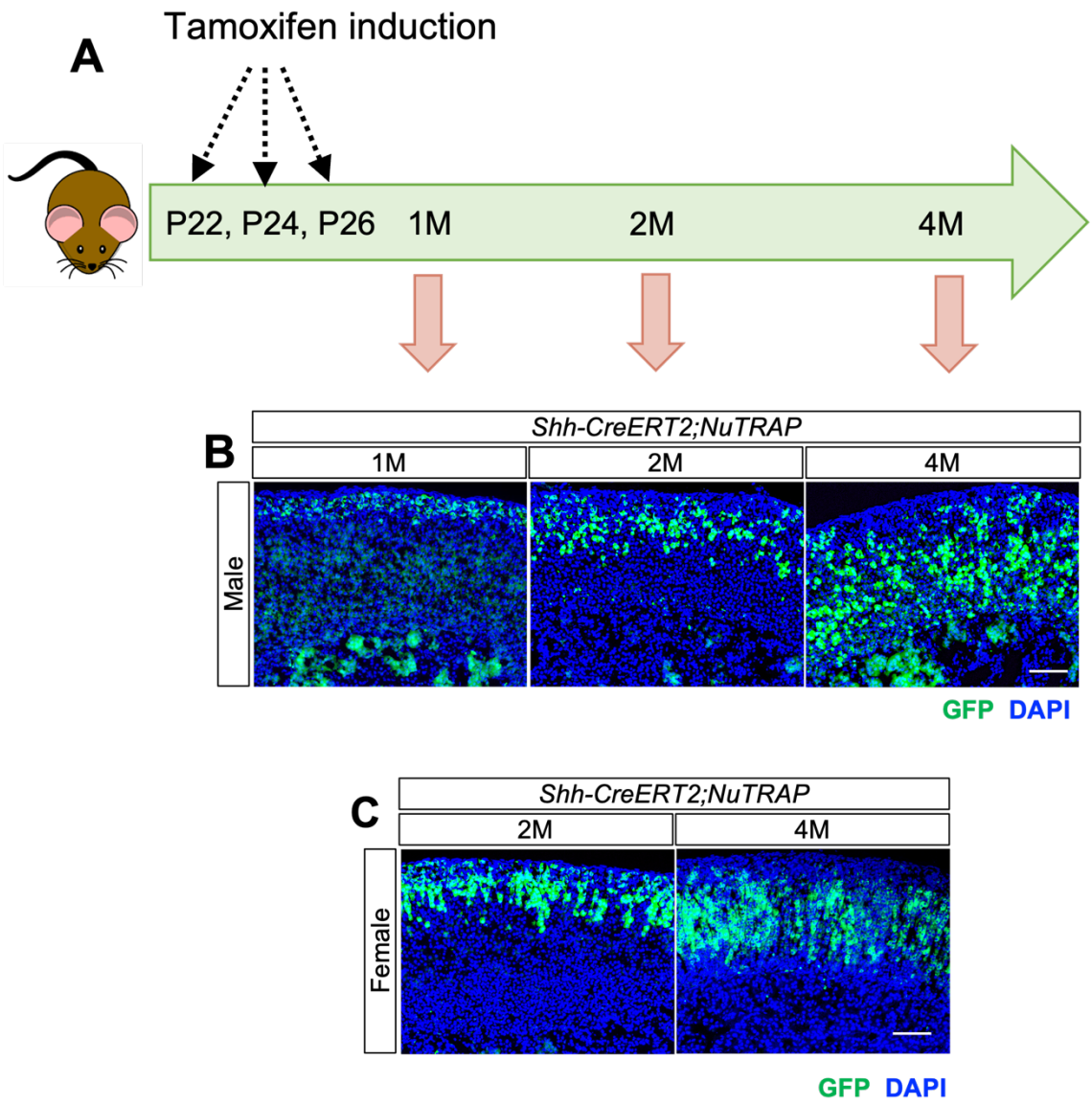

Figure 6.1 Cell lineage analysis (*Shh-CreER^{T2};NuTRAP*) for male and female mice. (A) Schematic diagram of tamoxifen treatment schedule. (B) Cells that were expressing *Shh* at the time of tamoxifen induction (P22-P26), marked by endogenous EGFP, are shown in 1, 2- and 4-month-old male mice. (C) *Shh*-expressing cells at the time of tamoxifen induction are shown in 2- and 4-month-old female mice. Scale bar, 100 µm.

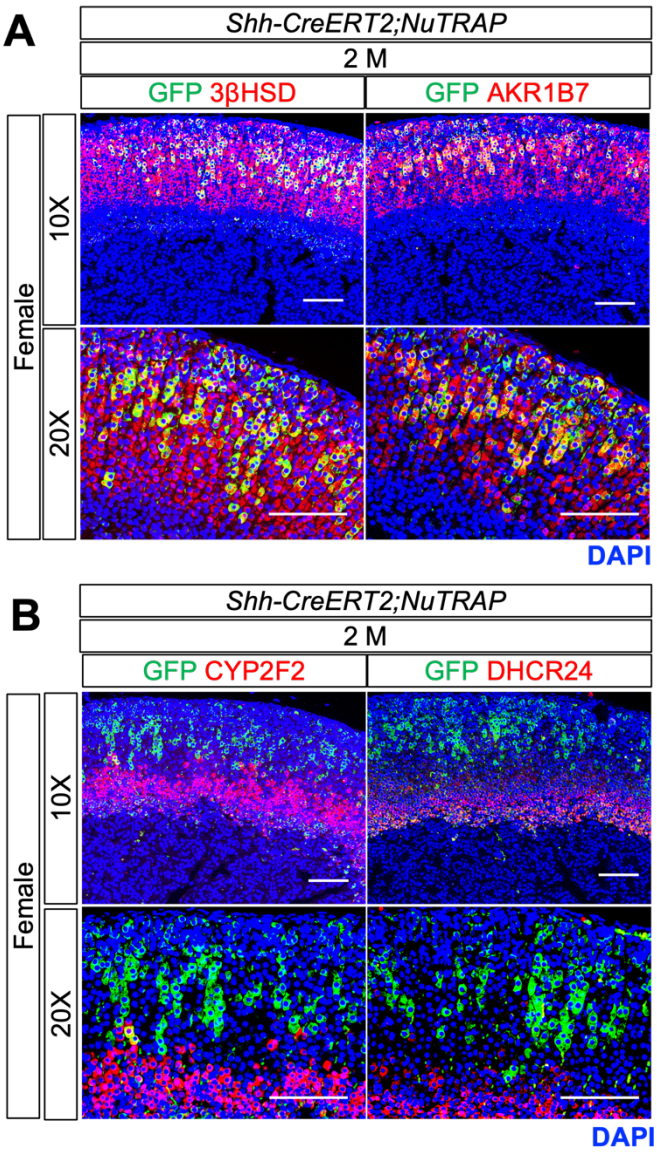

Figure 6.2 Cell lineage tracing at 2 months of age in females. (A) *Shh*-expressing cells at the time of tamoxifen induction co-immunostained with outer cortex markers at 2 months. (B) *Shh*-expressing cells at the time of tamoxifen induction co-immunostained with inner cortex markers at 2 months. Scale bar, 100 µm.

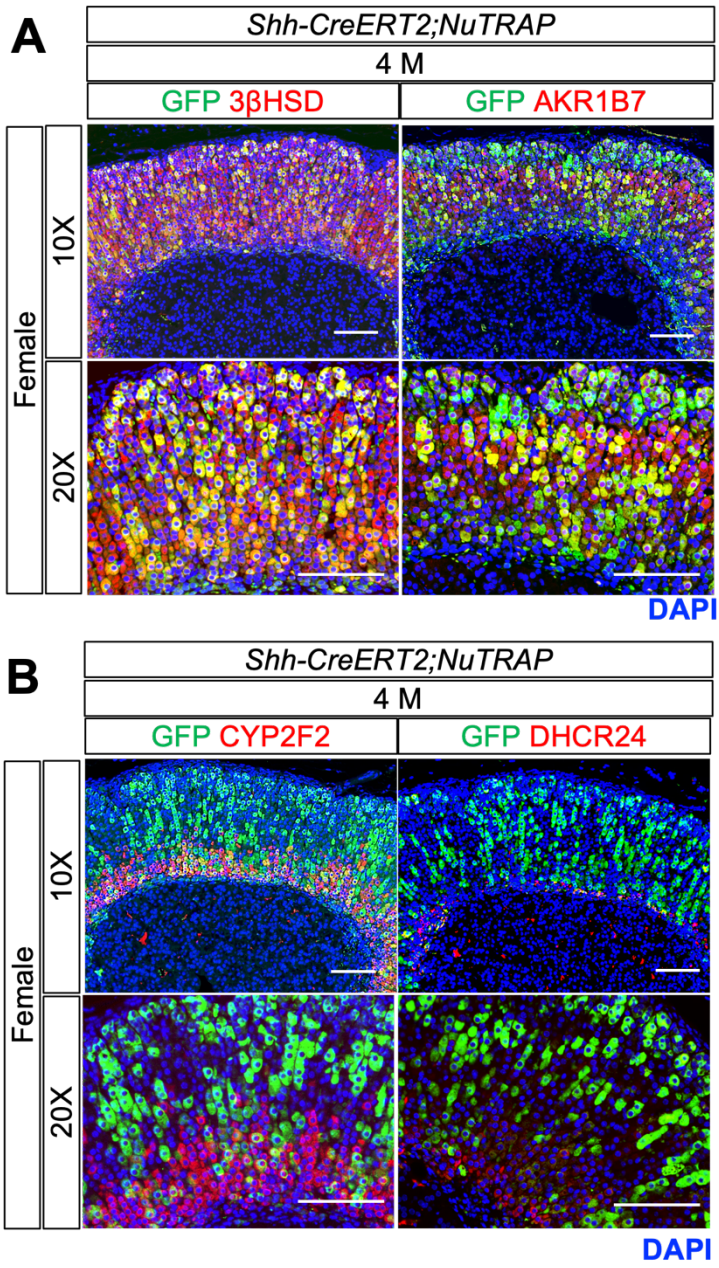

Figure 6.3 Cell lineage tracing at 4 months of age in females. (A) *Shh*-expressing cells at the time of tamoxifen induction coimmunostained with outer cortex markers at 4 months of age. (B) *Shh*-expressing cells at the time of tamoxifen induction coimmunostained with inner cortex markers at 4 months of age. Scale bar, 100 µm.

Conclusions

The adrenal cortex, an endocrine gland, consists of three unique regions: the zona glomerulosa, zona fasciculata, and zona reticularis (also known as the X-zone in mice). This organ is vital for maintaining homeostasis in adults by producing steroid hormones. To fulfill the hormonal requirements for steroid synthesis, it possesses the capability to naturally replenish aging cells. Cells in the innermost zone are considered as an aged cell population and ultimately undergo apoptosis. The factors that manipulate the cell fate of the aged cell population are not fully understood. In my thesis, I would like to answer three basic questions as follows: 1) What factors affect the aged cell population's fate? 2) What are the potential functions of the aged cell population? 3) What is the origin of the aged cell population?

Thyroid hormone exerts important functions on tissue development by binding to thyroid hormone receptors (TRs) in nucleus. The nuclear receptor corepressor (*Ncor1*) is known as the main corepressor that interacts with TRs. In the absence of thyroid hormone, NCOR1 is recruited by TRs to inhibit gene transcription. In chapter 2, we employed tissue-specific gene editing approaches to remove the *Ncor1* gene in adrenocortical cells of the adrenal gland. The removal of *Ncor1* was demonstrated to postpone the cell regression of the adrenal inner cortex.

Our previous study has demonstrated that thyroid hormone increased the expression of cholesterol synthesis-associated genes, and *Dhcr24* was one of these genes. In chapter 3, we also employed tissue-specific gene editing approaches to remove *Dhcr24* in adrenocortical cells of the

adrenal gland. *Dhcr24* acted as a master regulator of T3-mediated lipid accumulation and delayed cell regression in the adrenal inner cortex. The inner cortex zone could potentially serve as a backup tissue for steroidogenesis.

Glucocorticoids have short- and long-term effects on adrenal gland function and development. In chapter 4, RNA sequencing (RNA-seq) was performed to identify early transcriptomic responses to the synthetic glucocorticoid, dexamethasone (Dex), *in vitro* and *in vivo*. Adrenocortical Y-1 cells had a transient early response to Dex treatment *in vitro*. Furthermore, the differentially expressed genes (DEGs) had a minimal overlap with those in the 1-h Dex-treated group *in vivo* and *in vitro*.

Sonic hedgehog (SHH) protein is expressed in the subcapsular cortical region of the adrenal cortex. *Shh*-positive cells subsequently contribute to the formation of different cortical layers. In chapter 6, we conducted a lineage tracing experiment to track *Shh*-positive cells in post-weaning mice. It has been shown that the adrenal cortex undergoes replacement about every three months. Cells Shh-positive at 22-26 days of age reached the inner cortex and a small part of them become inner cortex marker positive cells. In chapter 5, we used a similar lineage tracing experiment to study the role of *Gli1* in another steroidogenesis organ, the testis. We successfully isolated cell-type-specific RNAs from heterogeneous tissue samples without cell sorting.

References

1. Gruenwald P. Embryonic and postnatal development of the adrenal cortex, particularly the zona glomerulosa and accessory nodules. *Anat Rec*. 1946;95:391-421.
2. Mesiano S, Jaffe RB. Developmental and functional biology of the primate fetal adrenal cortex. *Endocr Rev*. 1997;18(3):378-403.
3. Keegan CE, Hammer GD. Recent insights into organogenesis of the adrenal cortex. *Trends Endocrinol Metab*. 2002;13(5):200-208.
4. Hatano O, Takakusu A, Nomura M, Morohashi K. Identical origin of adrenal cortex and gonad revealed by expression profiles of Ad4BP/SF-1. *Genes Cells*. 1996;1(7):663-671.
5. Luo X, Ikeda Y, Parker KL. A cell-specific nuclear receptor is essential for adrenal and gonadal development and sexual differentiation. *Cell*. 1994;77(4):481-490.
6. Morohashi K. The ontogenesis of the steroidogenic tissues. *Genes Cells*. 1997;2(2):95-106.
7. Jirásek JE. Human fetal endocrines. *London: Martinus Nijhoff*. 1980:69–82.
8. McClellan MC, Brenner RM. Development of the fetal adrenals in nonhuman primates: electron microscopy. *Fetal endocrinology*. 1981:383-403.
9. Mesiano S, Coulter CL, Jaffe RB. Localization of cytochrome P450 cholesterol side-chain cleavage, cytochrome P450 17 alpha-hydroxylase/17, 20-lyase, and 3 beta-hydroxysteroid dehydrogenase isomerase steroidogenic enzymes in human and rhesus monkey fetal adrenal glands: reappraisal of functional zonation. *J Clin Endocrinol Metab*. 1993;77(5):1184-1189.

10. Sucheston ME, Cannon MS. Development of zonular patterns in the human adrenal gland. *J Morphol*. 1968;126(4):477-491.

11. Spencer SJ, Mesiano, S. and Jaffe, R.B. Programmed cell death in remodeling of the human fetal adrenal cortex: possible role of activin-A. *J Soc Gynecol Investig*. 1995;2(2):p.150.

12. Havelock JC, Auchus RJ, Rainey WE. The rise in adrenal androgen biosynthesis: adrenarche. *Semin Reprod Med*. 2004;22(4):337-347.

13. Yates R, Katugampola H, Cavlan D, Cogger K, Meimaridou E, Hughes C, Metherell L, Guasti L, King P. Adrenocortical development, maintenance, and disease. *Curr Top Dev Biol*. 2013;106:239-312.

14. Tanaka S, Matsuzawa A. Comparison of adrenocortical zonation in C57BL/6J and DDD mice. *Exp Anim*. 1995;44(4):285-291.

15. Tanaka S, Nishimura M, Kitoh J, Matsuzawa A. Strain difference of the adrenal cortex between A/J and SM/J mice, progenitors of SMXA recombinant inbred group. *Exp Anim*. 1995;44(2):127-130.

16. Tamura Y. Structural changes in the suprarenal gland of the mouse during pregnancy. *J Exp Biol*. 1926;4(1):81-92.

17. Howard‐Miller E. A transitory zone in the adrenal cortex which shows age and sex relationships. *Am J Anat*. 1927;40(2):251-293.

18. Jones IC. The disappearance of the X zone of the mouse adrenal cortex during first pregnancy. *Proc R Soc Lond B Biol Sci*. 1952;139(896):398-410.

19. Le Douarin NM, Teillet MA. Experimental analysis of the migration and differentiation of neuroblasts of the autonomic nervous system and of neurectodermal mesenchymal derivatives, using a biological cell marking technique. *Dev Biol*. 1974;41(1):162-184.

20. Furlan A, Dyachuk V, Kastriti ME, Calvo-Enrique L, Abdo H, Hadjab S, Chontorotzea T, Akkuratova N, Usoskin D, Kamenev D, Petersen J, Sunadome K, Memic F, Marklund U, Fried K, Topilko P, Lallemend F, Kharchenko PV, Ernfors P, Adameyko I. Multipotent peripheral glial cells generate neuroendocrine cells of the adrenal medulla. *Science*. 2017;357(6346).

21. Berger I, Werdermann M, Bornstein SR, Steenblock C. The adrenal gland in stress - Adaptation on a cellular level. *J Steroid Biochem Mol Biol*. 2019;190:198-206.

22. Cater DB, Lever JD. The zona intermedia of the adrenal cortex; a correlation of possible functional significance with development, morphology and histochemistry. *J Anat*. 1954;88(4):437-454.

23. Black VH, Robbins D, McNamara N, Huima T. A correlated thin-section and freeze-fracture analysis of guinea pig adrenocortical cells. *Am J Anat*. 1979;156(4):453-503.

24. Rhodin JA. The ultrastructure of the adrenal cortex of the rat under normal and experimental conditions. *J Ultrastruct Res*. 1971;34(1):23-71.

25. Sato T. The fine structure of the mouse adrenal X zone. *Z Zellforsch Mikrosk Anat*. 1968;87(3):315-329.

26. Pignatti E, Leng S, Carlone DL, Breault DT. Regulation of zonation and homeostasis in the adrenal cortex. *Mol Cell Endocrinol*. 2017;441:146-155.

27. Freedman BD, Kempna PB, Carlone DL, Shah M, Guagliardo NA, Barrett PQ, Gomez-Sanchez CE, Majzoub JA, Breault DT. Adrenocortical zonation results from lineage conversion of differentiated zona glomerulosa cells. *Dev Cell*. 2013;26(6):666-673.

28. Wood MA, Acharya A, Finco I, Swonger JM, Elston MJ, Tallquist MD, Hammer GD. Fetal adrenal capsular cells serve as progenitor cells for steroidogenic and stromal adrenocortical cell lineages in M. musculus. *Development*. 2013;140(22):4522-4532.

29. Walczak EM, Hammer GD. Regulation of the adrenocortical stem cell niche: implications for disease. *Nat Rev Endocrinol*. 2015;11(1):14-28.

30. Salmon TNaZ, R.L. A study of the life history of cortico-adrenal gland cells of the rat by means of trypan blue injections. *Anat Rec*. 1941;80(4):421-429.

31. Kim JH, Choi MH. Embryonic Development and Adult Regeneration of the Adrenal Gland. *Endocrinol Metab (Seoul)*. 2020;35(4):765-773.

32. Lerario AM, Finco I, LaPensee C, Hammer GD. Molecular Mechanisms of Stem/Progenitor Cell Maintenance in the Adrenal Cortex. *Front Endocrinol (Lausanne)*. 2017;8:52.

33. Kim AC, Reuter AL, Zubair M, Else T, Serecky K, Bingham NC, Lavery GG, Parker KL, Hammer GD. Targeted disruption of beta-catenin in Sf1-expressing cells impairs development and maintenance of the adrenal cortex. *Development*. 2008;135(15):2593-2602.

34. MacDonald BT, Tamai K, He X. Wnt/beta-catenin signaling: components, mechanisms, and diseases. *Dev Cell*. 2009;17(1):9-26.

35. Liu C, Li Y, Semenov M, Han C, Baeg GH, Tan Y, Zhang Z, Lin X, He X. Control of beta-catenin phosphorylation/degradation by a dual-kinase mechanism. *Cell*. 2002;108(6):837-847.

36. Aberle H, Bauer A, Stappert J, Kispert A, Kemler R. beta-catenin is a target for the ubiquitin-proteasome pathway. *EMBO J*. 1997;16(13):3797-3804.

37. Bhanot P, Brink M, Samos CH, Hsieh JC, Wang Y, Macke JP, Andrew D, Nathans J, Nusse R. A new member of the frizzled family from Drosophila functions as a Wingless receptor. *Nature*. 1996;382(6588):225-230.

38. Yang-Snyder J, Miller JR, Brown JD, Lai CJ, Moon RT. A frizzled homolog functions in a vertebrate Wnt signaling pathway. *Curr Biol*. 1996;6(10):1302-1306.

39. He X, Semenov M, Tamai K, Zeng X. LDL receptor-related proteins 5 and 6 in Wnt/beta-catenin signaling: arrows point the way. *Development*. 2004;131(8):1663-1677.

40. Eastman Q, Grosschedl R. Regulation of LEF-1/TCF transcription factors by Wnt and other signals. *Curr Opin Cell Biol*. 1999;11(2):233-240.

41. Daniels DL, Weis WI. Beta-catenin directly displaces Groucho/TLE repressors from Tcf/Lef in Wnt-mediated transcription activation. *Nat Struct Mol Biol*. 2005;12(4):364-371.

42. Mosimann C, Hausmann G, Basler K. Beta-catenin hits chromatin: regulation of Wnt target gene activation. *Nat Rev Mol Cell Biol*. 2009;10(4):276-286.

43. Berthon A, Martinez A, Bertherat J, Val P. Wnt/beta-catenin signalling in adrenal physiology and tumour development. *Mol Cell Endocrinol*. 2012;351(1):87-95.

44. Heikkila M, Peltoketo H, Leppaluoto J, Ilves M, Vuolteenaho O, Vainio S. Wnt-4 deficiency alters mouse adrenal cortex function, reducing aldosterone production. *Endocrinology*. 2002;143(11):4358-4365.

45. Eberhart CG, Argani P. Wnt signaling in human development: beta-catenin nuclear translocation in fetal lung, kidney, placenta, capillaries, adrenal, and cartilage. *Pediatr Dev Pathol*. 2001;4(4):351-357.

46. Berthon A, Sahut-Barnola I, Lambert-Langlais S, de Joussineau C, Damon-Soubeyrand C, Louiset E, Taketo MM, Tissier F, Bertherat J, Lefrancois-Martinez AM, Martinez A, Val P. Constitutive beta-catenin activation induces adrenal hyperplasia and promotes adrenal cancer development. *Hum Mol Genet*. 2010;19(8):1561-1576.

47. Haegel H, Larue L, Ohsugi M, Fedorov L, Herrenknecht K, Kemler R. Lack of beta-catenin affects mouse development at gastrulation. *Development*. 1995;121(11):3529-3537.

48. McMahon AP, Ingham PW, Tabin CJ. Developmental roles and clinical significance of hedgehog signaling. *Curr Top Dev Biol*. 2003;53:1-114.

49. King PJ, Guasti L, Laufer E. Hedgehog signalling in endocrine development and disease. *J Endocrinol*. 2008;198(3):439-450.

50. Gupta S, Takebe N, Lorusso P. Targeting the Hedgehog pathway in cancer. *Ther Adv Med Oncol*. 2010;2(4):237-250.

51. Ingham PW, McMahon AP. Hedgehog signaling in animal development: paradigms and principles. *Genes Dev*. 2001;15(23):3059-3087.

52. Cohen MM, Jr. The hedgehog signaling network. *Am J Med Genet A*. 2003;123A(1):5-28.

53. Bijlsma MF, Spek CA, Peppelenbosch MP. Hedgehog: an unusual signal transducer. *Bioessays*. 2004;26(4):387-394.

54. Jiang J, Hui CC. Hedgehog signaling in development and cancer. *Dev Cell*. 2008;15(6):801-812.

55. Bai CB, Auerbach W, Lee JS, Stephen D, Joyner AL. Gli2, but not Gli1, is required for initial Shh signaling and ectopic activation of the Shh pathway. *Development*. 2002;129(20):4753-4761.

56. Wang B, Fallon JF, Beachy PA. Hedgehog-regulated processing of Gli3 produces an anterior/posterior repressor gradient in the developing vertebrate limb. *Cell*. 2000;100(4):423-434.

57. Persson M, Stamataki D, te Welscher P, Andersson E, Bose J, Ruther U, Ericson J, Briscoe J. Dorsal-ventral patterning of the spinal cord requires Gli3 transcriptional repressor activity. *Genes Dev*. 2002;16(22):2865-2878.

58. Shimokawa T, Tostar U, Lauth M, Palaniswamy R, Kasper M, Toftgard R, Zaphiropoulos PG. Novel human glioma-associated oncogene 1 (GLI1) splice variants reveal distinct mechanisms in the terminal transduction of the hedgehog signal. *J Biol Chem*. 2008;283(21):14345-14354.

59. King P, Paul A, Laufer E. Shh signaling regulates adrenocortical development and identifies progenitors of steroidogenic lineages. *Proc Natl Acad Sci U S A*. 2009;106(50):21185-21190.

60. Huang CC, Miyagawa S, Matsumaru D, Parker KL, Yao HH. Progenitor cell expansion and organ size of mouse adrenal is regulated by sonic hedgehog. *Endocrinology*. 2010;151(3):1119-1128.

61. Ching S, Vilain E. Targeted disruption of Sonic Hedgehog in the mouse adrenal leads to adrenocortical hypoplasia. *Genesis*. 2009;47(9):628-637.

62. Finco I, Lerario AM, Hammer GD. Sonic Hedgehog and WNT Signaling Promote Adrenal Gland Regeneration in Male Mice. *Endocrinology*. 2018;159(2):579-596.

63. Stephens MA, Wand G. Stress and the HPA axis: role of glucocorticoids in alcohol dependence. *Alcohol Res*. 2012;34(4):468-483.

64. Lotfi CF, de Mendonca PO. Comparative Effect of ACTH and Related Peptides on Proliferation and Growth of Rat Adrenal Gland. *Front Endocrinol (Lausanne)*. 2016;7:39.

65. Clark BJ. ACTH Action on StAR Biology. *Front Neurosci*. 2016;10:547.

66. Hofland J, Delhanty PJ, Steenbergen J, Hofland LJ, van Koetsveld PM, van Nederveen FH, de Herder WW, Feelders RA, de Jong FH. Melanocortin 2 receptor-associated protein (MRAP) and MRAP2 in human adrenocortical tissues: regulation of expression and association with ACTH responsiveness. *J Clin Endocrinol Metab*. 2012;97(5):E747-754.

67. Clark AJL, Chan L. Stability and Turnover of the ACTH Receptor Complex. *Front Endocrinol (Lausanne)*. 2019;10:491.

68. Lefkowitz RJ, Roth J, Pricer W, Pastan I. ACTH receptors in the adrenal: specific binding of ACTH-125I and its relation to adenyl cyclase. *Proc Natl Acad Sci U S A*. 1970;65(3):745-752.

69. Mathieu M, Drelon C, Rodriguez S, Tabbal H, Septier A, Damon-Soubeyrand C, Dumontet T, Berthon A, Sahut-Barnola I, Djari C, Batisse-Lignier M, Pointud JC, Richard D, Kerdivel G, Calmejane MA, Boeva V, Tauveron I, Lefrancois-Martinez AM, Martinez A, Val P. Steroidogenic differentiation and PKA signaling are programmed by histone methyltransferase EZH2 in the adrenal cortex. *Proc Natl Acad Sci U S A*. 2018;115(52):E12265-E12274.

70. Gomez-Sanchez CE, Qi X, Velarde-Miranda C, Plonczynski MW, Parker CR, Rainey W, Satoh F, Maekawa T, Nakamura Y, Sasano H, Gomez-Sanchez EP. Development of monoclonal antibodies against human CYP11B1 and CYP11B2. *Mol Cell Endocrinol*. 2014;383(1-2):111-117.

71. Drelon C, Berthon A, Sahut-Barnola I, Mathieu M, Dumontet T, Rodriguez S, Batisse-Lignier M, Tabbal H, Tauveron I, Lefrancois-Martinez AM, Pointud JC, Gomez-Sanchez CE, Vainio S, Shan J, Sacco S, Schedl A, Stratakis CA, Martinez A, Val P. PKA inhibits WNT signalling in adrenal cortex zonation and prevents malignant tumour development. *Nat Commun*. 2016;7:12751.

72. Lala DS, Rice DA, Parker KL. Steroidogenic factor I, a key regulator of steroidogenic enzyme expression, is the mouse homolog of fushi tarazu-factor I. *Mol Endocrinol*. 1992;6(8):1249-1258.

73. Crawford PA, Sadovsky Y, Milbrandt J. Nuclear receptor steroidogenic factor 1 directs embryonic stem cells toward the steroidogenic lineage. *Mol Cell Biol*. 1997;17(7):3997-4006.

74. Sakai N, Terami H, Suzuki S, Haga M, Nomoto K, Tsuchida N, Morohashi K, Saito N, Asada M, Hashimoto M, Harada D, Asahara H, Ishikawa T, Shimada F, Sakurada K. Identification of NR5A1 (SF-1/AD4BP) gene expression modulators by large-scale gain and loss of function studies. *J Endocrinol*. 2008;198(3):489-497.

75. Kim AC, Barlaskar FM, Heaton JH, Else T, Kelly VR, Krill KT, Scheys JO, Simon DP, Trovato A, Yang WH, Hammer GD. In search of adrenocortical stem and progenitor cells. *Endocr Rev*. 2009;30(3):241-263.

76. Mitani F, Suzuki H, Hata J, Ogishima T, Shimada H, Ishimura Y. A novel cell layer without corticosteroid-synthesizing enzymes in rat adrenal cortex: histochemical detection and possible physiological role. *Endocrinology*. 1994;135(1):431-438.

77. Nishimoto K, Harris RB, Rainey WE, Seki T. Sodium deficiency regulates rat adrenal zona glomerulosa gene expression. *Endocrinology*. 2014;155(4):1363-1372.

78. Davies LA, Hu C, Guagliardo NA, Sen N, Chen X, Talley EM, Carey RM, Bayliss DA, Barrett PQ. TASK channel deletion in mice causes primary hyperaldosteronism. *Proc Natl Acad Sci U S A*. 2008;105(6):2203-2208.

79. McEwan PE, Vinson GP, Kenyon CJ. Control of adrenal cell proliferation by AT1 receptors in response to angiotensin II and low-sodium diet. *Am J Physiol*. 1999;276(2):E303-309.

80. McNeill H, Whitworth E, Vinson GP, Hinson JP. Distribution of extracellular signal-regulated protein kinases 1 and 2 in the rat adrenal and their activation by angiotensin II. *J Endocrinol*. 2005;187(1):149-157.

81. Xing Y, Lerario AM, Rainey W, Hammer GD. Development of adrenal cortex zonation. *Endocrinol Metab Clin North Am*. 2015;44(2):243-274.

82. Miller WL. Molecular biology of steroid hormone synthesis. *Endocr Rev*. 1988;9(3):295-318.

83. Brown MS, Kovanen PT, Goldstein JL. Receptor-mediated uptake of lipoprotein-cholesterol and its utilization for steroid synthesis in the adrenal cortex. *Recent Prog Horm Res*. 1979;35:215-257.

84. Azhar S, Reaven E. Scavenger receptor class BI and selective cholesteryl ester uptake: partners in the regulation of steroidogenesis. *Mol Cell Endocrinol*. 2002;195(1-2):1-26.

85. Connelly MA. SR-BI-mediated HDL cholesteryl ester delivery in the adrenal gland. *Mol Cell Endocrinol*. 2009;300(1-2):83-88.

86. Carr BR, Simpson ER. Lipoprotein utilization and cholesterol synthesis by the human fetal adrenal gland. *Endocr Rev*. 1981;2(3):306-326.

87. Kraemer FB. Adrenal cholesterol utilization. *Mol Cell Endocrinol*. 2007;265-266:42-45.

88. Hu J, Zhang Z, Shen WJ, Azhar S. Cellular cholesterol delivery, intracellular processing and utilization for biosynthesis of steroid hormones. *Nutr Metab (Lond)*. 2010;7:47.

89. Jefcoate C. High-flux mitochondrial cholesterol trafficking, a specialized function of the adrenal cortex. *J Clin Invest*. 2002;110(7):881-890.

90. Sewer MB, Waterman MR. ACTH modulation of transcription factors responsible for steroid hydroxylase gene expression in the adrenal cortex. *Microsc Res Tech*. 2003;61(3):300-307.

91. Payne AH, Hales DB. Overview of steroidogenic enzymes in the pathway from cholesterol to active steroid hormones. *Endocr Rev*. 2004;25(6):947-970.

92. Lachance Y, Luu-The V, Labrie C, Simard J, Dumont M, de Launoit Y, Guerin S, Leblanc G, Labrie F. Characterization of human 3 beta-hydroxysteroid dehydrogenase/delta 5-delta 4-isomerase gene and its expression in mammalian cells. *J Biol Chem*. 1992;267(5):3551.

93. Muller J. Regulation of aldosterone biosynthesis. Physiological and clinical aspects. *Monogr Endocrinol*. 1987;29:1-364.

94. El Ghorayeb N, Bourdeau I, Lacroix A. Role of ACTH and Other Hormones in the Regulation of Aldosterone Production in Primary Aldosteronism. *Front Endocrinol (Lausanne)*. 2016;7:72.

95. Gray SA, Mannan MA, O'Shaughnessy PJ. Development of cytochrome P450 17 alpha-hydroxylase (P450c17) mRNA and enzyme activity in neonatal ovaries of normal and hypogonadal (hpg) mice. *J Mol Endocrinol*. 1996;17(1):55-60.

96. Missaghian E, Kempna P, Dick B, Hirsch A, Alikhani-Koupaei R, Jegou B, Mullis PE, Frey BM, Fluck CE. Role of DNA methylation in the tissue-specific expression of the CYP17A1 gene for steroidogenesis in rodents. *J Endocrinol*. 2009;202(1):99-109.

97. Arlt W, Stewart PM. Adrenal corticosteroid biosynthesis, metabolism, and action. *Endocrinol Metab Clin North Am*. 2005;34(2):293-313, viii.

98. Beishuizen A, Thijs LG, Vermes I. Patterns of corticosteroid-binding globulin and the free cortisol index during septic shock and multitrauma. *Intensive Care Med*. 2001;27(10):1584-1591.

99. Prigent H, Maxime V, Annane D. Science review: mechanisms of impaired adrenal function in sepsis and molecular actions of glucocorticoids. *Crit Care*. 2004;8(4):243-252.

100. Chapman K, Holmes M, Seckl J. 11beta-hydroxysteroid dehydrogenases: intracellular gate-keepers of tissue glucocorticoid action. *Physiol Rev*. 2013;93(3):1139-1206.

101. Spiga F, Walker JJ, Terry JR, Lightman SL. HPA axis-rhythms. *Compr Physiol*. 2014;4(3):1273-1298.

102. Timmermans S, Souffriau J, Libert C. A General Introduction to Glucocorticoid Biology. *Front Immunol*. 2019;10:1545.

103. Giguere V, Hollenberg SM, Rosenfeld MG, Evans RM. Functional domains of the human glucocorticoid receptor. *Cell*. 1986;46(5):645-652.

104. Stahn C, Lowenberg M, Hommes DW, Buttgereit F. Molecular mechanisms of glucocorticoid action and selective glucocorticoid receptor agonists. *Mol Cell Endocrinol*. 2007;275(1-2):71-78.

105. Meijsing SH, Pufall MA, So AY, Bates DL, Chen L, Yamamoto KR. DNA binding site sequence directs glucocorticoid receptor structure and activity. *Science*. 2009;324(5925):407-410.

106. Buttgereit F, Scheffold A. Rapid glucocorticoid effects on immune cells. *Steroids*. 2002;67(6):529-534.

107. Scheller K, Sekeris CE, Krohne G, Hock R, Hansen IA, Scheer U. Localization of glucocorticoid hormone receptors in mitochondria of human cells. *Eur J Cell Biol*. 2000;79(5):299-307.

108. Moutsatsou P, Psarra AM, Tsiapara A, Paraskevakou H, Davaris P, Sekeris CE. Localization of the glucocorticoid receptor in rat brain mitochondria. *Arch Biochem Biophys*. 2001;386(1):69-78.

109. Akhtar MK, Kelly SL, Kaderbhai MA. Cytochrome b(5) modulation of 17alpha hydroxylase and 17-20 lyase (CYP17) activities in steroidogenesis. *J Endocrinol*. 2005;187(2):267-274.

110. Rainey WE, Nakamura Y. Regulation of the adrenal androgen biosynthesis. *J Steroid Biochem Mol Biol*. 2008;108(3-5):281-286.

111. Rege J, Nakamura Y, Satoh F, Morimoto R, Kennedy MR, Layman LC, Honma S, Sasano H, Rainey WE. Liquid chromatography-tandem mass spectrometry analysis of human adrenal vein 19-carbon steroids before and after ACTH stimulation. *J Clin Endocrinol Metab*. 2013;98(3):1182-1188.

112. Lazar MA. Thyroid hormone receptors: multiple forms, multiple possibilities. *Endocr Rev*. 1993;14(2):184-193.

113. Brent GA. Mechanisms of thyroid hormone action. *J Clin Invest*. 2012;122(9):3035-3043.

114. Cheng SY, Leonard JL, Davis PJ. Molecular aspects of thyroid hormone actions. *Endocr Rev*. 2010;31(2):139-170.

115. Mendoza A, Hollenberg AN. New insights into thyroid hormone action. *Pharmacol Ther*. 2017;173:135-145.

116. Gross J, Pitt-Rivers R. Physiological activity of 3:5:3'-L-triiodothyronine. *Lancet*. 1952;1(6708):593-594.

117. Pitt-Rivers R. Metabolic effects of compounds structurally related to thyroxine in vivo: thyroxine derivatives. *J Clin Endocrinol Metab*. 1954;14(11):1444-1450.

118. Friesema EC, Ganguly S, Abdalla A, Manning Fox JE, Halestrap AP, Visser TJ. Identification of monocarboxylate transporter 8 as a specific thyroid hormone transporter. *J Biol Chem*. 2003;278(41):40128-40135.

119. Friesema EC, Jansen J, Jachtenberg JW, Visser WE, Kester MH, Visser TJ. Effective cellular uptake and efflux of thyroid hormone by human monocarboxylate transporter 10. *Mol Endocrinol*. 2008;22(6):1357-1369.

120. Groeneweg S, van Geest FS, Peeters RP, Heuer H, Visser WE. Thyroid Hormone Transporters. *Endocr Rev*. 2020;41(2).

121. Teumer A, Chaker L, Groeneweg S, Li Y, Di Munno C, Barbieri C, Schultheiss UT, Traglia M, Ahluwalia TS, Akiyama M, Appel EVR, Arking DE, Arnold A, Astrup A, Beekman M, Beilby JP, Bekaert S, Boerwinkle E, Brown SJ, De Buyzere M, Campbell PJ, Ceresini G, Cerqueira C, Cucca F, Deary IJ, Deelen J, Eckardt KU, Ekici AB, Eriksson JG, Ferrrucci L, Fiers T, Fiorillo E, Ford I, Fox CS, Fuchsberger C, Galesloot TE, Gieger C, Gogele M, De Grandi A, Grarup N, Greiser KH, Haljas K, Hansen T, Harris SE, van Heemst D, den Heijer M, Hicks AA, den Hollander W, Homuth G, Hui J, Ikram MA, Ittermann T, Jensen RA, Jing J, Jukema JW, Kajantie E, Kamatani Y, Kasbohm E, Kaufman JM, Kiemeney LA, Kloppenburg M, Kronenberg F, Kubo M, Lahti J, Lapauw B, Li S, Liewald DCM, Lifelines Cohort S, Lim EM, Linneberg A, Marina M, Mascalzoni D, Matsuda K, Medenwald D, Meisinger C, Meulenbelt I, De Meyer T, Meyer Zu Schwabedissen HE, Mikolajczyk R, Moed M, Netea-Maier RT, Nolte IM, Okada Y, Pala M, Pattaro C, Pedersen O, Petersmann A, Porcu E, Postmus I, Pramstaller PP, Psaty BM, Ramos YFM, Rawal R, Redmond P, Richards JB, Rietzschel ER, Rivadeneira F, Roef G, Rotter JI, Sala CF, Schlessinger D, Selvin E, Slagboom PE, Soranzo N, Sorensen TIA, Spector TD, Starr JM, Stott DJ, Taes Y, Taliun D, Tanaka T, Thuesen B, Tiller D, Toniolo D, Uitterlinden AG, Visser WE, Walsh JP, Wilson SG, Wolffenbuttel BHR, Yang Q, Zheng HF, Cappola A,

Peeters RP, Naitza S, Volzke H, Sanna S, Kottgen A, Visser TJ, Medici M. Genome-wide analyses identify a role for SLC17A4 and AADAT in thyroid hormone regulation. *Nat Commun*. 2018;9(1):4455.

122. Pizzagalli F, Hagenbuch B, Stieger B, Klenk U, Folkers G, Meier PJ. Identification of a novel human organic anion transporting polypeptide as a high affinity thyroxine transporter. *Mol Endocrinol*. 2002;16(10):2283-2296.

123. Sap J, Munoz A, Damm K, Goldberg Y, Ghysdael J, Leutz A, Beug H, Vennstrom B. The c-erb-A protein is a high-affinity receptor for thyroid hormone. *Nature*. 1986;324(6098):635-640.

124. Tata JR, Widnell CC. Ribonucleic acid synthesis during the early action of thyroid hormones. *Biochem J*. 1966;98(2):604-620.

125. Weinberger C, Thompson CC, Ong ES, Lebo R, Gruol DJ, Evans RM. The c-erb-A gene encodes a thyroid hormone receptor. *Nature*. 1986;324(6098):641-646.

126. Izumo S, Mahdavi V. Thyroid hormone receptor alpha isoforms generated by alternative splicing differentially activate myosin HC gene transcription. *Nature*. 1988;334(6182):539-542.

127. Lazar MA, Hodin RA, Darling DS, Chin WW. Identification of a rat c-erbA alpha-related protein which binds deoxyribonucleic acid but does not bind thyroid hormone. *Mol Endocrinol*. 1988;2(10):893-901.

128. Mitsuhashi T, Tennyson GE, Nikodem VM. Alternative splicing generates messages encoding rat c-erbA proteins that do not bind thyroid hormone. *Proc Natl Acad Sci U S A*. 1988;85(16):5804-5808.

129. Hodin RA, Lazar MA, Wintman BI, Darling DS, Koenig RJ, Larsen PR, Moore DD, Chin WW. Identification of a thyroid hormone receptor that is pituitary-specific. *Science*. 1989;244(4900):76-79.

130. Wood WM, Dowding JM, Bright TM, McDermott MT, Haugen BR, Gordon DF, Ridgway EC. Thyroid hormone receptor beta2 promoter activity in pituitary cells is regulated by Pit-1. *J Biol Chem*. 1996;271(39):24213-24220.

131. Cheng SY. Multiple mechanisms for regulation of the transcriptional activity of thyroid hormone receptors. *Rev Endocr Metab Disord*. 2000;1(1-2):9-18.

132. Anyetei-Anum CS, Roggero VR, Allison LA. Thyroid hormone receptor localization in target tissues. *J Endocrinol*. 2018;237(1):R19-R34.

133. Jones I, Ng L, Liu H, Forrest D. An intron control region differentially regulates expression of thyroid hormone receptor beta2 in the cochlea, pituitary, and cone photoreceptors. *Mol Endocrinol*. 2007;21(5):1108-1119.

134. Williams GR. Cloning and characterization of two novel thyroid hormone receptor beta isoforms. *Mol Cell Biol*. 2000;20(22):8329-8342.

135. Gothe S, Wang Z, Ng L, Kindblom JM, Barros AC, Ohlsson C, Vennstrom B, Forrest D. Mice devoid of all known thyroid hormone receptors are viable but exhibit disorders of the pituitary-thyroid axis, growth, and bone maturation. *Genes Dev*. 1999;13(10):1329-1341.

136. Wikstrom L, Johansson C, Salto C, Barlow C, Campos Barros A, Baas F, Forrest D, Thoren P, Vennstrom B. Abnormal heart rate and body temperature in mice lacking thyroid hormone receptor alpha 1. *EMBO J*. 1998;17(2):455-461.

137. Yen PM, Ando S, Feng X, Liu Y, Maruvada P, Xia X. Thyroid hormone action at the cellular, genomic and target gene levels. *Mol Cell Endocrinol*. 2006;246(1-2):121-127.

138. Evans RM. The steroid and thyroid hormone receptor superfamily. *Science*. 1988;240(4854):889-895.

139. Kliewer SA, Umesono K, Mangelsdorf DJ, Evans RM. Retinoid X receptor interacts with nuclear receptors in retinoic acid, thyroid hormone and vitamin D3 signalling. *Nature*. 1992;355(6359):446-449.

140. Chen JD, Evans RM. A transcriptional co-repressor that interacts with nuclear hormone receptors. *Nature*. 1995;377(6548):454-457.

141. McKenna NJ, Lanz RB, O'Malley BW. Nuclear receptor coregulators: cellular and molecular biology. *Endocr Rev*. 1999;20(3):321-344.

142. Oberoi J, Fairall L, Watson PJ, Yang JC, Czimmerer Z, Kampmann T, Goult BT, Greenwood JA, Gooch JT, Kallenberger BC, Nagy L, Neuhaus D, Schwabe JW. Structural basis for the assembly of the SMRT/NCoR core transcriptional repression machinery. *Nat Struct Mol Biol*. 2011;18(2):177-184.

143. Privalsky ML. The role of corepressors in transcriptional regulation by nuclear hormone receptors. *Annu Rev Physiol*. 2004;66:315-360.

144. Mendoza A, Astapova I, Shimizu H, Gallop MR, Al-Sowaimel L, MacGowan SMD, Bergmann T, Berg AH, Tenen DE, Jacobs C, Lyubetskaya A, Tsai L, Hollenberg AN. NCoR1-independent mechanism plays a role in the action of the unliganded thyroid hormone receptor. *Proc Natl Acad Sci U S A*. 2017;114(40):E8458-E8467.

145. Xu L, Glass CK, Rosenfeld MG. Coactivator and corepressor complexes in nuclear receptor function. *Curr Opin Genet Dev*. 1999;9(2):140-147.

146. Hershkovitz L, Beuschlein F, Klammer S, Krup M, Weinstein Y. Adrenal 20alpha-hydroxysteroid dehydrogenase in the mouse catabolizes progesterone and 11-deoxycorticosterone and is restricted to the X-zone. *Endocrinology*. 2007;148(3):976-988.

147. Holmes PV, Dickson AD. X-zone degeneration in the adrenal glands of adult and immature female mice. *J Anat*. 1971;108(Pt 1):159-168.

148. Huang CC, Kraft C, Moy N, Ng L, Forrest D. A Novel Population of Inner Cortical Cells in the Adrenal Gland That Displays Sexually Dimorphic Expression of Thyroid Hormone Receptor-beta1. *Endocrinology*. 2015;156(6):2338-2348.

149. Lyu Q, Wang H, Kang Y, Wu X, Zheng HS, Laprocina K, Junghans K, Ding X, Huang CC. RNA-Seq Reveals Sub-Zones in Mouse Adrenal Zona Fasciculata and the Sexually Dimorphic Responses to Thyroid Hormone. *Endocrinology*. 2020;161(9).

150. Aranda A, Pascual A. Nuclear hormone receptors and gene expression. *Physiol Rev*. 2001;81(3):1269-1304.

151. Shibata H, Spencer TE, Onate SA, Jenster G, Tsai SY, Tsai MJ, O'Malley BW. Role of co-activators and co-repressors in the mechanism of steroid/thyroid receptor action. *Recent Prog Horm Res*. 1997;52:141-164; discussion 164-145.

152. Astapova I. Role of co-regulators in metabolic and transcriptional actions of thyroid hormone. *J Mol Endocrinol*. 2016;56(3):73-97.

153. Stolz V, et al. Nuclear receptor corepressor 1 controls regulatory T cell subset differentiation and effector function. *bioRxiv*. 2022.

154. Spencer SJ, Mesiano S, Lee JY, Jaffe RB. Proliferation and apoptosis in the human adrenal cortex during the fetal and perinatal periods: implications for growth and remodeling. *J Clin Endocrinol Metab*. 1999;84(3):1110-1115.

155. Hashimoto I, Wiest WG. Luteotrophic and luteolytic mechanisms in rat corpora lutea. *Endocrinology*. 1969;84(4):886-892.

156. Wiest WG. Conversion of progesterone to 4-pregnen-20 alpha-ol-3-one by rat ovarian tissue in vitro. *J Biol Chem*. 1959;234:3115-3121.

157. Zhang Q, Ding X. The CYP2F, CYP2G and CYP2J subfamilies. *Cytochrome P450: Role in the Metabolism and Toxicity of Drugs and Other Xenobiotics*. 2008;Jun 27:309-353.

158. Cruzan G, Bus JS, Banton MI, Sarang SS, Waites R, Layko DB, Raymond J, Dodd D, Andersen ME. Editor's Highlight: Complete Attenuation of Mouse Lung Cell Proliferation and Tumorigenicity in CYP2F2 Knockout and CYP2F1 Humanized Mice Exposed to Inhaled Styrene for up to 2 Years Supports a Lack of Human Relevance. *Toxicol Sci*. 2017;159(2):413-421.

159. Cruzan G, Bus J, Hotchkiss J, Harkema J, Banton M, Sarang S. CYP2F2-generated metabolites, not styrene oxide, are a key event mediating the mode of action of styrene-induced mouse lung tumors. *Regul Toxicol Pharmacol*. 2012;62(1):214-220.

160. Miller WL. Steroidogenic enzymes. *Endocr Dev*. 2008;13:1-18.

161. Miller WL, Bose HS. Early steps in steroidogenesis: intracellular cholesterol trafficking. *J Lipid Res*. 2011;52(12):2111-2135.

162. Mason JI, Rainey WE. Steroidogenesis in the human fetal adrenal: a role for cholesterol synthesized de novo. *J Clin Endocrinol Metab*. 1987;64(1):140-147.

163. Borkowski AJ, Levin S, Delcroix C, Mahler A, Verhas V. Blood cholesterol and hydrocortisone production in man: quantitative aspects of the utilization of circulating cholesterol by the adrenals at rest and under adrenocorticotropin stimulation. *J Clin Invest*. 1967;46(5):797-811.

164. Battista MC, Roberge C, Martinez A, Gallo-Payet N. 24-dehydrocholesterol reductase/seladin-1: a key protein differentially involved in adrenocorticotropin effects observed in human and rat adrenal cortex. *Endocrinology*. 2009;150(9):4180-4190.

165. Battista MC, Roberge C, Otis M, Gallo-Payet N. Seladin-1 expression in rat adrenal gland: effect of adrenocorticotropic hormone treatment. *J Endocrinol*. 2007;192(1):53-66.

166. Greeve I, Hermans-Borgmeyer I, Brellinger C, Kasper D, Gomez-Isla T, Behl C, Levkau B, Nitsch RM. The human DIMINUTO/DWARF1 homolog seladin-1 confers resistance to Alzheimer's disease-associated neurodegeneration and oxidative stress. *J Neurosci*. 2000;20(19):7345-7352.

167. Luciani P, Ferruzzi P, Arnaldi G, Crescioli C, Benvenuti S, Nesi G, Valeri A, Greeve I, Serio M, Mannelli M, Peri A. Expression of the novel adrenocorticotropin-responsive gene selective Alzheimer's disease indicator-1 in the normal adrenal cortex and in adrenocortical adenomas and carcinomas. *J Clin Endocrinol Metab*. 2004;89(3):1332-1339.

168. Sarkar D, Imai T, Kambe F, Shibata A, Ohmori S, Siddiq A, Hayasaka S, Funahashi H, Seo H. The human homolog of Diminuto/Dwarf1 gene (hDiminuto): a novel ACTH-responsive

gene overexpressed in benign cortisol-producing adrenocortical adenomas. *J Clin Endocrinol Metab*. 2001;86(11):5130-5137.

169. Rohanizadegan M, Sacharow S. Desmosterolosis presenting with multiple congenital anomalies. *Eur J Med Genet*. 2018;61(3):152-156.

170. Manna PR, Tena-Sempere M, Huhtaniemi IT. Molecular mechanisms of thyroid hormone-stimulated steroidogenesis in mouse leydig tumor cells. Involvement of the steroidogenic acute regulatory (StAR) protein. *J Biol Chem*. 1999;274(9):5909-5918.

171. Jana NR, Bhattacharya S. Binding of thyroid hormone to the goat testicular Leydig cell induces the generation of a proteinaceous factor which stimulates androgen release. *J Endocrinol*. 1994;143(3):549-556.

172. Manna PR, Kero J, Tena-Sempere M, Pakarinen P, Stocco DM, Huhtaniemi IT. Assessment of mechanisms of thyroid hormone action in mouse Leydig cells: regulation of the steroidogenic acute regulatory protein, steroidogenesis, and luteinizing hormone receptor function. *Endocrinology*. 2001;142(1):319-331.

173. Manna PR, Roy P, Clark BJ, Stocco DM, Huhtaniemi IT. Interaction of thyroid hormone and steroidogenic acute regulatory (StAR) protein in the regulation of murine Leydig cell steroidogenesis. *J Steroid Biochem Mol Biol*. 2001;76(1-5):167-177.

174. Kanuri B, Fong V, Ponny SR, Weerasekera R, Pulakanti K, Patel KS, Tyshynsky R, Patel SB. Generation and validation of a conditional knockout mouse model for desmosterolosis. *J Lipid Res*. 2021;62:100028.

175. Lyu Q, Zheng HS, Laprocina K, Huang CC. Microwaving and Fluorophore-Tyramide for Multiplex Immunostaining on Mouse Adrenals - Using Unconjugated Primary Antibodies from the Same Host Species. *J Vis Exp*. 2020(156).

176. Huang CC, Kang Y. The transient cortical zone in the adrenal gland: the mystery of the adrenal X-zone. *J Endocrinol*. 2019;241(1):R51-R63.

177. Boivin GP, Hickman DL, Creamer-Hente MA, Pritchett-Corning KR, Bratcher NA. Review of CO(2) as a Euthanasia Agent for Laboratory Rats and Mice. *J Am Assoc Lab Anim Sci*. 2017;56(5):491-499.

178. Zubair M, Ishihara S, Oka S, Okumura K, Morohashi K. Two-step regulation of Ad4BP/SF-1 gene transcription during fetal adrenal development: initiation by a Hox-Pbx1-Prep1 complex and maintenance via autoregulation by Ad4BP/SF-1. *Mol Cell Biol*. 2006;26(11):4111-4121.

179. Zubair M, Parker KL, Morohashi K. Developmental links between the fetal and adult zones of the adrenal cortex revealed by lineage tracing. *Mol Cell Biol*. 2008;28(23):7030-7040.

180. Lopez JP, Brivio E, Santambrogio A, De Donno C, Kos A, Peters M, Rost N, Czamara D, Bruckl TM, Roeh S, Pohlmann ML, Engelhardt C, Ressle A, Stoffel R, Tontsch A, Villamizar JM, Reincke M, Riester A, Sbiera S, Fassnacht M, Mayberg HS, Craighead WE, Dunlop BW, Nemeroff CB, Schmidt MV, Binder EB, Theis FJ, Beuschlein F, Andoniadou CL, Chen A. Single-cell molecular profiling of all three components of the HPA axis reveals adrenal ABCB1 as a regulator of stress adaptation. *Sci Adv*. 2021;7(5).

181. Mullur R, Liu YY, Brent GA. Thyroid hormone regulation of metabolism. *Physiol Rev*. 2014;94(2):355-382.

182. Sinha RA, Singh BK, Yen PM. Direct effects of thyroid hormones on hepatic lipid metabolism. *Nat Rev Endocrinol*. 2018;14(5):259-269.

183. Araki O, Ying H, Zhu XG, Willingham MC, Cheng SY. Distinct dysregulation of lipid metabolism by unliganded thyroid hormone receptor isoforms. *Mol Endocrinol*. 2009;23(3):308-315.

184. Maran RR. Thyroid hormones: their role in testicular steroidogenesis. *Arch Androl*. 2003;49(5):375-388.

185. Gallo-Payet N, Battista MC. Steroidogenesis-adrenal cell signal transduction. *Compr Physiol*. 2014;4(3):889-964.

186. Gersh I, Grollman A. The nature of the X‐zone of the adrenal gland of the mouse. *Anat Rec*. 1939;75(2):131-153.

187. Iivonen S, Hiltunen M, Alafuzoff I, Mannermaa A, Kerokoski P, Puolivali J, Salminen A, Helisalmi S, Soininen H. Seladin-1 transcription is linked to neuronal degeneration in Alzheimer's disease. *Neuroscience*. 2002;113(2):301-310.

188. Crameri A, Biondi E, Kuehnle K, Lutjohann D, Thelen KM, Perga S, Dotti CG, Nitsch RM, Ledesma MD, Mohajeri MH. The role of seladin-1/DHCR24 in cholesterol biosynthesis, APP processing and Abeta generation in vivo. *EMBO J*. 2006;25(2):432-443.

189. Cecchi C, Rosati F, Pensalfini A, Formigli L, Nosi D, Liguri G, Dichiara F, Morello M, Danza G, Pieraccini G, Peri A, Serio M, Stefani M. Seladin-1/DHCR24 protects neuroblastoma

cells against Abeta toxicity by increasing membrane cholesterol content. *J Cell Mol Med*. 2008;12(5B):1990-2002.

190. Kuehnle K, Crameri A, Kalin RE, Luciani P, Benvenuti S, Peri A, Ratti F, Rodolfo M, Kulic L, Heppner FL, Nitsch RM, Mohajeri MH. Prosurvival effect of DHCR24/Seladin-1 in acute and chronic responses to oxidative stress. *Mol Cell Biol*. 2008;28(2):539-550.

191. Wu C, Miloslavskaya I, Demontis S, Maestro R, Galaktionov K. Regulation of cellular response to oncogenic and oxidative stress by Seladin-1. *Nature*. 2004;432(7017):640-645.

192. Lu X, Li Y, Wang W, Chen S, Liu T, Jia D, Quan X, Sun D, Chang AK, Gao B. 3 beta-hydroxysteroid-Delta 24 reductase (DHCR24) protects neuronal cells from apoptotic cell death induced by endoplasmic reticulum (ER) stress. *PLoS One*. 2014;9(1):e86753.

193. Lu X, Kambe F, Cao X, Kozaki Y, Kaji T, Ishii T, Seo H. 3beta-Hydroxysteroid-delta24 reductase is a hydrogen peroxide scavenger, protecting cells from oxidative stress-induced apoptosis. *Endocrinology*. 2008;149(7):3267-3273.

194. Sarajarvi T, Haapasalo A, Viswanathan J, Makinen P, Laitinen M, Soininen H, Hiltunen M. Down-regulation of seladin-1 increases BACE1 levels and activity through enhanced GGA3 depletion during apoptosis. *J Biol Chem*. 2009;284(49):34433-34443.

195. Preston MI. Effects of thyroxin injections on the suprarenal glands of the mouse. *Endocrinology*. 1928;12(3):323-334.

196. Stahn C, Buttgereit F. Genomic and nongenomic effects of glucocorticoids. *Nat Clin Pract Rheumatol*. 2008;4(10):525-533.

197. Panettieri RA, Schaafsma D, Amrani Y, Koziol-White C, Ostrom R, Tliba O. Non-genomic Effects of Glucocorticoids: An Updated View. *Trends Pharmacol Sci*. 2019;40(1):38-49.

198. Trevino LS, Gorelick DA. The Interface of Nuclear and Membrane Steroid Signaling. *Endocrinology*. 2021;162(8).

199. Uchoa ET, Aguilera G, Herman JP, Fiedler JL, Deak T, de Sousa MB. Novel aspects of glucocorticoid actions. *J Neuroendocrinol*. 2014;26(9):557-572.

200. Lopez-Maury L, Marguerat S, Bahler J. Tuning gene expression to changing environments: from rapid responses to evolutionary adaptation. *Nat Rev Genet*. 2008;9(8):583-593.

201. Yosef N, Regev A. Impulse control: temporal dynamics in gene transcription. *Cell*. 2011;144(6):886-896.

202. Dallman MF, Akana SF, Levin N, Walker CD, Bradbury MJ, Suemaru S, Scribner KS. Corticosteroids and the control of function in the hypothalamo-pituitary-adrenal (HPA) axis. *Ann N Y Acad Sci*. 1994;746:22-31; discussion 31-22, 64-27.

203. Foradori CD, Mackay L, Huang CJ, Kemppainen RJ. Expression of Rasd1 in mouse endocrine pituitary cells and its response to dexamethasone. *Stress*. 2021;24(5):659-666.

204. Trzeciak WH, LeHoux JG, Waterman MR, Simpson ER. Dexamethasone inhibits corticotropin-induced accumulation of CYP11A and CYP17 messenger RNAs in bovine adrenocortical cells. *Mol Endocrinol*. 1993;7(2):206-213.

205. Martin LJ, Tremblay JJ. Glucocorticoids antagonize cAMP-induced Star transcription in Leydig cells through the orphan nuclear receptor NR4A1. *J Mol Endocrinol*. 2008;41(3):165-175.

206. Koibuchi F, Ritoh N, Aoyagi R, Funakoshi-Tago M, Tamura H. Dexamethasone suppresses neurosteroid biosynthesis via downregulation of steroidogenic enzyme gene expression in human glioma GI-1 cells. *Biol Pharm Bull*. 2014;37(7):1241-1247.

207. Paez-Pereda M, Kovalovsky D, Hopfner U, Theodoropoulou M, Pagotto U, Uhl E, Losa M, Stalla J, Grubler Y, Missale C, Arzt E, Stalla GK. Retinoic acid prevents experimental Cushing syndrome. *J Clin Invest*. 2001;108(8):1123-1131.

208. Kallio MA, Tuimala JT, Hupponen T, Klemela P, Gentile M, Scheinin I, Koski M, Kaki J, Korpelainen EI. Chipster: user-friendly analysis software for microarray and other high-throughput data. *BMC Genomics*. 2011;12:507.

209. Dobin A, Davis CA, Schlesinger F, Drenkow J, Zaleski C, Jha S, Batut P, Chaisson M, Gingeras TR. STAR: ultrafast universal RNA-seq aligner. *Bioinformatics*. 2013;29(1):15-21.

210. Anders S, Pyl PT, Huber W. HTSeq--a Python framework to work with high-throughput sequencing data. *Bioinformatics*. 2015;31(2):166-169.

211. Love MI, Huber W, Anders S. Moderated estimation of fold change and dispersion for RNA-seq data with DESeq2. *Genome Biol*. 2014;15(12):550.

212. Raudvere U, Kolberg L, Kuzmin I, Arak T, Adler P, Peterson H, Vilo J. g:Profiler: a web server for functional enrichment analysis and conversions of gene lists (2019 update). *Nucleic Acids Res*. 2019;47(W1):W191-W198.

213. Yu G, Wang LG, Han Y, He QY. clusterProfiler: an R package for comparing biological themes among gene clusters. *OMICS*. 2012;16(5):284-287.

214. Chan WH, Komada M, Fukushima T, Southard-Smith EM, Anderson CR, Wakefield MJ. RNA-seq of Isolated Chromaffin Cells Highlights the Role of Sex-Linked and Imprinted Genes in Adrenal Medulla Development. *Sci Rep*. 2019;9(1):3929.

215. Dumontet T, Sahut-Barnola I, Septier A, Montanier N, Plotton I, Roucher-Boulez F, Ducros V, Lefrancois-Martinez AM, Pointud JC, Zubair M, Morohashi KI, Breault DT, Val P, Martinez A. PKA signaling drives reticularis differentiation and sexually dimorphic adrenal cortex renewal. *JCI Insight*. 2018;3(2).

216. Spiga F, Zavala E, Walker JJ, Zhao Z, Terry JR, Lightman SL. Dynamic responses of the adrenal steroidogenic regulatory network. *Proc Natl Acad Sci U S A*. 2017;114(31):E6466-E6474.

217. Wong DL, Lesage A, Siddall B, Funder JW. Glucocorticoid regulation of phenylethanolamine N-methyltransferase in vivo. *FASEB J*. 1992;6(14):3310-3315.

218. Wurtman RJ, Axelrod J. Adrenaline synthesis: control by the pituitary gland and adrenal glucocorticoids. *Science*. 1965;150(3702):1464-1465.

219. Ju Y, Mizutani T, Imamichi Y, Yazawa T, Matsumura T, Kawabe S, Kanno M, Umezawa A, Kangawa K, Miyamoto K. Nuclear receptor 5A (NR5A) family regulates 5-aminolevulinic acid synthase 1 (ALAS1) gene expression in steroidogenic cells. *Endocrinology*. 2012;153(11):5522-5534.

220. Imamichi Y, Mizutani T, Ju Y, Matsumura T, Kawabe S, Kanno M, Yazawa T, Miyamoto K. Transcriptional regulation of human ferredoxin 1 in ovarian granulosa cells. *Mol Cell Endocrinol*. 2013;370(1-2):1-10.

221. Aigueperse C, Val P, Pacot C, Darne C, Lalli E, Sassone-Corsi P, Veyssiere G, Jean C, Martinez A. SF-1 (steroidogenic factor-1), C/EBPbeta (CCAAT/enhancer binding protein), and ubiquitous transcription factors NF1 (nuclear factor 1) and Sp1 (selective promoter factor 1) are required for regulation of the mouse aldose reductase-like gene (AKR1B7) expression in adrenocortical cells. *Mol Endocrinol*. 2001;15(1):93-111.

222. Oakley RH, Cidlowski JA. The biology of the glucocorticoid receptor: new signaling mechanisms in health and disease. *J Allergy Clin Immunol*. 2013;132(5):1033-1044.

223. Picard D, Yamamoto KR. Two signals mediate hormone-dependent nuclear localization of the glucocorticoid receptor. *EMBO J*. 1987;6(11):3333-3340.

224. Pedram A, Razandi M, Aitkenhead M, Hughes CC, Levin ER. Integration of the non-genomic and genomic actions of estrogen. Membrane-initiated signaling by steroid to transcription and cell biology. *J Biol Chem*. 2002;277(52):50768-50775.

225. John S, Sabo PJ, Thurman RE, Sung MH, Biddie SC, Johnson TA, Hager GL, Stamatoyannopoulos JA. Chromatin accessibility pre-determines glucocorticoid receptor binding patterns. *Nat Genet*. 2011;43(3):264-268.

226. Vockley CM, D'Ippolito AM, McDowell IC, Majoros WH, Safi A, Song L, Crawford GE, Reddy TE. Direct GR Binding Sites Potentiate Clusters of TF Binding across the Human Genome. *Cell*. 2016;166(5):1269-1281 e1219.

227. Severinova E, Alikunju S, Deng W, Dhawan P, Sayed N, Sayed D. Glucocorticoid Receptor-Binding and Transcriptome Signature in Cardiomyocytes. *J Am Heart Assoc*. 2019;8(6):e011484.

228. Fu M, Sun T, Bookout AL, Downes M, Yu RT, Evans RM, Mangelsdorf DJ. A Nuclear Receptor Atlas: 3T3-L1 adipogenesis. *Mol Endocrinol*. 2005;19(10):2437-2450.

229. Richard AC, Lun ATL, Lau WWY, Gottgens B, Marioni JC, Griffiths GM. T cell cytolytic capacity is independent of initial stimulation strength. *Nat Immunol*. 2018;19(8):849-858.

230. Ipseiz N, Uderhardt S, Scholtysek C, Steffen M, Schabbauer G, Bozec A, Schett G, Kronke G. The nuclear receptor Nr4a1 mediates anti-inflammatory effects of apoptotic cells. *J Immunol*. 2014;192(10):4852-4858.

231. Kassel O, Herrlich P. Crosstalk between the glucocorticoid receptor and other transcription factors: molecular aspects. *Mol Cell Endocrinol*. 2007;275(1-2):13-29.

232. Reddy TE, Pauli F, Sprouse RO, Neff NF, Newberry KM, Garabedian MJ, Myers RM. Genomic determination of the glucocorticoid response reveals unexpected mechanisms of gene regulation. *Genome Res*. 2009;19(12):2163-2171.

233. Paust HJ, Loeper S, Else T, Bamberger AM, Papadopoulos G, Pankoke D, Saeger W, Bamberger CM. Expression of the glucocorticoid receptor in the human adrenal cortex. *Exp Clin Endocrinol Diabetes*. 2006;114(1):6-10.

234. Tacon LJ, Soon PS, Gill AJ, Chou AS, Clarkson A, Botling J, Stalberg PL, Skogseid BM, Robinson BG, Sidhu SB, Clifton-Bligh RJ. The glucocorticoid receptor is overexpressed in malignant adrenocortical tumors. *J Clin Endocrinol Metab*. 2009;94(11):4591-4599.

235. Dardis A, Miller WL. Dexamethasone does not exert direct intracellular feedback on steroidogenesis in human adrenal NCI-H295A cells. *J Endocrinol*. 2003;179(1):131-142.

236. Vahl TP, Ulrich-Lai YM, Ostrander MM, Dolgas CM, Elfers EE, Seeley RJ, D'Alessio DA, Herman JP. Comparative analysis of ACTH and corticosterone sampling methods in rats. *Am J Physiol Endocrinol Metab*. 2005;289(5):E823-828.

237. Liston C, Gan WB. Glucocorticoids are critical regulators of dendritic spine development and plasticity in vivo. *Proc Natl Acad Sci U S A*. 2011;108(38):16074-16079.

238. Wurtman RJ. Control of epinephrine synthesis in the adrenal medulla by the adrenal cortex: hormonal specificity and dose-response characteristics. *Endocrinology*. 1966;79(3):608-614.

239. Wurtman RJ, Axelrod J. Control of enzymatic synthesis of adrenaline in the adrenal medulla by adrenal cortical steroids. *J Biol Chem*. 1966;241(10):2301-2305.

240. Einer-Jensen N, Carter AM. Local transfer of hormones between blood vessels within the adrenal gland may explain the functional interaction between the adrenal cortex and medulla. *Med Hypotheses*. 1995;44(6):471-474.

241. Huang CC, Shih MC, Hsu NC, Chien Y, Chung BC. Fetal glucocorticoid synthesis is required for development of fetal adrenal medulla and hypothalamus feedback suppression. *Endocrinology*. 2012;153(10):4749-4756.

242. Evinger MJ, Towle AC, Park DH, Lee P, Joh TH. Glucocorticoids stimulate transcription of the rat phenylethanolamine N-methyltransferase (PNMT) gene in vivo and in vitro. *Cell Mol Neurobiol*. 1992;12(3):193-215.

243. Frahm KA, Peffer ME, Zhang JY, Luthra S, Chakka AB, Couger MB, Chandran UR, Monaghan AP, DeFranco DB. Research Resource: The Dexamethasone Transcriptome in Hypothalamic Embryonic Neural Stem Cells. *Mol Endocrinol*. 2016;30(1):144-154.

244. Szyf M, Milstone DS, Schimmer BP, Parker KL, Seidman JG. cis modification of the steroid 21-hydroxylase gene prevents its expression in the Y1 mouse adrenocortical tumor cell line. *Mol Endocrinol*. 1990;4(8):1144-1152.

245. Thorngate FE, Strockbine PA, Erickson SK, Williams DL. Altered adrenal gland cholesterol metabolism in the apoE-deficient mouse. *J Lipid Res*. 2002;43(11):1920-1926.

246. El Wakil A, Mari B, Barhanin J, Lalli E. Genomic analysis of sexual dimorphism of gene expression in the mouse adrenal gland. *Horm Metab Res*. 2013;45(12):870-873.

247. Frahm KA, Waldman JK, Luthra S, Rudine AC, Monaghan-Nichols AP, Chandran UR, DeFranco DB. A comparison of the sexually dimorphic dexamethasone transcriptome in mouse cerebral cortical and hypothalamic embryonic neural stem cells. *Mol Cell Endocrinol*. 2018;471:42-50.

248. Wallensteen L, Zimmermann M, Thomsen Sandberg M, Gezelius A, Nordenstrom A, Hirvikoski T, Lajic S. Sex-Dimorphic Effects of Prenatal Treatment With Dexamethasone. *J Clin Endocrinol Metab*. 2016;101(10):3838-3846.

249. Kreider ML, Levin ED, Seidler FJ, Slotkin TA. Gestational dexamethasone treatment elicits sex-dependent alterations in locomotor activity, reward-based memory and hippocampal cholinergic function in adolescent and adult rats. *Neuropsychopharmacology*. 2005;30(9):1617-1623.

250. Duma D, Collins JB, Chou JW, Cidlowski JA. Sexually dimorphic actions of glucocorticoids provide a link to inflammatory diseases with gender differences in prevalence. *Sci Signal*. 2010;3(143):ra74.

251. Kananen K, Markkula M, Mikola M, Rainio EM, McNeilly A, Huhtaniemi I. Gonadectomy permits adrenocortical tumorigenesis in mice transgenic for the mouse inhibin alpha-subunit promoter/simian virus 40 T-antigen fusion gene: evidence for negative autoregulation of the inhibin alpha-subunit gene. *Mol Endocrinol*. 1996;10(12):1667-1677.

252. Quinn MA, Cidlowski JA. Endogenous hepatic glucocorticoid receptor signaling coordinates sex-biased inflammatory gene expression. *FASEB J*. 2016;30(2):971-982.

253. Tejos-Bravo M, Oakley RH, Whirledge SD, Corrales WA, Silva JP, Garcia-Rojo G, Toledo J, Sanchez W, Roman-Albasini L, Aliaga E, Aguayo F, Olave F, Maracaja-Coutinho V, Cidlowski JA, Fiedler JL. Deletion of hippocampal Glucocorticoid receptors unveils sex-biased microRNA expression and neuronal morphology alterations in mice. *Neurobiol Stress*. 2021;14:100306.

254. Cruz-Topete D, Oakley RH, Carroll NG, He B, Myers PH, Xu X, Watts MN, Trosclair K, Glasscock E, Dominic P, Cidlowski JA. Deletion of the Cardiomyocyte Glucocorticoid Receptor Leads to Sexually Dimorphic Changes in Cardiac Gene Expression and Progression to Heart Failure. *J Am Heart Assoc*. 2019;8(15):e011012.

255. Yang KC, Yamada KA, Patel AY, Topkara VK, George I, Cheema FH, Ewald GA, Mann DL, Nerbonne JM. Deep RNA sequencing reveals dynamic regulation of myocardial

noncoding RNAs in failing human heart and remodeling with mechanical circulatory support. *Circulation*. 2014;129(9):1009-1021.

256. Soumillon M, Necsulea A, Weier M, Brawand D, Zhang X, Gu H, Barthes P, Kokkinaki M, Nef S, Gnirke A, Dym M, de Massy B, Mikkelsen TS, Kaessmann H. Cellular source and mechanisms of high transcriptome complexity in the mammalian testis. *Cell Rep*. 2013;3(6):2179-2190.

257. Lake BB, Ai R, Kaeser GE, Salathia NS, Yung YC, Liu R, Wildberg A, Gao D, Fung HL, Chen S, Vijayaraghavan R, Wong J, Chen A, Sheng X, Kaper F, Shen R, Ronaghi M, Fan JB, Wang W, Chun J, Zhang K. Neuronal subtypes and diversity revealed by single-nucleus RNA sequencing of the human brain. *Science*. 2016;352(6293):1586-1590.

258. Heiman M, Kulicke R, Fenster RJ, Greengard P, Heintz N. Cell type-specific mRNA purification by translating ribosome affinity purification (TRAP). *Nat Protoc*. 2014;9(6):1282-1291.

259. Bertin B, Renaud Y, Aradhya R, Jagla K, Junion G. TRAP-rc, Translating Ribosome Affinity Purification from Rare Cell Populations of Drosophila Embryos. *J Vis Exp*. 2015(103).

260. Thellmann M, Andersen TG, Vermeer JE. Translating Ribosome Affinity Purification (TRAP) to Investigate Arabidopsis thaliana Root Development at a Cell Type-Specific Scale. *J Vis Exp*. 2020(159).

261. Moran P, Guo Y, Yuan R, Barnekow N, Palmer J, Beck A, Ren B. Translating Ribosome Affinity Purification (TRAP) for RNA Isolation from Endothelial Cells In vivo. *J Vis Exp*. 2019(147).

262. Roh HC, Tsai LT, Lyubetskaya A, Tenen D, Kumari M, Rosen ED. Simultaneous Transcriptional and Epigenomic Profiling from Specific Cell Types within Heterogeneous Tissues In Vivo. *Cell Rep*. 2017;18(4):1048-1061.

263. Varjosalo M, Taipale J. Hedgehog: functions and mechanisms. *Genes Dev*. 2008;22(18):2454-2472.

264. Mueller O LS, Schroeder A. RNA integrity number (RIN)–standardization of RNA quality control. *Agilent application note, publication*. 2004(1):1-8.

265. Benton L, Shan LX, Hardy MP. Differentiation of adult Leydig cells. *J Steroid Biochem Mol Biol*. 1995;53(1-6):61-68.

266. Monder C, Hardy MP, Blanchard RJ, Blanchard DC. Comparative aspects of 11 beta-hydroxysteroid dehydrogenase. Testicular 11 beta-hydroxysteroid dehydrogenase: development of a model for the mediation of Leydig cell function by corticosteroids. *Steroids*. 1994;59(2):69-73.

267. Bitgood MJ, Shen L, McMahon AP. Sertoli cell signaling by Desert hedgehog regulates the male germline. *Curr Biol*. 1996;6(3):298-304.

268. Beverdam A, Svingen T, Bagheri-Fam S, Bernard P, McClive P, Robson M, Khojasteh MB, Salehi M, Sinclair AH, Harley VR, Koopman P. Sox9-dependent expression of Gstm6 in Sertoli cells during testis development in mice. *Reproduction*. 2009;137(3):481-486.

269. Gross A, Schoendube J, Zimmermann S, Steeb M, Zengerle R, Koltay P. Technologies for Single-Cell Isolation. *Int J Mol Sci*. 2015;16(8):16897-16919.

270. Ziegenhain C, Vieth B, Parekh S, Reinius B, Guillaumet-Adkins A, Smets M, Leonhardt H, Heyn H, Hellmann I, Enard W. Comparative Analysis of Single-Cell RNA Sequencing Methods. *Mol Cell*. 2017;65(4):631-643 e634.

271. Nguyen QH, Pervolarakis N, Nee K, Kessenbrock K. Experimental Considerations for Single-Cell RNA Sequencing Approaches. *Front Cell Dev Biol*. 2018;6:108.

272. Chucair-Elliott AJ, Ocanas SR, Stanford DR, Ansere VA, Buettner KB, Porter H, Eliason NL, Reid JJ, Sharpe AL, Stout MB, Beckstead MJ, Miller BF, Richardson A, Freeman WM. Inducible cell-specific mouse models for paired epigenetic and transcriptomic studies of microglia and astroglia. *Commun Biol*. 2020;3(1):693.

273. Barsoum I, Yao HH. Redundant and differential roles of transcription factors Gli1 and Gli2 in the development of mouse fetal Leydig cells. *Biol Reprod*. 2011;84(5):894-899.

274. Mori H, Shimizu D, Fukunishi R, Christensen AK. Morphometric analysis of testicular Leydig cells in normal adult mice. *Anat Rec*. 1982;204(4):333-339.

275. Villavicencio EH, Walterhouse DO, Iannaccone PM. The sonic hedgehog-patched-gli pathway in human development and disease. *Am J Hum Genet*. 2000;67(5):1047-1054.

276. Briscoe J, Therond PP. The mechanisms of Hedgehog signalling and its roles in development and disease. *Nat Rev Mol Cell Biol*. 2013;14(7):416-429.

277. Grabek A, Dolfi B, Klein B, Jian-Motamedi F, Chaboissier MC, Schedl A. The Adult Adrenal Cortex Undergoes Rapid Tissue Renewal in a Sex-Specific Manner. *Cell Stem Cell*. 2019;25(2):290-296 e292.